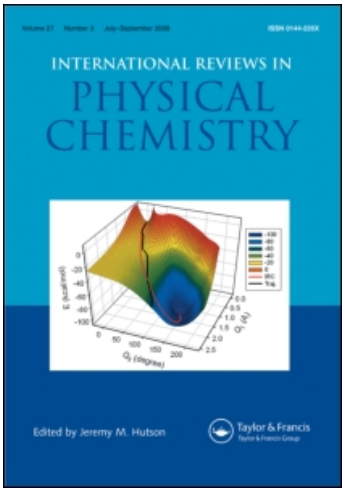

International Reviews in Physical Chemistry
Publication details, including instructions for authors and subscription information:
http://www.informaworld.com/smpp/title~content=t713724383

What are the basic mechanisms of electronic transitions in molecular dynamic processes?

Hiroki Nakamura[a]
[a] Division of Theoretical Studies, Institute for Molecular Science, Myodaiji, Okazaki, Japan

To cite this Article Nakamura, Hiroki(1991) 'What are the basic mechanisms of electronic transitions in molecular dynamic processes?', International Reviews in Physical Chemistry, 10: 2, 123 — 188
To link to this Article: DOI: 10.1080/01442359109353256
URL: http://dx.doi.org/10.1080/01442359109353256

INTERNATIONAL REVIEWS IN PHYSICAL CHEMISTRY, 1991, VOL. 10, NO. 2, 123–188

What are the basic mechanisms of electronic transitions in molecular dynamic processes?

by HIROKI NAKAMURA
Division of Theoretical Studies,
Institute for Molecular Science, Myodaiji, Okazaki 444, Japan

The basic mechanisms of electronic transitions in molecular processes and their theoretical treatments are summarized and reviewed. These are the non-adiabatic (either radially or rotationally induced) transitions and the decay (auto-ionization) mechanisms of 'superexcited states'. The interdisciplinarity of the concept of non-adiabatic transition is emphasized, and the present status of the semiclassical theory is inclusively summarized together with some numerical applications. Particular emphasis is put on the non-adiabatic tunnelling process which is supposed to be an important key mechanism for state (or phase) change in various fields. Definitions of two kinds of superexcited state are given, and their peculiarities and richness in their participating dynamic processes are explained. The multichannel quantum defect theory is outlined and recommended as a powerful theoretical tool for dealing with the various dynamic processes such as photo-ionization, photodissociation, auto-ionization, dissociative recombination and associative ionization. Some numerical applications are also presented in order to promote the understanding of the mechanisms. The underlying philosophy throughout this paper is to try to clarify the basic mechanisms of electronic transitions and to formulate them in a unified way as much as possible.

1. Introduction

Recent progress in laser and synchrotron radiation technology has made it possible to explore the world of highly excited states of molecules efficiently. In particular, the multiphoton ionization (MPI) technique has enabled us to investigate in detail the excited states of specified symmetry (Lawley 1985, Kimura 1987). Electronically highly excited states have intriguing characteristics compared with ground and lower excited states. These characteristics may be summarized as follows.

(1) There is strong coupling between electronic and nuclear degrees of freedom.
(2) Many competitive channels are open.
(3) The states contribute largely to oscillator strength distribution.
(4) They are sensitive to an external perturbation such as collision with other particle or external field.
(5) Various transitions among them occur with high probability compared with those in the ordinary first kind of collision processes between unexcited species.

For highly excited states, the Born–Oppenheimer approximation breaks down at least locally in a certain region of nuclear configuration, and the non-Born–Oppenheimer couplings play an essential role. In some cases even the definition itself of the Born–Oppenheimer (adiabatic) state loses its meaning because of the spontaneous decay (auto-ionization) at a fixed nuclear configuration. In general, states are densely populated in the high-energy region, and their contribution to oscillator strength distribution is naturally significant (Berkowitz 1979, Inokuti 1967, 1981). Figure 1

0144-235X/91 $3·00

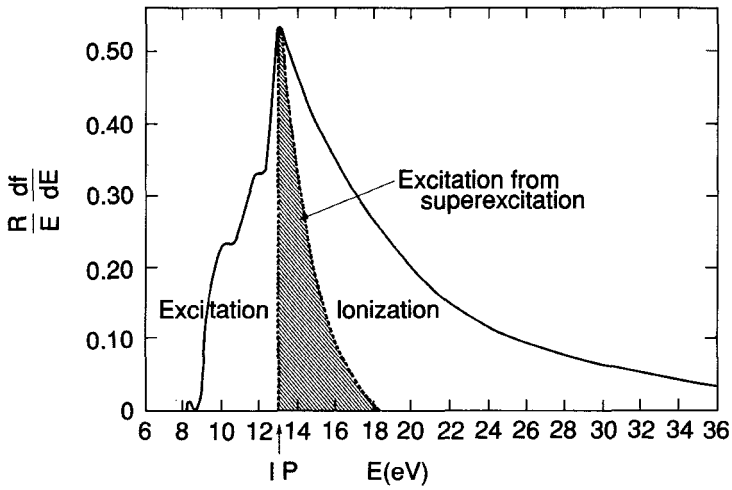

Figure 1. Oscillator strength distribution of CH_4 where R is the Rydberg energy (Inokuti 1967, Platzman 1962a).

shows, as an example, the oscillator strength distribution of CH_4 (Inokuti 1967). As is seen clearly, there is a large contribution from the energy region near and above the first ionization threshold which is designated as IP in the figure. Because of the high density, the excited states in this energy region are sensitive to an external perturbation and various dynamic processes such as auto-ionization, pre-dissociation and non-adiabatic transition can occur. These processes are basically competitive with each other and present intriguing challenging problems to be investigated. In these processes, the internal excitation energy can be effectively employed to induce state change (the collision process of this type is called collision of the second kind (Mitchell and Zemansky 1934, Nakamura and Matsuzawa 1970)); thus the transition (reaction) occurs more efficiently than that in collision of the first kind, in which the relative kinetic energy is used to excite the internal degrees of freedom. Furthermore the mechanisms of the dynamic processes involving excited states are rich in variety and present interesting targets of pure theoretical investigation as well (McGowan 1981, Nakamura 1984a).

The diversity of the dynamic processes involving excited species may be easily shown by listing the examples such as

$M+h\nu \rightarrow M^* \rightarrow M^+ + e$,	resonant photo-ionization, auto-ionization,
$M+h\nu \rightarrow M^* \rightarrow A+B$,	resonant photodissociation, pre-dissociation,
$M^*+\text{field} \rightarrow M^+ + e$,	field ionization,
$M^*+\text{field} \rightarrow A+B$,	field dissociation,
$e+M^+ \rightarrow A^*+B$,	dissociative recombination,
$e+M^+ \rightarrow A^+ + B^-$,	ion-pair formation,
$A^*+B \rightarrow AB^+ + e$,	associative ionization,
$A^*+B \rightarrow A+B^+ + e$,	Penning ionization,
$A^*+BC \rightarrow AB^+ + C+e$,	chemi-ionization,
$AB+h\nu \rightarrow AB^* \rightarrow BA$,	photoisomerization.

Excited states participating in these processes are classified as follows:

(1) ordinary valence electron excited states, either optically allowed or metastable;

(2) Rydberg states, in which one valence electron is excited into a high Rydberg orbital;
(3) two- (or many)-valence-electron (or one-inner-shell-electron) excited states embedded in the electronic continuum.

Internal energy of rovibrationally excited Rydberg states belonging to (2) can easily be larger than the lowest ionization potential. Electronic excitation energy of the states belonging to the above category (3) is also larger than the lowest ionization potential. These states, being unstable against auto-ionization, have very peculiar properties, and are called 'superexcited states' (Platzman 1962a, b, Inokuti 1967, Berkowitz 1979). We call the states of category (3) 'superexcited states of first kind', and the rovibrationally excited Rydberg states 'superexcited states of second kind'. These superexcited states play an important role as the intermediate states of the various dynamic processes mentioned above. The physics and chemistry of these states will open a new and exciting area of science.

One of the most basic questions about these highly excited states is: what are the basic interactions which cause the various dynamic processes? Transitions among the valence electron excited states are generally induced by the so-called non-adiabatic couplings, that is non-adiabatic radial coupling or non-adiabatic rotational (Coriolis) coupling. The former applies to the transitions among the adiabatic states of the same electronic symmetry. The latter applies, on the other hand, to those between the adiabatic states of the different electronic symmetry. Non-adiabatic transition is a very general interdisciplinary concept and represents a key mechanism of various kinds of state-changing phenomena not only in atomic and molecular dynamic processes (Child 1979, Lam and George 1979, Crothers 1981, Nikitin and Umanskii 1984, Eu 1984, Nakamura 1986, 1988) but also in many other fields such as condensed phase physics, surface physics and even biological systems (Nasu and Kayanuma 1980, Kayanuma 1982, 1984a, b, 1985, Wolynes 1987, DeVault 1984, Yoshimori and Tsukada 1985). Avoided crossings are also closely related to the chaotic behaviour of a spectrum (Ramaswamy and Marcus 1981) and even to soliton-like structure (Gaspard *et al.* 1989). Semiclassical theory for the non-adiabatic transitions has been quite well developed for one-dimensional two-state problems (Barany 1979, Nakamura 1988). However, it is not a clever way to deal with the transitions among the Rydberg states from the viewpoint of non-adiabatic transition. This is basically because the period τ_n of the Rydberg electron orbital motion ($\tau_n \approx 1{\cdot}5 \times 10^{-16} n^3$ s with n the principal quantum number) becomes easily comparable with or larger than that of the nuclear vibrational motion and because the Born–Oppenheimer adiabatic approximation does not hold well. A much better treatment is to regard the interaction between the Rydberg electron and the ionic core other than the pure Coulombic interaction as a perturbation. This residual interaction is effectively well represented by the R-dependent quantum defect $\mu_\Lambda(R)$, where R is the internuclear distance. The quantum defect $\mu_\Lambda(R)$ is the same quantity as that usually used to express the potential energy of the Rydberg state $(n\Lambda)$ as

$$E_{n\Lambda}(R) = E_{\text{ion}}(R) - \tfrac{1}{2}[n - \mu_\Lambda(R)]^{-2} \text{ (in atomic units)}, \tag{1.1}$$

where $E_{\text{ion}}(R)$ is the potential energy of the core ion and Λ represents the quantum number other than the principal quantum number n. The R dependence of this quantum defect causes auto-ionization of the vibrationally excited Rydberg state. The multichannel quantum defect theory (MQDT) provides us with a powerful tool for investigating the various processes involving Rydberg states in a unified way (Seaton

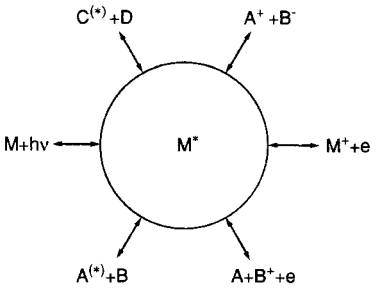

Figure 2. Schematic unified representation of the various dynamic processes, spectroscopic as well as scattering. It is most important to understand the central part M*.

1983, Fano 1970, 1975, Jungen and Atabek 1977, Greene and Jungen 1985). The first kind of superexcited state, on the other hand, has a completely different auto-ionization mechanism. Since this state is embedded in the electronic continuum, this cannot be defined as an ordinary Born–Oppenheimer adiabatic state; in other words, this cannot be an eigenstate of the electronic Hamiltonian H_{el} defined at fixed internuclear configuration. Auto-ionization occurs by the coupling of this state to the electronic continuum through H_{el} itself, or the electron–electron repulsion (electron correlation). This coupling is called 'electronic coupling' and is expressed as

$$V(R)=\langle\phi_{cont}|H_{el}|\phi_d\rangle, \tag{1.2}$$

where ϕ_d is the electronic wavefunction of the superexcited state and ϕ_{cont} is the electronic wavefunction of the continuum.

This review article is organized as follows. In section 2, I would like to emphasize that there is no essential difference between spectroscopic and scattering problems from the theoretical viewpoint of understanding the fundamental mechanisms. The various processes listed above can be schematically summarized in figure 2. The central part M* represents the excited (or superexcited) unstable intermediate state. The most important thing is to understand the properties of this state. Differences in the various dynamic processes, whether they are scattering processes or spectroscopic processes, consist of the boundary conditions. However, the essential physics must be the same as that occurring in the central circle of M*. One of the most typical mechanisms working there is non-adiabatic transition. This transition itself occurs very locally in the region of avoided crossing between adiabatic states and has nothing to do with boundary conditions. Thus the basic theory for non-adiabatic transition can be applied to both spectroscopic and scattering problems. Section 3 is devoted to a summary of the present status of the semiclassical theory of non-adiabatic transition. Inter-disciplinarity of the concept is emphasized, and the basic unified semiclassical theory for one-dimensional radially as well as rotationally induced transitions is reviewed. Particular emphasis is also put on non-adiabatic tunnelling. In section 4 the dynamics of superexcited states are clarified. The basic theories for dealing with the dynamic processes are briefly explained. The MQDT is one of the most powerful theories which enables us to treat the various processes in a unified way. This is outlined in this section. As practical examples of dynamic processes, photo-ionization and auto-ionization of NO, and dissociative recombination and associative ionization of H_2 are discussed. Two mechanisms of auto-ionization (vibrational auto-ionization and electronic auto-ionization) are clarified. The MQDT analysis of the multiphoton ionization (MPI)

experiment is shown to be very powerful and useful. The importance of the dissociative superexcited states of first kind in various dynamic processes is particularly emphasized. Based on the author's viewpoint, section 5 summarizes the subjects to be investigated in future in relation to those discussed in the text. Appendix A describes the derivation of the most sophisticated semiclassical formulae for the Landau–Zener-type and Rosen–Zener-type non-adiabatic transitions. Appendix B derives the reduced S matrix for the non-adiabatic tunnelling. Appendix C proves the unitarity of the S matrix in the MQDT. Atomic units are used throughout this paper.

2. No essential difference between spectroscopic and scattering problems?

Without doubt the experimental set-up for the studies of spectroscopic problems is very different from that of scattering processes. With respect to the mechanisms of the actual physical processes, however, there is not a large difference. As is easily conceivable, photodissociation can be formally decomposed into the following two processes: initial photoabsorption to an excited state and dissociation (half-collision) on the potential energy surface of this excited state. The photodissociation cross-section can actually be expressed in terms of the scattering matrix relevant to the collision process (Beswick *et al.* 1977, Takatsuka and Gordon 1981, Sato *et al.* 1986). Furthermore, in most scattering processes the essential part of the transition occurs in a spatially localized interaction region (reaction zone). The most important thing is to understand and formulate the phenomena occurring there. Once we can do that, then the theory can be used to analyse the spectroscopic processes governed by the same mechanism as well. The most typical example is the non-adiabatic transition. Suppose that we have non-adiabatically coupled two-state systems such as those shown in figure 3. The non-adiabatic transition occurs in a very much spatially localized region near the avoided crossing point. This transition is the same for the three different problems: the inelastic scattering problem (figure 3 (*a*)), the elastic scattering problem

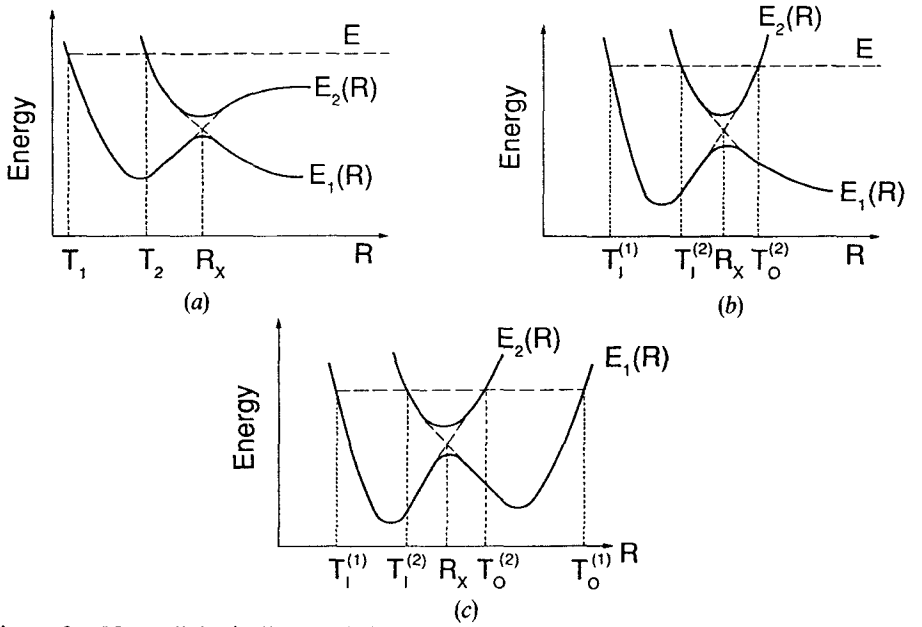

Figure 3. Non-adiabatically coupled two-state problems: (*a*) inelastic scattering; (*b*) elastic scattering or pre-dissociation; (*c*) the perturbed bound-state problem.

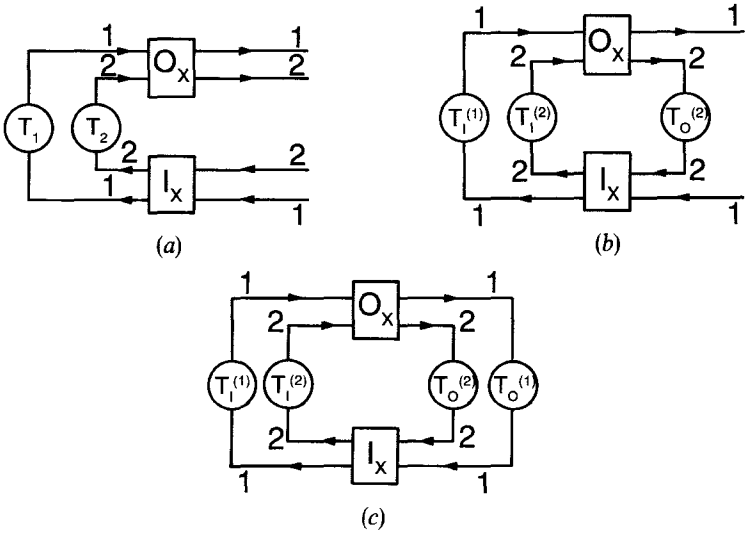

Figure 4. Diagrams corresponding to figure 3.

with resonance or a pre-dissociation process (figure 3(*b*)) and the perturbed bound-state problem (figure 3(*c*)). These three cases can be depicted diagrammatically as in figures 4(*a*)–(*c*). Each arrow indicates the wave propagation on the corresponding potential energy curve. $\mathbf{O}_X$ ($\mathbf{I}_X$) represents a matrix of the non-adiabatic transition at the avoided crossing point R_X for the outgoing (incoming) segment of wave propagation. $(O_X)_{ij}[(I_X)_{ij}]$ is the amplitude for the transition $j \to i$. The circle with T represents the wave reflection at the corresponding turning point. The diagrammatic technique such as the one devised by Child (1974a) can be employed to analyse these three problems. In the case of inelastic scattering (figure 4(*a*)), the 2×2 scattering matrix $\mathbf{S}$ can be expressed as follows (Nakamura 1982, 1984a, b, 1988):

$$\mathbf{S} = \mathbf{P}^{+}_{\infty X}\mathbf{O}_X\mathbf{P}_{XTX}\mathbf{I}_X\mathbf{P}^{-}_{X\infty}, \tag{2.1}$$

where $\mathbf{P}^{(\pm)}_{A\ldots B}$ is a diagonal matrix, representing the adiabatic wave propagation from B to A. In the case of elastic scattering (figure 4(*b*)), the scattering matrix $\exp(2i\eta)$ with phase shift η is given by

$$\exp(2i\eta) = \exp(2i\eta^{(0)})\,[S^{(0)}_{11} - |S^{(0)}|(P_{XT_OX})_{22}][1 - S^{(0)}_{22}(P_{XT_OX})_{22}]^{-1}, \tag{2.2}$$

where $|\ldots|$ designates a determinant, $\eta^{(0)}$ is the scattering phase shift for $R \geqslant R_X$ on the adiabatic potential 1, and

$$\mathbf{S}^{(0)} = \mathbf{O}_X\mathbf{P}_{XT_IX}\mathbf{I}_X, \tag{2.3}$$

which represents the scattering matrix for $R \leqslant R_X$. By analysing the resonance structure in the energy dependence of the phase shift, we can derive the expressions for the resonance position and pre-dissociation lifetime. In the third case of the perturbed bound-state problem (figure 4(*c*)), channel 1 is also closed and the diagrammatic technique leads to the following secular equation:

$$|\mathbf{O}_X\mathbf{P}_{XT_IX}\mathbf{I}_X\mathbf{P}_{XT_OX} - 1| = 0. \tag{2.4}$$

It is now clear that the most basic physics in these three problems consists in the non-adiabatic transition and the knowledge about $\mathbf{I}_X$ and $\mathbf{O}_X$ is most crucial, irrespective of

the boundary conditions. Even the bound-state problem shares the essential mechanisms with the scattering problem. The more detailed physics about $\mathbf{I}_X$ and $\mathbf{O}_X$ will be discussed in the next section.

The scattering matrix may be generally expressed as

$$\mathbf{S}=\mathbf{S}^{\text{out}}\mathbf{S}^{\text{centre}}\mathbf{S}^{\text{in}}, \tag{2.5}$$

where $\mathbf{S}^{\text{in}}$ and $\mathbf{S}^{\text{out}}$ represent the incoming and outgoing parts of the scattering process, and $\mathbf{S}^{\text{centre}}$ is responsible for the central mechanism of the process which is independent of the boundary conditions. As is easily conjectured now, knowledge of $\mathbf{S}^{\text{centre}}$ can be directly used for problems other than the scattering process, probably even for problems in the condensed medium. In this sense, the concept and the theory of non-adiabatic transition, for instance, can be quite universal.

Another good example is the basic idea of the quantum defect theory (Seaton 1983, Fano 1970, 1975, Jungen and Atabek 1977, Greene and Jungen 1985), which gives a uniform description of the Rydberg states and continuum and can describe the various processes in a unified way. For simplicity, let us consider the energy region near the first ionization potential of a diatomic molecule with no superexcited state of the first kind nearby. Even in this simple system we have the following three kinds of problem: the perturbed bound(-Rydberg)-states problem, auto-ionization of internally excited Rydberg states or resonant elastic electron scattering by molecular ion, and inelastic electron scattering. The basic idea of the theory consists in realizing the fact that the physics of the Rydberg electron in the inner region of the electron coordinate space ($r \lesssim r_0$) is quite different from that in the outer region ($r \gtrsim r_0$). In the inner region the electron moves together with the other electrons in the ionic core and the ordinary Born–Oppenheimer approximation is expected to hold well. The total wavefunction of the system can then be expanded in terms of the Born–Oppenheimer basis functions, in which the wavefunction of the Rydberg electron is expressed by using the R-dependent quantum defect $\mu(R)$. This R-dependent quantum defect represents the effects of all the complicated interactions between the Rydberg electron and the core electrons in the inner region. In the outer region, on the other hand, the Rydberg electron moves rather independently from the core. The angular momentum of the electron becomes a good quantum number together with the quantum numbers of the ionic core. The important physical parameter here is the phase shift of the wavefunction measured from the one-centre Coulomb wave. The total wavefunction can be approximated by the close-coupling-type expansion. In the intermediate region ($r \approx r_0$) both Born–Oppenheimer and close-coupling expansions are assumed to hold, and then the basis transformation between the two expansions leads to the coupled linear equations for the expansion coefficients. The key quantities in the present problem within the rotationally unresolved regime are

$$\mathscr{C}^{(\Lambda)}_{v^+v}=\langle v^+|\cos[\pi\mu_\Lambda(R)]|v\rangle, \tag{2.6a}$$

$$\mathscr{S}^{(\Lambda)}_{v^+v}=\langle v^+|\sin[\pi\mu_\Lambda(R)]|v\rangle, \tag{2.6b}$$

where $|v^+\rangle$ represents a vibrational state of the ion and $|v\rangle$ represents a vibrational state of the molecule in a Rydberg state. Depending on the boundary conditions to be imposed on the wavefunction in the outer region, the system of linear equations lead to a secular equation in the case of the bound-state problem or to an expression for the S matrix in the case of the scattering problem. Here again the differences among the

various processes appear only after the boundary conditions are applied. The essential physics occurring in these processes are the same and determined in the inner region; in other words, the basic quantities defined by equation (2.6) are the same for the various processes, namely the physical quantities observed in the asymptotic region are basically determined by the parameters defined in the inner region which is free from boundary condition. The MQDT will be explained in more detail in section 4.

Now, we go back to figure 2, which tells us generally that the key to comprehend the various processes in a unified way as much as possible is to grasp the dynamic as well as the static properties of the central unstable excited or superexcited state M*. The various boundary conditions can be taken into account later. This is what I meant by saying that there is no big difference between spectroscopic and scattering problems. Also, the basic theory for the key mechanisms such as non-adiabatic transition can have a general applicability to a variety of problems.

3. Non-adiabatic transition

3.1. *What is a non-adiabatic transition?*

A non-adiabatic transition is a very general interdisciplinary concept, meaning a transition among the adiabatic states defined as the eigenstates of a system under consideration at a fixed 'adiabatic parameter R'. This transition is induced by a variation in the parameter R. The adiabatic states as a function of R make good basis states when the separability of the parameter R from other variables holds well, or the variation in R is much slower than the motion with respect to the other variables. In this case it is said that the 'adiabaticity' holds well. The adiabaticity breaks down, or the non-adiabatic transition occurs efficiently in such a region of R where the adiabatic states come close together. When the symmetries of the states are the same, they cannot cross each other (the Neumann–Wigner non-crossing rule) and we have a situation like that shown in figure 3. This is called the avoided crossing of adiabatic states. A non-adiabatic transition occurs very locally in the region of this avoided crossing. The broken lines in figure 3 are called diabatic states, which cannot be defined uniquely but provide us with a useful concept sometimes. If the variation in R is very rapid, then the non-adiabatic transition occurs with unit probability, namely the system propagates along the diabatic states.

A non-adiabatic transition presents a key mechanism of a variety of physical and chemical phenomena, as was mentioned before. The most typical examples are, as is well known, atomic and molecular collisions and spectroscopic processes (Child 1979, Lam and George 1979, Crothers 1981, Nikitin and Umanskii 1984, Eu 1984, Nakamura 1986, 1988). Other examples are a vibrational transition in a chemical reaction (Ohsaki and Nakamura 1990), nuclear collision (Abe and Park 1983, Imanishi and von Oertzen 1987), energy relaxation and phase transition in condensed phase physics (Nasu and Kayanuma 1980, Kayanuma 1982, 1984a, b, 1985), dynamic processes on a solid surface (Yoshimori and Tsukada 1985), and electron and proton transfer in biological as well as chemical systems (DeVault 1984, Wolynes 1987). A non-adiabatic transition is also one of the key mechanisms causing chaotic behaviour of the quantum energy spectrum (Ramaswamy and Marcus 1981). In most cases the adiabatic parameter R is some kind of space coordinate. This parameter, however, can be anything in principle. For instance, it can be a field strength in atomic and molecular processes in an external fields (Kleppner *et al.* 1983), or the electron density in the resonant neutrino conversion in the Sun (Schwarzschild 1986).

In the case of atomic and molecular dynamic processes in which we are interested, R is the interatomic distance and the adiabatic states are the ordinary Born–Oppenheimer states. The interaction to cause a non-adiabatic transition between them is a matrix element of the operator $\partial/\partial R$ with respect to the electronic wavefunctions which depend on R parametrically. Because of the large mass disparity between an electron and a nucleus, the electronic motion is much faster than the nuclear motion and the separability between R and the electronic coordinates holds well generally unless the nuclear relative kinetic energy is very high. The localizability of the non-adiabatic transition at the avoided crossing point is very well satisfied. This is because the smaller the amount of energy transferred between different kinds of degrees of freedom, the more probable the transition is.

3.2. *Radial and rotational (Coriolis) couplings*

There are two different mechanisms in the electronically non-adiabatic transitions between the Born–Oppenheimer adiabatic states: one is a transition induced by the relative translational motion of nuclei and the other by the rotational motion. These are explained in this section.

For simplicity let us consider the case of a diatomic molecule AB. The Hamiltonian H of the system in the fixed-space coordinate system is given by

$$H = -\frac{\hbar^2}{2\mu_{AB}}\nabla_R^2 + H_{el}, \tag{3.1}$$

where H_{el} represents the electronic Hamiltonian at fixed R, and μ_{AB} is the reduced mass of the two atoms. Transformation to the fixed-molecule coordinate system changes equation (3.1) to (Thorson 1961)

$$\begin{aligned} H &= -\frac{\hbar^2}{2\mu_{AB}}\frac{1}{R^2}\left(\frac{\partial}{\partial R}R^2\frac{\partial}{\partial R}\right) + \frac{\hbar^2}{2\mu_{AB}R^2}(J-L)^2 + H_{el} \\ &= -\frac{\hbar^2}{2\mu_{AB}}\frac{1}{R^2}\left(\frac{\partial}{\partial R}R^2\frac{\partial}{\partial R}\right) + H_{rot} + H_{cor} + H' + H_{el}, \end{aligned} \tag{3.2}$$

$$H_{rot} = -\frac{\hbar^2}{2\mu_{AB}R^2}(J^2 - 2\Lambda^2), \tag{3.3a}$$

$$H_{cor} = -\frac{\hbar^2}{2\mu_{AB}R^2}(L_+U_+ + L_-U_-), \tag{3.3b}$$

$$H' = \frac{\hbar^2}{2\mu_{AB}R^2}L^2, \tag{3.3c}$$

where H_{rot} represents the rotational motion of a molecule, H_{cor} is the Coriolis interaction, J is the total angular momentum operator and L is the electronic angular momentum operator. The operators $L_\pm$ and $U_\pm$ are explicitly given as follows:

$$L_\pm = L_\xi \pm iL_\eta, \tag{3.4}$$

$$U_\pm = \mp\frac{\partial}{\partial\Theta} + \frac{i}{\sin\Theta}\frac{\partial}{\partial\Phi} + L_\zeta\cot\Theta, \tag{3.5}$$

where L_ξ, L_η and L_ζ are the components of L in the fixed-molecule coordinate system with the ζ axis along the molecular axis and (Θ, Φ) are the ordinary angle variables to

define the molecular axis orientation in the fixed-space system. The ordinary Born–Oppenheimer adiabatic states are defined by the following conventional eigenvalue problem:

$$H_{el}\Psi^{el}(\mathbf{r}:R|\Lambda)=E(R:\Lambda)\Psi^{el}(\mathbf{r}:R|\Lambda). \tag{3.6}$$

Non-adiabatic transitions between these states of the same electronic symmetry (the same Λ) are induced by the first term of equation (3.2), that is by the coupling

$$T_{rad}=\left\langle \Psi_1^{el}(\mathbf{r}:R|\Lambda)\left|\frac{\partial}{\partial R}\Psi_2^{el}(\mathbf{r}:R|\Lambda)\right.\right\rangle. \tag{3.7}$$

The other operators have no off-diagonal element in the manifold of the same $|\Lambda|$. H' also couples the states with the same Λ, but its contribution is small and is usually neglected. The coupling (3.7) is called 'non-adiabatic radial coupling' and causes the non-adiabatic transition to be very much localized at the avoided crossing point between $E_1(R:\Lambda)$ and $E_2(R:\Lambda)$. This spatial localization can be seen as follows. If we use the Hellmann–Feynman theorem, we obtain

$$T_{rad}=\langle\Psi_1^{el}|\frac{\partial H_{el}}{\partial R}|\Psi_2^{el}\rangle\Big/[E_1(R:\Lambda)-E(R:\Lambda)]^2. \tag{3.8}$$

This simply tells us that the coupling has a strong peak at the avoided crossing point where the adiabatic energy difference $|E_1(R:\Lambda)-E_2(R:\Lambda)|$ becomes a minimum. From the energetics point of view also, the avoided crossing point is the position for the transition to occur most dominantly. The transitions between the adiabatic states of different electronic symmetries (different $|\Lambda|$) are, on the other hand, induced by the Coriolis coupling H_{cor} and have quite different porperties. In order to derive the explicit expression for the corresponding coupling matrix element, let us introduce the electronic–rotational basis functions defined as (Nakamura 1984a, Mies 1980)

$$\Phi_{\pm}^J(\Lambda)=\frac{1}{\sqrt{2}}[\Psi^{el}(\mathbf{r}:R|\Lambda^+)\pm\Psi^{el}(\mathbf{r}:R|\Lambda^-)]Y(\hat{R}:J\Lambda),\quad \text{for } \Lambda\neq 0, \tag{3.9}$$

$$\Phi_{\pm}^J(\Sigma)=\Psi^{el}(\mathbf{r}:R|\Sigma^{\pm})Y(\hat{R}:J\Sigma),\quad \text{for } \Lambda=0, \tag{3.10}$$

where $Y(\hat{R}:J\Lambda)$ is the eigenfunction of H_{rot}:

$$H_{rot}Y(\hat{R}:J\Lambda)=[J(J+1)-2\Lambda^2]Y(\hat{R}:J\Lambda). \tag{3.11}$$

There is no coupling between the two sets $\{\Phi_+^J(\Lambda)\}$ and $\{\Phi_-^J(\Lambda)\}$. The Coriolis (or non-adiabatic rotational) coupling matrix element within each set is explicitly given by

$$\begin{aligned}T_{rot}&=\langle\Phi_{\pm}^J(\Lambda_1)|H_{cor}|\Phi_{\pm}^J(\Lambda_2)\rangle\\&=-\frac{\hbar^2}{2\mu_{AB}R^2}[\lambda_-(J,\Lambda_2^+)\delta(\Lambda_1^+,\Lambda_2^+-1)\\&\quad\times\langle\Psi^{el}(\Lambda_1^+)|L_-|\Psi^{el}(\Lambda_2^+)\rangle+\lambda_+(J,\Lambda_2^+)\delta(\Lambda_1^+,\Lambda_2^++1)\\&\quad\times\langle\Psi^{el}(\Lambda_1^+)|L_+|\Psi^{el}(\Lambda_2^+)\rangle],\end{aligned} \tag{3.12}$$

where

$$\lambda_{\pm}(J,\Lambda)=[(J+\Lambda)(J\pm\Lambda+1)]^{1/2}. \tag{3.13}$$

The transitions induced by this coupling are generally not very strong compared with the transitions induced by T_{rad}. However, this coupling plays an important role in various processes, since this couples the states of different symmetries which cannot be coupled by T_{rad}. For instance, this is known to play a decisive role in some ion–atom collision proccesses (Wille and Hippler 1986). In spectroscopic problems, this coupling is called 'heterogeneous perturbation' in contrast with the homogeneous perturbation for the radial coupling case (Herzberg 1950). As can be easily conjectured from equations (3.8) and (3.12), the two kinds of non-adiabatic transition have quite different properties from each other. Since the electronic matrix elements $\langle \Psi^{el}(\Lambda_1)|L_{\pm}|\Psi^{el}(\Lambda_2)\rangle$ in equation (3.12) are generally moderately varying functions of R, the Coriolis coupling T_{rot} has a strong peak at the closest approach (turning point). On the other hand, the corresponding adiabatic potential energy curves can have a real crossing because of the symmetry difference. This means that in contrast with the radially induced non-adiabatic transition the rotationally induced transition cannot be spatially localized, because the crossing point is most favourable from the energetics point of view, while the turning point is most important as far as the coupling strength is concerned.

In the purely quantum-mechanical treatment the total wavefunction $\Psi(\mathbf{r}, \mathbf{R})$ which is a solution of the Schrödinger equation

$$H\Psi_{\pm} = E\Psi_{\pm} \tag{3.14}$$

is usually expanded in terms of $\Phi^J_{\pm}(\mathbf{r}, \hat{R}: R|\Lambda)$ as

$$\Psi_{\pm} = \sum_j \sum_{m\Lambda} \Phi^J_{\pm}(\mathbf{r}, \hat{R}: R|m\Lambda) F^J_{m\Lambda}(R), \tag{3.15}$$

where m distinguishes between the states of the same electronic symmetry Λ, and $F^J_{m\Lambda}(R)$ represents the relative translational motion in the state $(m\Lambda)$. Insertion of equation (3.15) into equation (3.14) leads to the conventional close-coupling equations for $F^J_{m\Lambda}(R)$, in which both T_{rad} and T_{rot} play essential roles in coupling the various states.

Actual numerical calculation is carried out either by direct solution of the above-mentioned coupled equations in the adiabatic state representation or by introducing some kind of adiabatic-to-diabatic transformation (Baer 1985). In eaither case, however, we need information on T_{rad} and T_{rot}. In spite of the recent progress of the quantum-chemical computational technique, however, such information on T_{rad} and T_{rot} is still very scarce, unfortunately. Here, we explain a quite different approach, that is the semiclassical analytical theory for a non-adiabatic transition. This is discussed in the following sections.

3.3. *Semiclassical theory for radially induced non-adiabatic transitions*

Curve-crossing problems have a long history, and the Landau–Zener transition probability for one passage of the crossing point is well known. This is given by

$$p^{(0)}_{LZ} = \exp(-2\delta^{(0)}_{LZ}) = \exp\left(-2\frac{\pi V^2}{\hbar v_X \Delta F}\right), \tag{3.16}$$

where V is the coupling strength between the two diabatic (crossing) states $V_1(R)$ and $V_2(R)$, ΔF is the difference between the slopes of the diabatic potential curves and v_X is the velocity of the relative motion at the crossing point R_X. For the overall scattering

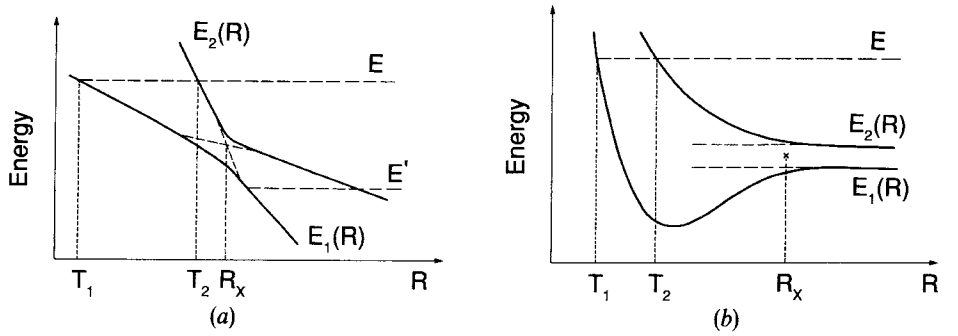

Figure 5. Two typical curve-crossing schemes: (*a*) Landau–Zener type where E' represents the case when the avoided crossing point is located in the classically inaccessible region; (*b*) Rosen–Zener type.

process which involves the two passages of the crossing point (once on the way in and once on the way out), the total transition probability is given by

$$\mathscr{P}_{LZ}^{(0)} = 2p_{LZ}^{(0)}(1 - p_{LZ}^{(0)}). \tag{3.17}$$

Equation (3.16) is very useful especially for understanding the qualitative nature of a non-adiabatic transition. However, we should be careful, because this is not quantitatively accurate. For instance, this cannot be used in the case when the crossing point is located in the classically forbidden region (the case of $E = E'$ in figure 5 (*a*)). The following are assumed in the derivation of equation (3.16).

(1) Diabatic potentials are assumed to be linear.
(2) Diabatic coupling V is constant.
(3) Relative translational motion is assumed to be a straight line with constant velocity v_X.

After the pioneering work by Landau (1932), Zener (1932) and Stückelberg (1932), many studies have been carried out by many workers, and we have now quite a sophisticated formula for the radially induced non-adiabatic transition (Barany 1979, Crothers 1981, Nakamura 1986, 1988).

In addition to the above-mentioned so-called Landau–Zener-type non-adiabatic transition, there is another important kind of non-crossing non-adiabatic radially induced transition, namely the Rosen–Zener (1932) (or Demkov (1964)) type, in which the diabatic potential curves $V_1(R)$ and $V_2(R)$ are parallel ($V_2 - V_1 = \text{constant} = \Delta$) and the diabatic coupling V has a strong exponential dependence on R ($V = A\exp(-\alpha R)$) (see figure 5 (*b*)). Although the corresponding adiabatic potentials have no conspicuous avoided crossing, the transition occurs quite locally at R_X where the two adiabatic curves start to diverge. Exact definition of R_X is given below. The original formula for the overall transition probability $\mathscr{P}_{RZ}$ is given by

$$\mathscr{P}_{RZ}^{(0)} = 4p_{RZ}^{(0)}(1 - p_{RZ}^{(0)}) \sin^2\left(\frac{2A}{\pi\alpha v_X}\right)$$

$$= \operatorname{sech}^2\left(\frac{\pi\Delta}{2\hbar\alpha v_X}\right) \sin^2\left(\frac{2A}{\pi\alpha v_X}\right), \tag{3.18}$$

where

$$p_{RZ}^{(0)}=\left[1+\exp\left(\frac{\pi\Delta}{\hbar\alpha v_X}\right)\right]^{-1}. \tag{3.19}$$

In the limit $\Delta\to 0$ the formula coincides with that for the exact resonant case (Mott and Massey 1965). It should be noted that both $p_{LZ}^{(0)}$ and $p_{RZ}^{(0)}$ go to zero (no non-adiabatic transition) in the low-velocity limit ($v_X\to 0$) but, in the high-velocity limit ($v_X\to\infty$), $p_{LZ}^{(0)}\to 1$ while $p_{RZ}^{(0)}\to\frac{1}{2}$. In the limit $\Delta\to 0$, $p_{RZ}^{(0)}$ also goes to $\frac{1}{2}$. A quite sophisticated formula for the Rosen–Zener-type transition is also now available (Crothers 1976, Nakamura 1986, 1988).

In the following, we present the best semiclassical formulae for both the Landau–Zener- and the Rosen–Zener-type non-adiabatic transitions. Derivation of these formulae is given in Appendix A, being based on the comparison equation method (Miller and Good 1953) and the spirit of the path-integral formulation (Miller and George 1972, Miller 1974). In the case of the Landau–Zener-type two-state full collision process depicted in figure 5(*a*), the 2×2 scattering matrix is given by equation (2.1). Each matrix in this expression is explicitly given as follows (Nakamura 1982, 1984a, b, 1987, 1988):

$$[P_{\infty X}^{+}]_{nm}=[P_{X\infty}^{-}]_{nm}$$

$$=\delta_{nm}\exp\left(\mathrm{i}\int_{R_X}^{\infty}[k_n(R)-k_n(\infty)]\,\mathrm{d}R-\mathrm{i}k_n(\infty)R_X\right), \tag{3.20}$$

$$[P_{XTX}]_{nm}=\delta_{nm}\exp\left(2\mathrm{i}\int_{T_n}^{R_X}k_n(R)\,\mathrm{d}R+\mathrm{i}\frac{\pi}{2}\right), \tag{3.21}$$

$$\mathbf{O}_X=\begin{pmatrix}(1-p_{LZ})^{1/2}\exp(\mathrm{i}\phi_S) & -p_{LZ}^{1/2}\exp(-\mathrm{i}\sigma_0)\\ p_{LZ}^{1/2}\exp(\mathrm{i}\sigma_0) & (1-p_{LZ})^{1/2}\exp(-\mathrm{i}\phi_S)\end{pmatrix}, \tag{3.22}$$

$$\mathbf{I}_X=\tilde{\mathbf{O}}_X \qquad \text{(transposed)}, \tag{3.23}$$

where

$$p_{LZ}=\exp(-2\delta), \tag{3.24}$$

$$\sigma_0+\mathrm{i}\delta=\int_{R_X}^{R_*}[k_1(R)-k_2(R)]\,\mathrm{d}R, \tag{3.25}$$

$$\phi_S=\frac{\delta}{\pi}\ln\left(\frac{\delta}{\pi}\right)-\frac{\delta}{\pi}+\frac{\pi}{4}-\arg\left[\Gamma\left(1+\frac{\mathrm{i}\delta}{\pi}\right)\right], \tag{3.26}$$

$$E_1(R_*)=E_2(R_*), \tag{3.27}$$

$$R_X=R_c(R_*), \tag{3.28}$$

$$k_n(R)=\left(\frac{2\mu}{\hbar^2}[E-E_n(R)]\right)^{1/2}. \tag{3.29}$$

As was explained before, the matrices $\mathbf{P}_{A\ldots B}$ represent the wave propagation from B to A without any transition along the adiabatic potential curves. The matrices $(I_X)_{nm}$ and $(O_X)_{nm}$ give the non-adiabatic transition amplitudes for the m-to-n transition in the

incoming and outgoing segments respectively. R_* is a complex intersection point of the two adiabatic potentials $E_1(R)$ and $E_2(R)$ in the upper half of the complex R plane. The scattering matrix element and the overall probability for the transition $1 \leftrightarrow 2$ are given by

$$S_{21}^{LZ} = S_{12}^{LZ} = 2i[p_{LZ}(1-p_{LZ})]^{1/2} \sin(\sigma + \phi_S) \times \exp\left(i \int_{T_1}^{\infty} [k_1(R) - k_1(\infty)]\, dR - ik_1(\infty)T_1 + i \int_{T_2}^{\infty} [k_2(R) - k_2(\infty)]\, dR - ik_2(\infty)T_2 \right), \tag{3.30}$$

$$\mathscr{P}_{LZ} = |S_{21}^{LZ}|^2 = 4p_{LZ}(1-p_{LZ}) \sin^2(\sigma + \phi_S), \tag{3.31}$$

where

$$\sigma = \sigma_0 + \int_{T_1}^{R_X} k_1(R)\, dR - \int_{T_2}^{R_X} k_2(R)\, dR. \tag{3.32}$$

Equations (3.24) and (3.31) replace equations (3.16) and (3.17) respectively. It should be noted that the integration of equation (3.25) is a complex integral in the complex R plane, and p_{LZ} looks completely different from $p_{LZ}^{(0)}$. However, it can be shown that p_{LZ} reduces to $p_{LZ}^{(0)}$, when the adiabatic potentials are obtained by diagonalizing the diabatic Hamiltonian matrix and all the assumptions mentioned before are satisfied. The phase terms appearing in equations (3.30) and (3.31) are completely missing in equation (3.17). The work of Stückelberg (1932) is in this sense more elaborate than those of Landau and of Zener and gives a sine term as in equation (3.31). The phase ϕ_S is due to the non-adiabatic transition and is called the Stokes phase correction. When the total phase $\sigma + \phi_S$ is large and the random phase approximation can be applied ($\sin^2 \approx \frac{1}{2}$), then equation (3.31) reduces to equation (3.17) when p_{LZ} is replaced by $p_{LZ}^{(0)}$. One interesting point to note in the above-mentioned sophisticated semiclassical theory is that the non-adiabatic radial coupling matrix element T_{rad} defined by equation (3.7) or (3.8) does not appear anywhere in the formula and only the information about the adiabatic potentials $E_n(R)$ is required. Interestingly, T_{rad} is effectively replaced by the complex integration to define δ. As is shown in Appendix A, the adiabatic energy difference $\Delta E(R) \equiv E_2(R) - E_1(R)$ has a complex zero R_* of order $\frac{1}{2}$ and T_{rad} has a pole of order unity there:

$$T_{rad} \approx \frac{i}{4(R - R_*)}. \tag{3.33}$$

This analytical property of $\Delta E(R)$ and T_{rad} in the complex R plane underlies the derivation of the Landau–Zener and Rosen–Zener formulae. The fact that the pre-exponential factor of p_{LZ} is unity originates in this property (Demkov *et al.* 1978).

In the case of the Rosen–Zener-type collision process depicted in figure 5(*b*), the scattering matrix is also given by equation (2.1). The difference from the Landau–Zener case appears in the matrices $\mathbf{O}_X$ and $\mathbf{I}_X (= \tilde{\mathbf{O}}_X)$ as follows:

$$\mathbf{O}_X = \begin{pmatrix} (1-p_{RZ})^{1/2} & -p_{RZ}^{1/2} \exp(-i\sigma_0) \\ p_{RZ}^{1/2} \exp(i\sigma_0) & (1-p_{RZ})^{1/2} \end{pmatrix}, \tag{3.34}$$

$$p_{RZ} = [1 + \exp(2\delta)]^{-1}. \tag{3.35}$$

It should be noted that σ_0 and δ are the same as defined by equation (3.25), that R_* is the complex zero closest to the real axis in the upper half of the complex R plane and that the Stokes phase correction ϕ_S does not appear. The scattering matrix element and the overall probability for the transition $1 \leftrightarrow 2$ are given by

$$S_{21}^{RZ} = S_{12}^{RZ} = 2i[p_{RZ}(1-p_{RZ})]^{1/2} \sin\sigma \times \exp\left(i \int_{T_1}^{\infty} [k_1(R) - k_1(\infty)]\, dR - ik_1(\infty)T_1 + i \int_{T_2}^{\infty} [k_2(R) - k_2(\infty)]\, dR - ik_2(\infty)T_2 \right), \tag{3.36}$$

$$\mathscr{P}_{RZ} = |S_{21}^{RZ}|^2 = 4p_{RZ}(1-p_{RZ}) \sin^2\sigma = \operatorname{sech}^2\delta \sin^2\sigma. \tag{3.37}$$

When the diabatic potentials satisfy the conditions of the original Rosen–Zener model ($V_2 - V_1 = \text{constant} = \Delta$ and $V = A \exp(-\alpha R)$), it can be directly shown that δ defined by equation (3.25) reduces to $\pi\Delta/2\hbar\alpha v_X$ (see equation (3.18)). The analytical property of ΔE and T_{rad} is the same as that of the Landau–Zener case. The difference between the Landau–Zener and Rosen–Zener formulae comes from the different asymptotic expressions of the Weber function used in the comparison equation method (see Appendix A).

It should be noted that the formulae presented here are valid for the case when the turning points are smaller than the avoided crossing point, namely the case when the avoided crossing point is located in a classically accessible region of R. When the turning point becomes larger than the avoided crossing point (the case $E = E'$ in figure 5(*a*)), the phase integral between the two points is pure imaginary and a certain modification of the above formulae becomes necessary (Suzuki *et al.* 1984). For instance, when both T_1 and T_2 are larger than R_X, the exponent parameter δ should be modified as follows:

$$\delta = \operatorname{Im}\left(\int_{R_X}^{R_*} [k_1(R) - k_2(R)]\, dR \right) + \int_{R_X}^{T_2} |k_2(R)|\, dR - \int_{R_X}^{T_1} |k_1(R)|\, dR. \tag{3.38}$$

3.4. *Unified semiclassical theory*

As was mentioned before, the Coriolis coupling problem has quite a different property from the radial-coupling problem. As a naive extension, the *original* Landau–Zener formula may be considered to be applicable directly to a rotational-coupling problem, in which the Coriolis coupling plays a role of a diabatic coupling potential and the adiabatic potentials are taken to be the diabatic potential energies. This idea does not work well, however, because the Coriolis coupling has quite a strong R dependence (Russek 1971). Also, the Landau–Zener formula is not applicable to the case of the σ–π degeneracy at the united atom limit $R = 0$ (Wille and Hippler 1986), since the Coriolis coupling has a pole of second order at the crossing point $R = 0$.

A good analytical theory to deal with the rotationally induced non-adiabatic transitions is thus required. A unified treatment of the two kinds of non-adiabatic transition (radially induced and rotationally induced) would be more desirable. Furthermore, in order for such a theory for two-state problem to be extendable to a

multilevel curve crossing problem, a transition (either radially induced or rotationally induced) should be made to occur spatially locally at a certain internuclear distance. Here, we introduce the dynamical-state (DS) representation which meets all the requirements mentioned above (Crothers 1971, Nakamura and Namiki 1980, 1981, Nakamura 1982, 1984a, b, 1986, 1988).

The DSs are defined as the eigenstates of the Hamiltonian (see equation (3.2))

$$H_{\rm dyn} \equiv H_{\rm el} + H_{\rm rot} + H_{\rm cor} + H' \tag{3.39}$$

as

$$H_{\rm dyn} \Psi_n^J(\mathbf{r}, \hat{R}: R) = E_n^J(R) \Psi_n^J(\mathbf{r}, \hat{R}: R). \tag{3.40}$$

As is clear from this definition, the DSs are the eigenstates of the rotating collision complex at a fixed size of the complex and thus are dependent on the total angular momentum J. In other words, the states are completely diagonal with respect to nuclear and electronic rotations. The wavefunction $\Psi^J(\mathbf{r}, \hat{R}: R)$ can be expanded in terms of the electronic–rotational basis functions defined by equations (3.9) and (3.10), namely the eigenvalues $E^J(R)$ are obtained by diagonalizing a matrix of $H_{\rm dyn}$ spanned by the electronic–rotational basis functions. Since the dynamical states are the eigenstates of $H_{\rm dyn}$, transitions between them are exclusively induced by the first term of equation (3.2), that is all transitions are reduced to the radially induced ones irrespective of the type of original coupling in the adiabatic-state representation.

In order to show more explicitly the nature of this new (DS) representation, let us consider the simplest two-state case composed of one Π state and one Σ state:

$$\Psi^J = C_\Sigma^J \Phi^J(\Sigma) + C_\Pi^J \Phi_+^J(\Pi). \tag{3.41}$$

The conventional diagonalization of a 2×2 matrix leads to

$$E_{1,2}^J(R) = \tfrac{1}{2}\{E_J(R:\Pi) + E_J(R:\Sigma) \pm [(\Delta E(R))^2 + 4V_J^2(R)]^{1/2}\}, \tag{3.42}$$

where

$$V_J(R) = \frac{\hbar^2}{2\mu_{\rm AB}R^2} \lambda_+(J, \Sigma) V_0, \tag{3.43}$$

$$\Delta E(R) = E_J(R:\Pi) - E_J(R:\Sigma), \tag{3.44}$$

$$E_J(R:\Lambda) = E(R:\Lambda) + \frac{\hbar^2}{2\mu_{\rm AB}R^2}[J(J+1) - 2\Lambda^2] + \frac{\hbar^2}{2\mu_{\rm AB}R^2}\langle L^2 \rangle_\Lambda, \tag{3.45}$$

$$V_0 = \langle \Psi^{\rm el}(\Sigma) | L_- | \Psi^{\rm el}(\Pi^+) \rangle. \tag{3.46}$$

The radial coupling between Ψ_1^J and Ψ_2^J is given by

$$\left\langle \Psi_1^J \middle| \frac{\partial \Psi_2^J}{\partial R} \right\rangle = C_\Sigma^J \frac{{\rm d}C_\Pi^J}{{\rm d}R} + \frac{{\rm d}C_\Sigma^J}{{\rm d}R} C_\Pi^J$$

$$= \left(\frac{{\rm d}(\Delta E)}{{\rm d}R} V_J - \frac{{\rm d}V_J}{{\rm d}R} \Delta E \right) \Big/ [E_1^J(R) - E_2^J(R)]^2. \tag{3.47}$$

It is easily seen that the new states $E_{1,2}^J(R)$ avoid crossing each other and that the analytical properties are the same as those of the ordinary radial coupling case in the adiabatic-state representation, namely the DS energy difference $E_2^J(R) - E_1^J(R)$ has a complex zero of order $\frac{1}{2}$ and the radial coupling (equation (3.47)) between them has a

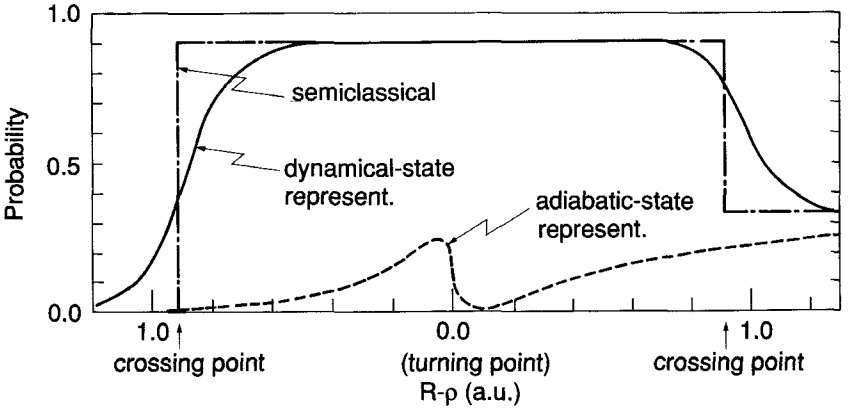

Figure 6. The localization of the rotationally induced transition in the DS representation. The model potential is given by equation (3.48) (Nakamura and Namiki 1981). The collision velocity v is 0·5 atomic units and the impact parameter ρ is 0·6 atomic units.

pole of order unity there. This is true even for the case of the σ–π degeneracy at $R=0$. Thus the analytical theory described in the previous section can be applied to the rotational-coupling problem. Furthermore, the avoided crossings between the adiabatic states of the same symmetry remain avoided in the DS representation, although they can be deformed by rotational couplings with other states. Thus, once we move into the DS representation, the radial and rotational couplings can be treated in a unified way by the semiclassical theories described in the previous section. Also, all non-adiabatic transitions are localized at the new avoided crossing points. Localization of rotationally induced transition in the DS representation is demonstrated in figure 6, where the following model potential is used to simulate the two-state ($1\pi_u$ and $2\sigma_u$) problem in the $Ne^+ + Ne$ collision system:

$$\Delta E(R)=2{\cdot}71\left(\frac{1}{1{\cdot}5}-\frac{1}{R}\right)\text{atomic units,} \tag{3.48}$$

$$V_0=1{\cdot}42\,\text{atomic units.} \tag{3.49}$$

The step function in the figure represents the semiclassical approximation. The asymptotic value on the way out at $R>\mathrm{Re}(R_*)$ equals $\mathscr{P}_{\mathrm{LZ}}$ given by equation (3.31). In the adiabatic-state representation the transition is not localized anywhere. The usefulness of the DS representation has been further demonstrated by Suzuki *et al.* (1984) and Nakamura (1983, 1984 a, b).

The idea of this representation can be summarized and generalized as follows. In general, whatever the coupling which can be defined at fixed R, we employ the representation in which this coupling is diagonalized. Once we move into this new representation, the semiclassical theory presented here can be applied in a unified way irrespective of the nature of the original coupling. The idea can be, in principle, generalized to more complicated systems by employing the hyperspherical coordinate system. The hyper-radius ρ represents the size of the rotating collision complex and plays the same role as R. The total Hamiltonian in the fixed-body frame can be generally expressed as

$$H=-\frac{\hbar^2}{2\mu_N}\frac{1}{\rho^{3N-4}}\frac{\partial}{\partial\rho}(\rho^{3N-4})\frac{\partial}{\partial\rho}+H_{\mathrm{dyn}}, \tag{3.50}$$

$$H_{\rm dyn}=\frac{\hbar^2}{2\mu_N}\frac{\Lambda^2(\Omega)}{\rho^2}+H_{\rm el}, \tag{3.51}$$

where N is the number of particles in the system, $\Lambda(\Omega)$ represents the grand angular momentum operator with respect to the angle variables Ω (the total of the hyperspherical angle variables and the Euler angles). The DSs are defined as the eigenstates of $H_{\rm dyn}$.

3.5. *Multilevel curve-crossing problem*

As is clear from the previous two sections, the two-state curve-crossing problem can be analysed quite accurately by the sophisticated semiclassical theory, irrespective of the kind of coupling that is responsible for the transition and of the kind of problem (scattering, spectroscopic or bound state) concerned. In reality, however, on many occasions we have to deal with multilevel systems.

Demkov and Osherov (1968) showed that in a special level scheme such as that shown in figure 7 the overall transition probabilities can be simply expressed as a product of the non-adiabatic transition probability at each crossing point no matter how close to each other the levels are. In the more realistic cases such as that shown later in figure 9 (*a*), the transition probabilities cannot be so simple and the phase terms should be taken into account. Woolley (1971) showed the importance of the phase terms by considering certain model systems with rather well separated crossing points. Korsch (1983) studied the similar three-state problem using the Magnus approximation.

The general multilevel problem is too difficult (almost impossible) to be formulated fully analytically. It is easily conjectured, however, that the scattering matrix for a multilevel system can be explicitly expressed in the form of a matrix product just like equation (2.1), if the avoided crossing points are well separated from each other. Taking, for instance, the three-state problem shown in figure 8, we can express the scattering matrix as (Nakamura 1982)

$$\mathbf{S}=\mathbf{P}^{+}_{\infty \rm A}\mathbf{O}_{\rm A}\mathbf{P}_{\rm AB}\mathbf{O}_{\rm B}\mathbf{P}_{\rm BTB}\mathbf{I}_{\rm B}\mathbf{P}_{\rm BA}\mathbf{I}_{\rm A}\mathbf{P}^{-}_{\rm A\infty}, \tag{3.52}$$

where A and B represent the outer and inner avoided crossing points respectively. The meanings of the various matrices are basically the same as before, although all of them

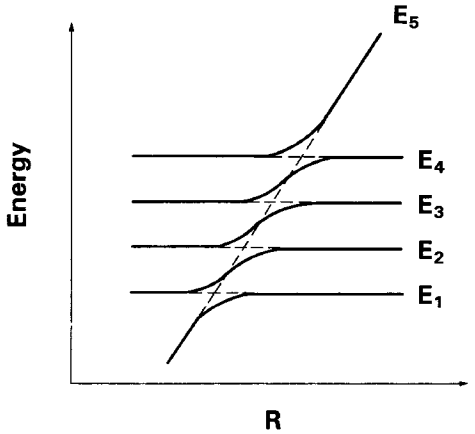

Figure 7. Potential-energy-level scheme studied by Demkov and Osherov (1968).

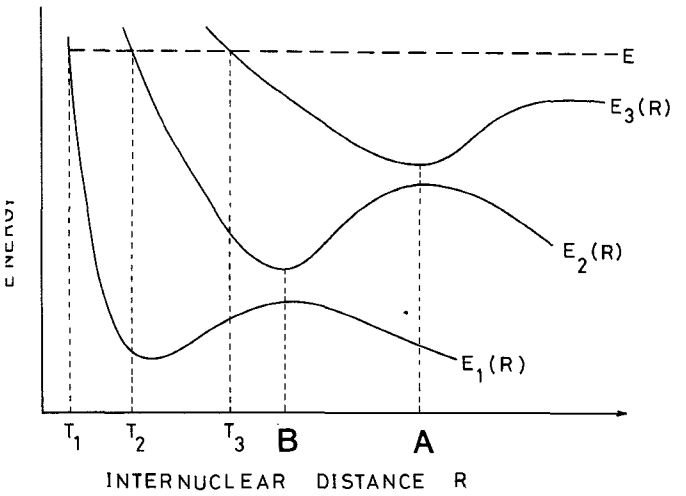

Figure 8. An example of a three-state potential diagram.

are 3×3 matrices in the present case. The matrices **O** and **I** have the non-zero 2×2 submatrices defined by equations (3.22) and (3.23). For instance, $\mathbf{I}_B$ in equation (3.52) is given by

$$\mathbf{I}_B = \begin{bmatrix} (1-p_B)^{1/2}\exp(i\phi_S^B) & p_B^{1/2}\exp(i\sigma_0^B) & 0 \\ -p_B^{1/2}\exp(-i\sigma_0^B) & (1-p_B)^{1/2}\exp(-i\phi_S^B) & 0 \\ 0 & 0 & 1 \end{bmatrix}. \tag{3.53}$$

This simple generalization of the two-state semiclassical theory has been applied to the model three- and four-state systems, and even to the cases in which the avoided crossings cannot be regarded as isolated from each other. Although it is not easy to formulate a quantitative criterion for the validity of the approximation, the numerical studies indicate that the applicability may be surprisingly wider than usually anticipated (Nakamura 1987). Here, we report the results of the four-state case. The model potential system employed is shown in figure 9. The diabatic potentials are (in atomic units)

$$\left.\begin{aligned} V_1(R) &= V_0 \exp\left(\frac{-R}{b}\right), \\ V_2(R) &= V_1(R) + V_{20}, \\ V_3(R) &= d\exp[-a(R-R_e)]\{\exp[-a(R-R_e)]-2\} + V_{30}, \\ V_4(R) &= V_3(R) + V_{40}, \end{aligned}\right\} \tag{3.54}$$

where

$$\left.\begin{aligned} &V_0 = 129{\cdot}62, \qquad V_{20} = 0{\cdot}03\text{–}0{\cdot}01, \\ &V_{30} = 0{\cdot}06, \qquad V_{40} = 0{\cdot}02\text{–}0{\cdot}004, \\ &b = 0{\cdot}5915, \qquad a = 0{\cdot}3, \qquad R_e = 6{\cdot}0, \qquad d = 0{\cdot}16. \end{aligned}\right\} \tag{3.55}$$

The diabatic couplings are taken as follows:

$$V_{13} = V_{14} = V_{23} = V_{24} = 0{\cdot}002. \tag{3.56}$$

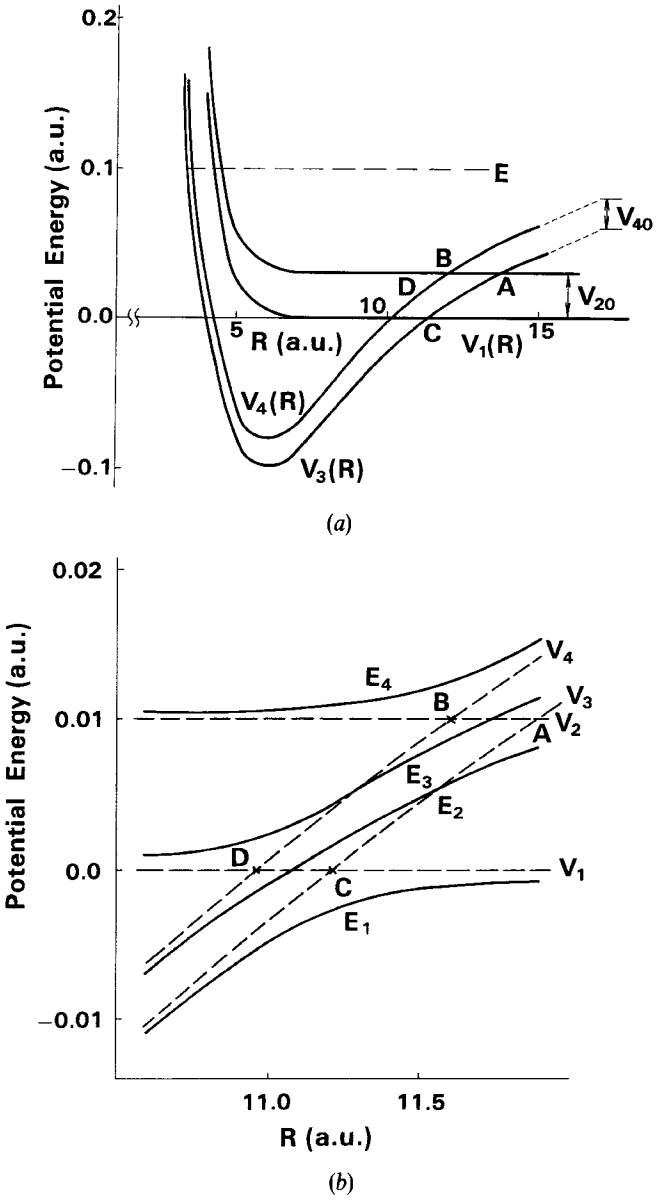

Figure 9. (*a*) The four-state model potential system of equation (3.54) (the case when $V_{20}=0{\cdot}03$ atomic units and $V_{40}=0{\cdot}02$ atomic units). (*b*) Potential curves of the four-state model system with $V_{20}=0{\cdot}01$ atomic units and $V_{40}=0{\cdot}004$ atomic units: (——), adiabatic potential energies; (– – –), diabatic potential energies. Only the vicinity of the crossings is shown (Nakamura 1987).

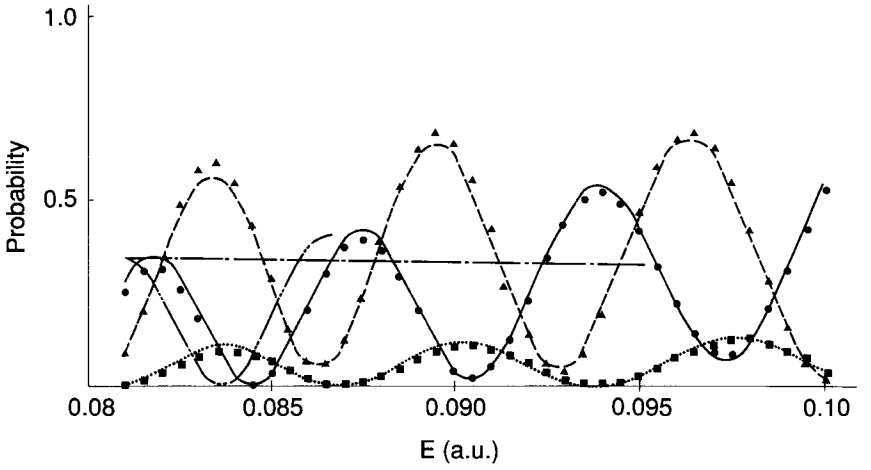

(*a*)

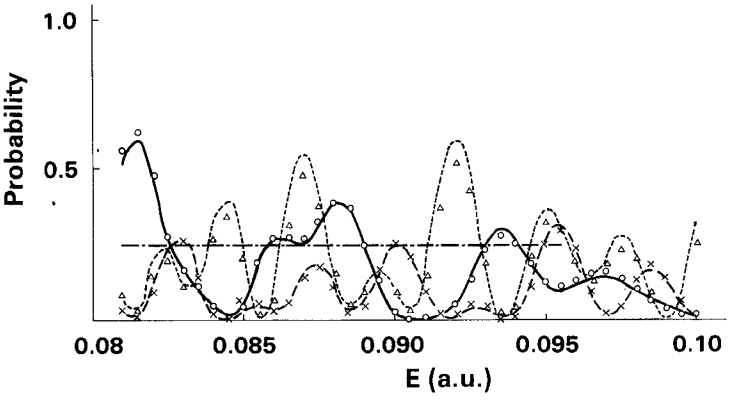

(*b*)

Figure 10. Transition probability P as a function of energy E for the four-state system ($V_{20}=0{\cdot}03$ atomic units and $V_{40}=0{\cdot}004$ atomic units) (Nakamura 1987).

(*a*)

	P_{12}	P_{13}	P_{14}
Semiclassical	——	– – –	·····
Exact	●	▲	■

The dash–dot line is the semiclassical result for P_{12} with phases totally neglected. The dash–two-dot line is that with the Stokes phase ϕ_S neglected.

(*b*)

	P_{23}	P_{34}	P_{24}
Semiclassical	——	-----	– – –
Exact	○	△	×

The dash–dot line is the same as above for P_{23}.

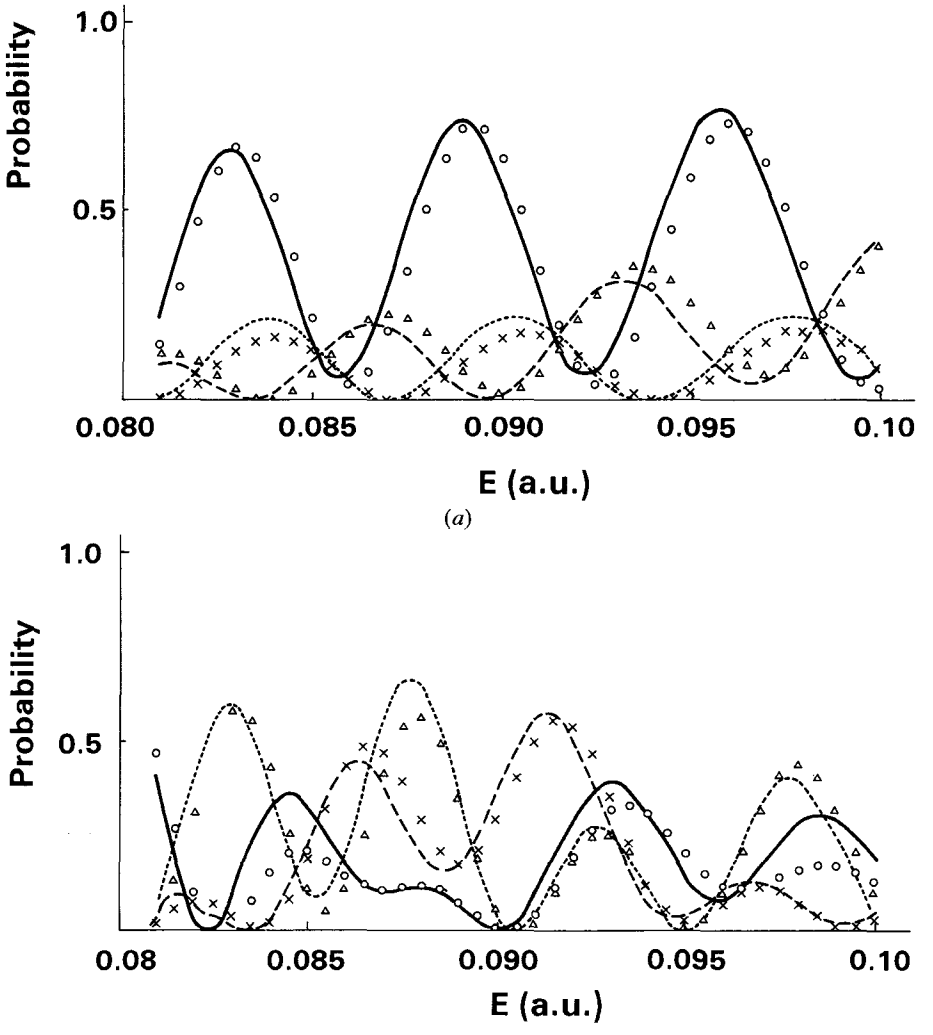

Figure 11. The same as figure 10 for $V_{20}=0{\cdot}01$ atomic units and $V_{40}=0{\cdot}004$ atomic units. (*a*) (○), P_{12}; (△), P_{13}; (×), P_{14}. (*b*) The same as figure 10(*b*).

The level separations are typical orders of vibrational energy spacing. Figure 9(*b*) magnifies the potential curves in the vicinity of the crossings for the case $V_{20}=0{\cdot}01$ and $V_{40}=0{\cdot}004$. The numerical results for the transition probabilities are shown in figures 10 and 11 for the cases $(V_{20}, V_{40})=(0{\cdot}03, 0{\cdot}004)$ and $(V_{20}, V_{40})=(0{\cdot}01, 0{\cdot}004)$ respectively. For simplicity, we have assumed that $\sigma_0 \approx 0$ and $\delta \approx \delta_{LZ}^{(0)}$ estimated from the diabatic potentials. The R_X are also approximated to be the crossing points of the diabatic potentials. The exact numerical solutions are obtained by using the R matrix propagation method of Light and Walker (1976). The agreement between the exact numerical and approximate semiclassical results is surprisingly good. The importance of the phases should be noticed. The chain lines in figure 10 represent the results for P_{12} (figure 10(*a*)) and P_{23} (figure 10(*b*)) with all phases neglected. Without phases no oscillation as a function of E appears. The significance of the Stokes phase ϕ_S can also

be seen from figure 10. The difference between the solid and the dash–two-dots curve in figure 10 (*a*) is the manifestation of the effect of ϕ_S. In the two-state approximation, the non-adiabatic coupling $T_{12}(R)$ can be estimated as follows (see equation (3.47)):

$$T_{12}(R)=\left(\frac{dV_{12}}{dR}\Delta\epsilon_{12}(R)-V_{12}(R)\frac{d[\Delta\epsilon_{12}(R)]}{dR}\right)\Big/[(\Delta\epsilon_{12})^2+4V_{12}^2]$$
$$\approx -\frac{\Delta F}{4V_{12}}\frac{(2V_{12}/\Delta F)^2}{(R-R_X)^2+(2V_{12}/\Delta F)^2}, \tag{3.57}$$

where $\Delta\epsilon_{12}=V_1(R)-V_2(R)\approx\Delta F(R-R_X)$ and V_{12} is assumed to be constant in the second equation. The coupling $T_{12}(R)$ takes half of the maximum value at $R=R_X\pm 2V_{12}/\Delta F$. In the present case where $V_{20}=0{\cdot}01$ and $V_{40}=0{\cdot}004$ (figure 9 (*b*)), $2V_{12}/\Delta F\approx 0{\cdot}3$, while $|R_X^A-R_X^B|\approx 0{\cdot}28$. This means that both couplings overlap substantially on the real R axis. In spite of this substantial overlap, the semiclassical treatment based on the two-state theory works very well. This is probably because the fundamental analytical properties of adiabatic coupling in the complex R plane are correctly taken into account in the basic two-state theory. When the potentials satisfy well the assumptions of the original Landau–Zener model as is the case studied here, we can use the replacements $\sigma_0\approx 0$ and $\delta_{LZ}\approx\delta_{LZ}^{(0)}$ and avoid the complex integration in equation (3.25), which is a great inconvenience of semiclassical theory. The results shown in figures 10 and 11 are very encouraging, but this is just a case study and more extensive work is necessary.

3.6. *Non-adiabatic tunnelling*

Tunnelling through a potential barrier has been the subject of theoretical interest and practical importance in various fields since the early days of quantum mechanics. One-dimensional tunnelling has presented a very good subject for semiclassical theory. The theory is now well developed and has been successful in interpreting various interesting phenomena (Jortner and Pullman 1986). However, the multidimensional theory still remains to be developed, unfortunately (Razavy and Pimpale 1988).

Here, we consider a seemingly similar but actually quite different problem, that is tunnelling through the potential barrier which is created by the interaction with another state (figure 12). The diabatic curves have slopes of different sign, and the coupling between them creates the barrier. In other words, without this diabatic coupling, no transition from the right side to the left side or vice versa can occur. The ordinary tunnelling of the single potential mentioned above corresponds to the strong diabatic coupling limit, in which the upper adiabatic potential curve is located far above and can be forgotten. In general, however, this non-adiabatic tunnelling has quite a different nature from the single-potential tunnelling. This is not necessarily well recognized. In a sense, the non-adiabatic tunnelling process can be controlled by the diabatic coupling. For instance, it can be switched on and off by switching the coupling. This type of transition must present a very important mechanism of state (or phase) change in various fields. Because of the mathematical difficulty, however, a good approximate analytical solution has not yet been obtained, unfortunately. Analysing the several formulae proposed so far, the present author has recently reported the working equations for non-adiabatic tunnelling (Nakamura 1987). In this section these formulae are presented together with the numerical applications.

The first most basic question is the non-adiabatic tunnelling probability. Several studies have been reported so far (Ovchinnikova 1965, Laing *et al.* 1977, Coveney *et al.*

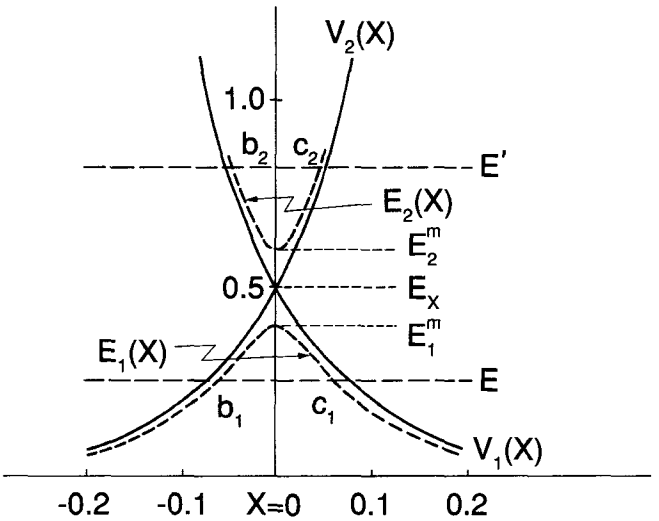

Figure 12. Model potential system for non-adiabatic tunnelling (equation (3.66)) (Nakamura 1987): (– – –) adiabatic potential energies; (——), diabatic potential energies.

1985). Among them the work by Coveney *et al.* (1985) is most elaborate. The formula that they recommend is a kind of renormalization of the perturbation expression obtained by Ovchinnikova (1965) and is given by

$$P_{\mathrm{L}}=\frac{B(\delta)\exp(-2\tau)}{1+B(\delta)\exp(-2\tau)}, \tag{3.58}$$

where

$$B(\delta)=\frac{2\pi}{\Gamma^2(\delta/\pi)}\left(\frac{\delta}{\pi}\right)^{2(\delta/\pi)-1}\exp\left(-\frac{2\delta}{\pi}\right), \tag{3.59}$$

$$\tau=\begin{cases}\displaystyle\int_{b_1}^{c_1}|k_1(R)|\,\mathrm{d}R>0 & (b_1,c_1:\text{real}), \quad \text{for } E\leqslant E_1^m,\\ \displaystyle-\left|\int_{b_1}^{c_1}k_1(R)\,\mathrm{d}R\right|<0 & (b_1,c_1:\text{imaginary}), \quad \text{for } E\geqslant E_1^m,\end{cases} \tag{3.60}$$

δ is defined by (see equation (3.25))

$$\delta=\mathrm{Im}\left(\int_{R_{\mathrm{X}}}^{R_*}[\kappa_2(R)-\kappa_1(R)]\,\mathrm{d}R\right) \tag{3.61}$$

with

$$\kappa_n(R)=\left(\frac{2\mu}{\hbar^2}[E_n(R)-E]\right)^{1/2}, \quad n=1,2. \tag{3.62}$$

If the adiabatic potentials $E_n(R)$ are obtained from the linear diabatic potentials $V_n(R)=F_n(R-R_{\mathrm{X}})$ and the constant diabatic coupling as in the original Landau–Zener model, then δ is reduced to

$$\delta=\frac{\pi V^2}{\hbar\tilde{v}_{\mathrm{X}}\Delta F}, \tag{3.63}$$

where $\Delta F = |F_1 - F_2|$ and $\tilde{v}_X$ is the absolute value of the imaginary velocity at the crossing point. Equation (3.63) has the same form as $\delta_{LZ}^{(0)}$ in equation (3.16). The function $B(\delta)$ is a monotonic function of δ (Child 1974b). The integration limits b_1 and c_1 are the turning points of the lower adiabatic potential (see figure 12). These are real when the energy E is lower than the maximum E_1^m of the lower adiabatic potential and pure imaginary, otherwise. It should be noted that, in the adiabatic limit ($\delta \to \infty$), $B(\delta) \to 1$ and P_L coincides with the single-potential tunnelling probability T (see equation (3.65 *a*)) and that, in the diabatic limit ($\delta \to 0$), $B(\delta) \to 2\delta$ and $P_L \to 2\delta \exp(-2\tau) \to 0$. Equation (3.58) works acceptably well at lower energies $E \lesssim E_2^m$, the minimum of the upper adiabatic potential. In other words, this formula cannot be used at higher energies $E \gtrsim E_2^m$. The formula that we recommend at these higher energies is

$$P_H = \frac{1+\cos(2\phi)}{1+d+\cos(2\phi)} T, \tag{3.64}$$

where

$$T = \frac{\exp(-2\tau)}{1+\exp(-2\tau)}, \tag{3.65 a}$$

$$\phi = -\gamma_2(b_2, c_2) + \phi_S, \tag{3.65 b}$$

$$\gamma_2(b_2, c_2) = \int_{b_2}^{c_2} k_2(R)\,dR, \tag{3.65 c}$$

$$d = \frac{p^2}{2(1-p)}. \tag{3.65 d}$$

The integration limits b_2 and c_2 are the turning points of the upper adiabatic potential and thus $\gamma_2 = 0$ for $E \leqslant E_2^m$. The phase ϕ_S is the Stokes phase defined by equation (3.26) and p is given by equation (3.24). The first factor in equation (3.64) is the same as that obtained by Ovchinnikova (1965), if ϕ_S is neglected. The second factor T represents the probability of tunnelling through the lower adiabatic potential.

The results of numerical applications are shown in figure 13 (Nakamura 1987). The model potential employed here is the following (see figure 12) (in atomic units):

$$V_1(x) = V_{10}\exp(-ax), \qquad V_2(x) = V_{10}\exp(ax), \qquad V_{12}(x) = V_0 \exp\left(-\frac{a}{2}x^2\right), \tag{3.66}$$

where $V_{10} = 0{\cdot}5$, $a = 10$ and $V_0 = 0{\cdot}05$ (weak), $0{\cdot}1$ (intermediate), $0{\cdot}2$ (strong). The reduced mass μ is taken to be 1000. As is seen from figure 13, equation (3.64) with the tunnelling correction works quite well even at $E \lesssim E_2^m$. The broken curves in figure 13 represent the single-potential tunnelling probability T. It should be noted that the definition of δ is not necessarily unique in the energy range $E_1^m \leqslant E \leqslant E_2^m$. Here the following expression was employed:

$$\delta = \frac{2\mu}{\hbar^2} \operatorname{Im}\left(\int_{R_X}^{R_*} \frac{E_2(R) - E_1(R)}{|k_1(R)| + |k_2(R)|}\,dR \right). \tag{3.67}$$

Another different expression was also tried, but no substantial deviation in the final results was found. Thus, as is seen from figure 13, the combination of equation (3.58)

and (3.64) can be regarded as almost usable in the whole energy range, although the approximation becomes slightly worse in the region of the crossing of the two approximate results.

In order to analyse the various problems associated with non-adiabatic tunnelling, knowledge of only the probability such as equation (3.58) and (3.64) is not sufficient. The most comprehensive quantity is the following matrix **A** (the reduced **S** matrix) which connects the waves on both sides of the tunnelling barrier (see figure 15 later) (Nakamura 1987):

$$\begin{bmatrix} V_1' \\ U_1'' \end{bmatrix} = \mathbf{A} \begin{bmatrix} V_1'' \\ U_1' \end{bmatrix}, \tag{3.68}$$

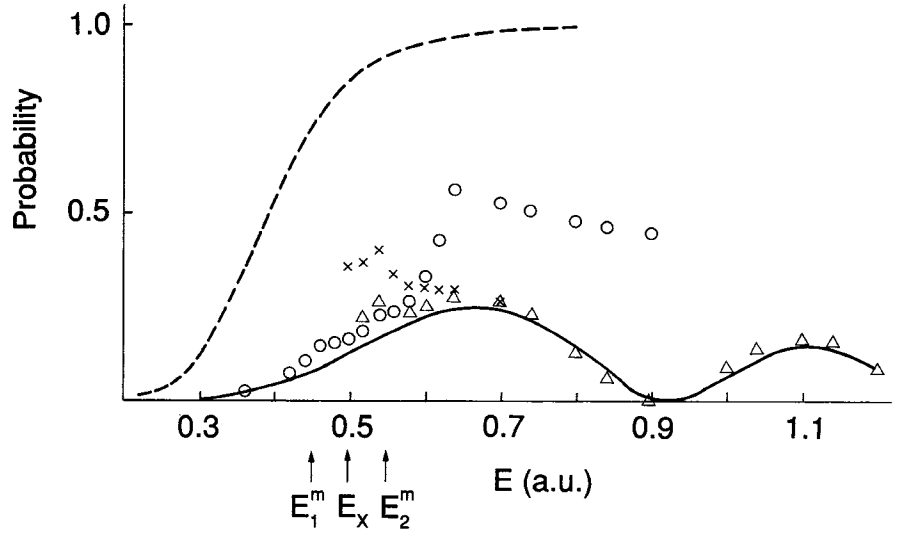

(*a*)

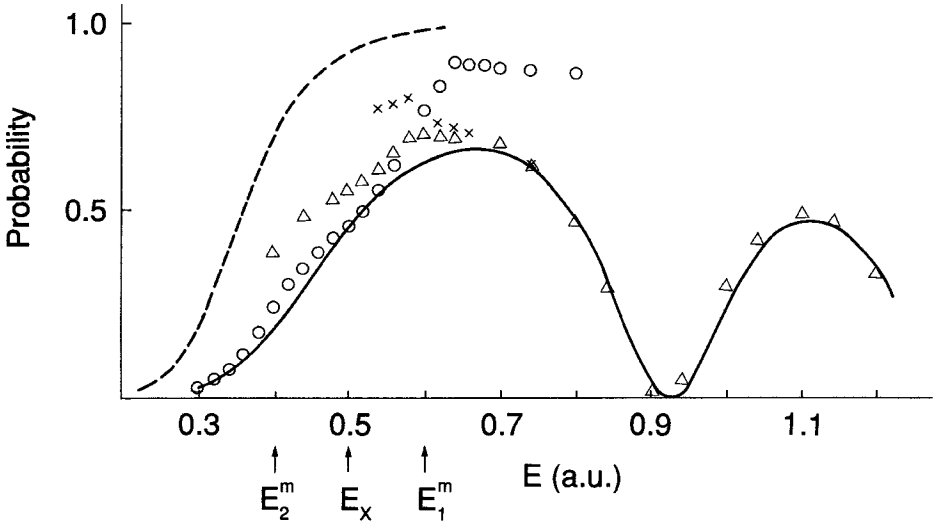

(*b*)

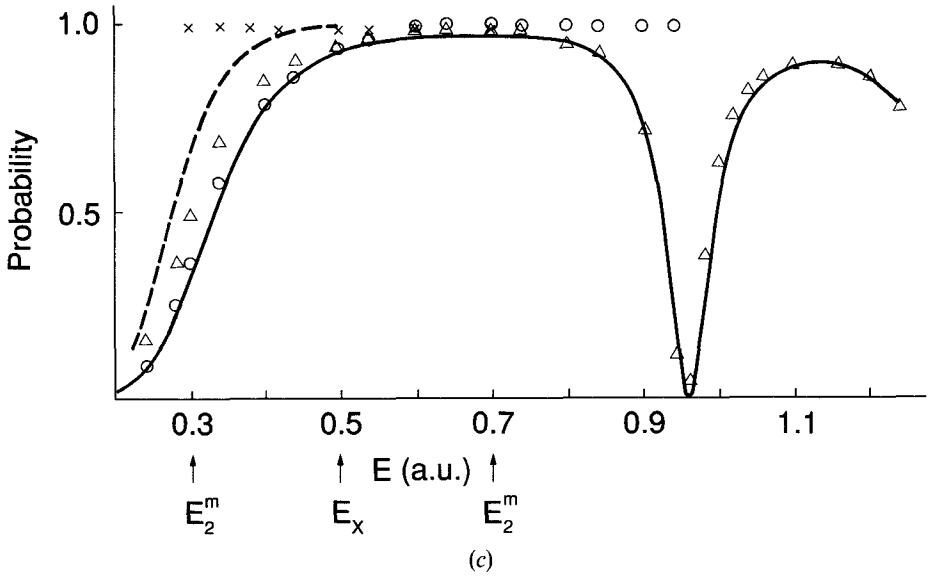

(*c*)

Figure 13. Non-adiabatic tunnelling probability as a function of energy E for (*a*) $V_0 = 0{\cdot}05$ atomic units (weak-coupling case), (*b*) $V_0 = 0{\cdot}1$ atomic units (intermediate-coupling case) and (*c*) $V_0 = 0{\cdot}2$ atomic units (strong-coupling case): ——, exact numerical result; – – –, single-potential tunnelling probability; (○) equation (3.58); (△), equation (3.64); (×), equation (3.64) without tunnelling correction (Nakamura 1987).

where V_1' and V_1'' are the coefficients of the outgoing and incoming waves along the lower adiabatic potential $E_1(R)$ on the right side of the tunnelling region and U_1' and U_1'' those on the left side. The wavefunctions in each region are given by

$$\Psi_{\text{right}} \approx -V_1' \exp\left(\mathrm{i}\int_{c_1}^{R} k_1(R)\,\mathrm{d}R\right) + V_1'' \exp\left(-\mathrm{i}\int_{c_1}^{R} k_1(R)\,\mathrm{d}R\right), \tag{3.69}$$

$$\Psi_{\text{left}} \approx -U_1' \exp\left(\mathrm{i}\int_{b_1}^{R} k_1(R)\,\mathrm{d}R\right) + U_1'' \exp\left(-\mathrm{i}\int_{b_1}^{R} k_1(R)\,\mathrm{d}R\right). \tag{3.70}$$

Let us first consider the low-energy case for which A is denoted as A^{L} below. The non-adiabatic tunnelling probability is given by $|A_{12}^{\mathrm{L}}|^2 = |A_{21}^{\mathrm{L}}|^2 = P_{\mathrm{L}}$. The final expressions for the matrix $\mathbf{A}^{\mathrm{L}}$ are

$$A_{11}^{\mathrm{L}} = A_{22}^{\mathrm{L}} = (1 - P_{\mathrm{L}})^{1/2} \exp(\tfrac{1}{2}\pi\mathrm{i}), \tag{3.71 a}$$

$$A_{12}^{\mathrm{L}} = A_{21}^{\mathrm{L}} = P_{\mathrm{L}}^{1/2} \exp(-\tfrac{1}{2}\pi\mathrm{i}). \tag{3.71 b}$$

The phase factors are determined from the following conditions.

(1) There should be unitarity and symmetry of the matrix **A**.
(2) $A_{11}^{\mathrm{L}} = A_{22}^{\mathrm{L}}$.
(3) The scattering phase shift in the case of the potential system such as that shown in figure 14 should coincide with the corresponding proper one in the diabatic (no tunnelling) limit ($\eta_1^{(0)}(c_1) + \pi/4$) and the adiabatic ($\delta \to \infty$) limit (equation (3.72)) below with P_{L} replaced by T).

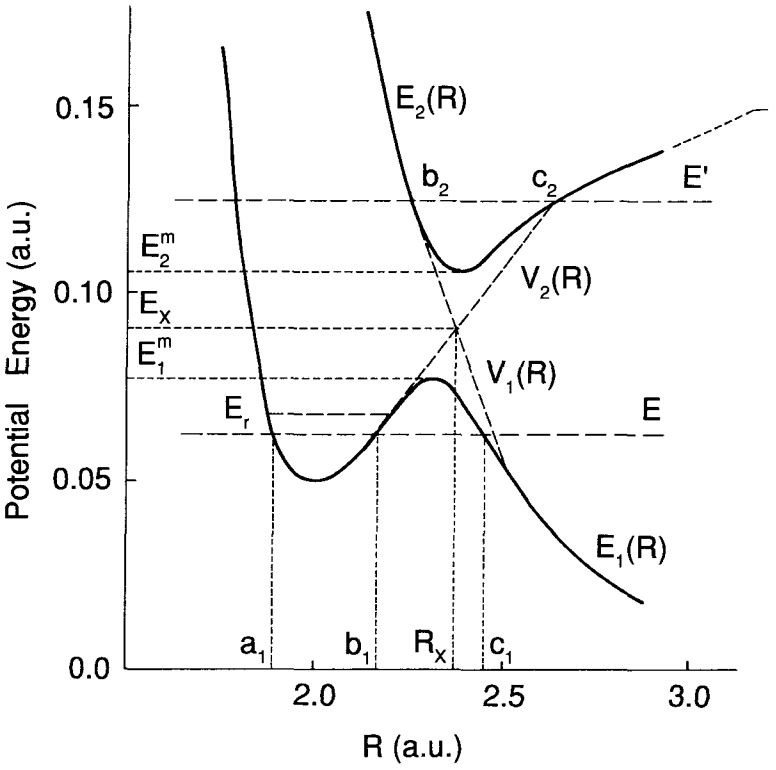

Figure 14. Two-state curve crossing system for elastic scattering accompanied by non-adiabatic tunnelling. E_r represents a resonance position.

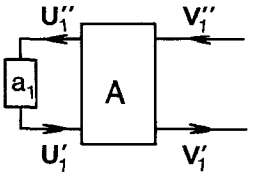

Figure 15. Diagram for the energy $E \leqslant E_1^m$.

The scattering phase shift η in the case of energy E in figure 14, whose corresponding diagram is shown in figure 15, is given as follows:

$$\eta_L = \eta_1^{(0)}(c_1) + \frac{\pi}{4} + \tan^{-1}\left(\frac{1-(1-P_L)^{1/2}}{1+(1-P_L)^{1/2}} \tan\left[\gamma_1(a_1, b_1)\right]\right), \tag{3.72}$$

where

$$\gamma_1(a_1, b_1) = \int_{a_1}^{b_1} k_1(R)\,\mathrm{d}R, \tag{3.73}$$

$$\eta_1^{(0)}(c_1) = \int_{c_1}^{\infty} [k_1(R) - k_1(\infty)]\,\mathrm{d}R - k_1(\infty)c_1. \tag{3.74}$$

The position E_r and width Γ of a resonance, if any, are roughly given by

$$E = E_r \leftrightarrow \gamma_1(a_1, b_1) = (n + \tfrac{1}{2})\pi, \quad n = 0, 1, 2, \ldots, \tag{3.75}$$

$$\Gamma \approx 2\frac{1-(1-P_L)^{1/2}}{1+(1-P_L)^{1/2}}\left(\frac{d\gamma_1(a_1, b_1)}{dE}\right)^{-1}_{E_r}. \tag{3.76}$$

Let us next consider the higher-energy case E' in figure 14. The corresponding diagram is shown in figure 16. By using the diagrammatic technique explained before, we can obtain the following expressions for the reduced **S** matrix (denoted as $\tilde{\mathbf{A}}^H$) corresponding to the first term in equation (3.64):

$$\tilde{A}^H_{11} = ip[1+(1-p)\exp(-2i\phi)]^{-1}\exp[2i\gamma_2(b_2, R_X) - 2i\sigma_0], \tag{3.77a}$$

$$\tilde{A}^H_{22} = ip[1+(1-p)\exp(-2i\phi)]^{-1}\exp[2i\gamma_2(R_X, c_2) + 2i\sigma_0], \tag{3.77b}$$

$$\tilde{A}^H_{12} = \tilde{A}^H_{21} = 2(1-p)^{1/2}[1+(1-p)\exp(-2i\phi)]^{-1}\cos\phi\exp[i\gamma_2(b_2, c_2)]. \tag{3.77c}$$

The first factor in equation (3.64) is equal to $|\tilde{A}^H_{12}|^2$. The derivation of equations (3.77) is given in Appendix B. Taking into account the tunnelling correction, we have proposed the following final expressions for the reduced **S** matrix:

$$A^H_{11} = -i(1-P_H)^{1/2}\exp[2i\gamma_2(b_2, R_X) - 2i\sigma_0 - i\tilde{\varphi}], \tag{3.78a}$$

$$A^H_{22} = -i(1-P_H)^{1/2}\exp[2i\gamma_2(R_X, c_2) + 2i\sigma_0 - i\tilde{\varphi}], \tag{3.78b}$$

$$A^H_{12} = A^H_{21} = \tilde{A}^H_{12}T^{1/2} = P_H^{1/2}\exp[i\gamma_2(b_2, c_2) - i\tilde{\varphi}], \tag{3.78c}$$

where

$$\tilde{\varphi} = -\tan^{-1}\left(\frac{(1-p)\sin(2\phi)}{1+(1-p)\cos(2\phi)}\right). \tag{3.79}$$

It can easily be shown that the matrix $\mathbf{A}^H$ is unitary and symmetric. The scattering phase shift is given by

$$\eta_H = \eta_1^{(0)}(R_X) + \frac{\pi}{4} + \gamma_2(b_2, R_X) - \sigma_0 - \tfrac{1}{2}\tilde{\varphi} + \tan^{-1}\left(\frac{1-(1-P_H)^{1/2}}{1+(1-P_H)^{1/2}}\tan\Theta\right), \tag{3.80}$$

where

$$\Theta = \gamma_2(R_X, c_2) - \tfrac{1}{2}\tilde{\varphi} + \sigma_0 + \gamma_1(a_1, R_X). \tag{3.81}$$

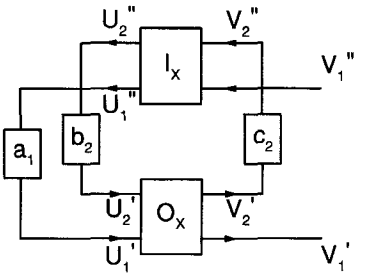

Figure 16. Diagram for the energy $E \geqslant E_2^m$.

The numerical application was made to the following model potential system (see figure 14):

$$\left.\begin{aligned} V_1(R) &= V_{10}\exp[-3(R-R_X)], \\ V_2(R) &= 0{\cdot}15+0{\cdot}1\exp[-3(R-2)]\{\exp[-3(R-2)]-2\}, \\ V_{12}(R) &= 0{\cdot}015\exp[-1{\cdot}5(R-R_X)^2], \end{aligned}\right\} \tag{3.82}$$

where the crossing point $R_X = 2{\cdot}35$ and V_{10} can be expressed as a function of R_X. The elastic scattering cross-section defined as

$$\sigma = \frac{2\pi\hbar^2}{\mu E}\sin^2\eta \tag{3.83}$$

is shown in figures 17 and 18. Except for the energy region $E \approx 0{\cdot}1$ au, the semiclassical approximation works well. In particular, the resonance at $E \approx 0{\cdot}069$ is reproduced well by the semiclassical theory. The combination of equations (3.71) and (3.78) again proves to be of practical use.

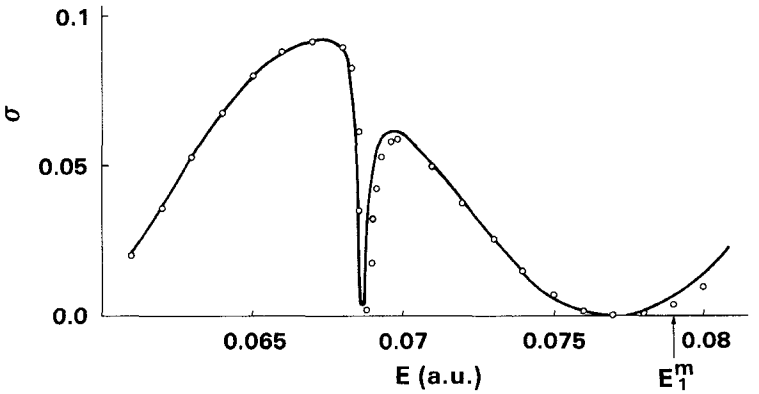

Figure 17. Elastic scattering cross-section as a function of energy: (——), exact numerical result; (○), semiclassical (equations (3.72) and (3.83)) (Nakamura 1987).

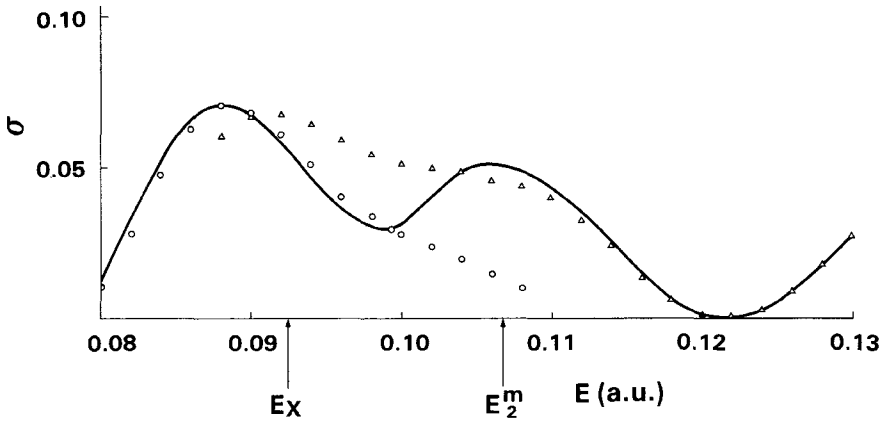

Figure 18. The same as figure 17 at higher energies: (△), semiclassical (equations (3.80) and (3.83)).

4. Dynamics of superexcited states of molecules

4.1. *What is a superexcited state?*

As has already been explained in section 1, a 'superexcited state' is defined as a state such that its internal excitation energy is higher than the first (lowest) ionization potential. This state is thus unstable against auto-ionization. However, this is different from an atomic auto-ionizing state in the sense that it can end up with neutral dissociation without ionization. The shaded area above the ionization potential in figure 1 actually shows this contribution. This is one of the peculiar characteristics of a molecular superexcited state. According to the above definition, a molecular negative ion whose electronic energy is higher than that of its corresponding neutral state can also be a superexcited state. However, in this article we confine ourselves only to the neutral superexcited states. As is easily seen from figure 1, the superexcited states contribute much to the oscillator strength distribution and are expected to play an important role as intermediate states in various dynamic processes (Inokuti 1967, 1981, Berkowitz 1979, Hatano 1988). The concept of superexcitation was actually first introduced by Platzman (1962a, b) in order to understand the molecular excitation processes in radiation chemistry.

According to the differences in auto-ionization mechanism, we classify the superexcited states into the following two (Nakamura 1984a, Nakamura and Takagi 1990):

(1) multiply (or inner-shell) excited state, which is called a 'superexcited state of first kind' and
(2) rovibrationally excited Rydberg state, which is called a 'superexcited state of second kind'.

In the first kind the electronic excitation energy itself is higher than the ionization potential at least in a certain finite range of internuclear distance (figure 19). Most typical examples are the doubly (two-valence-electron) excited states and the inner-shell-electron excited states. Auto-ionization of this kind of superexcited state is basically caused by electron correlation and can occur even if the nuclei were clamped, that is even at fixed internuclear distance. The coupling to the continuum is effectively expressed by the electronic coupling defined by equation (1.2), and the state can be characterized by the local complex potential

$$W(R)=E_{\mathrm{d}}(R)-\frac{\mathrm{i}}{2}\Gamma(R), \tag{4.1}$$

where

$$E_{\mathrm{d}}(\mathbf{R})=\langle\phi_{\mathrm{d}}|H_{\mathrm{el}}|\phi_{\mathrm{d}}\rangle, \tag{4.2}$$

$$\begin{aligned}\Gamma(R)&=2\pi|V(R)|^2\\&=2\pi|\langle\phi_{\mathrm{cont}}|H_{\mathrm{el}}|\phi_{\mathrm{d}}\rangle|^2.\end{aligned} \tag{4.3}$$

It should be noted that the continuum wavefunction ϕ_{cont} is energy-normalized. The auto-ionization lifetime $\tau(R)$ at fixed R is equal to

$$\tau(R)=\frac{\hbar}{\Gamma(R)}. \tag{4.4}$$

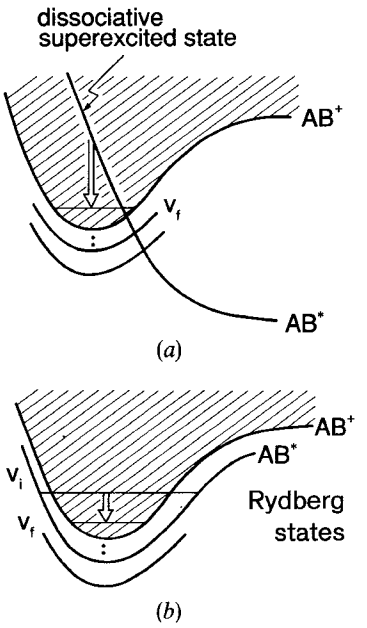

Figure 19. A schematic potential diagram for auto-ionization: (*a*) auto-ionization of the dissociative superexcited state of the first kind (electronic auto-ionization); (*b*) auto-ionization of the superexcited state of the second kind (vibrational auto-ionization).

This type of auto-ionization is called 'electronic auto-ionization'. For instance, Penning ionization $A^* + B \rightarrow A + B^+ + e$, $AB^+ + e$, in which the excitation energy of A* is larger than the ionization potential of B and the quasi-molecular state A*B generally corresponds to an inner-shell excited state, can be treated well by this local complex potential method (Nakamura 1969, 1971, Nakamura and Matsuzawa 1970, Miller 1970, Niehaus 1981).

The auto-ionization mechanism of a superexcited state of the second kind is completely different from that of the first kind. The electronic excitation energy is lower than the ionization potential in the whole range of R, and the auto-ionization is induced by the coupling between electronic motion and nuclear motion, that is by the energy transfer from the nuclear degree of freedom to the electronic degree of freedom (see figure 19). This process can, in principle, be regarded as a non-adiabatic transition but cannot be well treated in terms of the non-adiabatic couplings described in section 3.2. This is because there is no conspicuous avoided crossing between the Rydberg states and, more seriously, the adiabatic approximation does not hold well. As was mentioned in section 1, the period of the Rydberg electron orbital motion ($\tau_n \approx 1{\cdot}5 \times 10^{-16} n^3$ s) can easily be compared with that of nuclear vibrational motion at $n \gtrsim 10$. A much more elegant treatment is that of a kind of diabatic-state representation. This is made possible by the MQDT, in which the R-dependent quantum defect $\mu(R)$ defined by equation (1.1) represents a kind of diabatic coupling potential (Fano 1970, 1975, 1981, 1983, Jungen and Atabek 1977, Golubkov and Ivanov 1981, 1984, Golubkov *et al.* 1983, Seaton 1983, Mies 1984, Mies and Julienne 1984, Greene and Jungen 1985, Sobolewski and Domcke 1987, 1988). This type of auto-ionization is called 'vibrational auto-ionization'. It should be noted that the above-mentioned classification cannot be unique, because the core-excited Rydberg states converging to an excited molecular ion

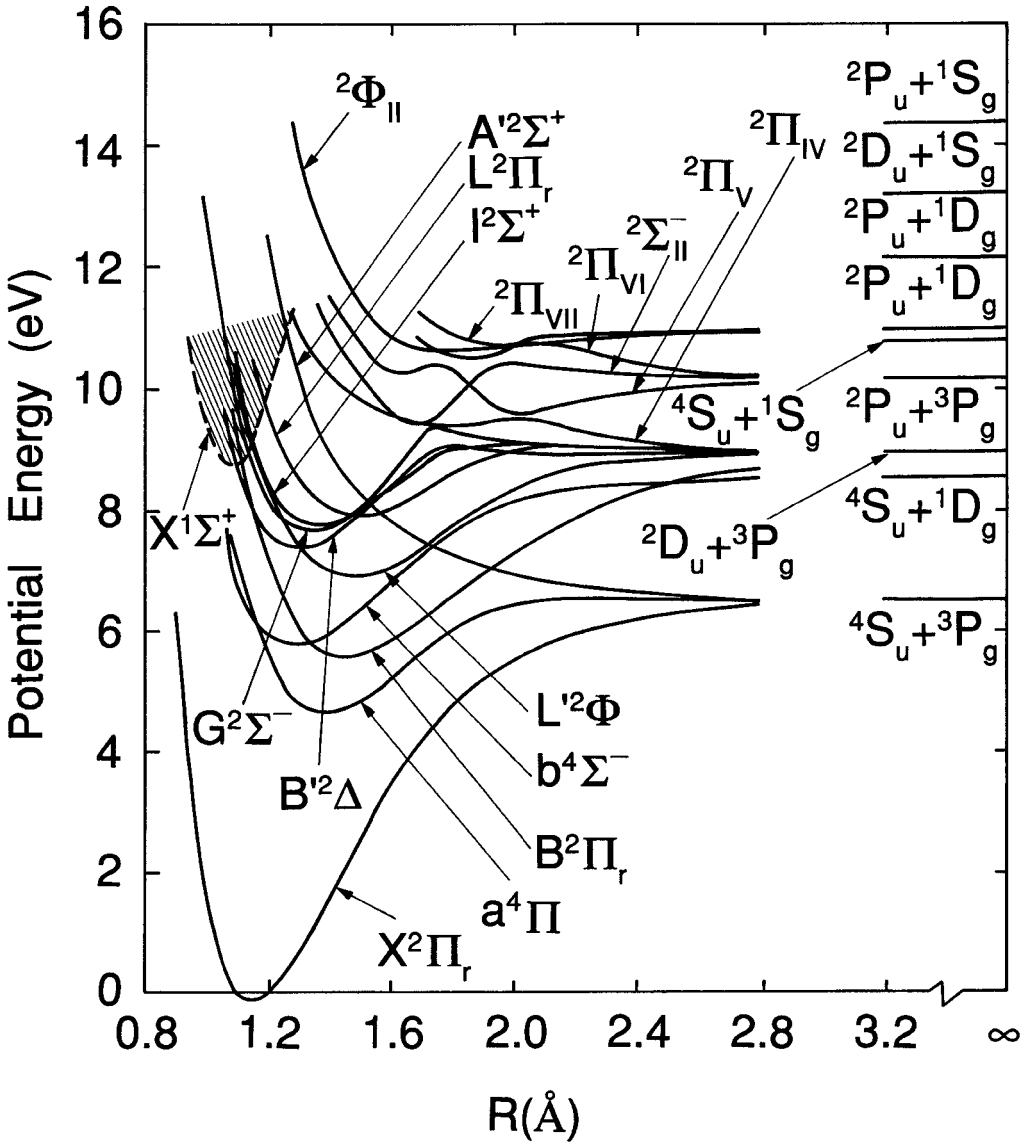

Figure 20. Potential curves of NO (Mitchels 1981).

can be of the first kind as well as of the second kind at the same time. These are of the first kind, because they auto-ionize to the lower ionization continuum by the first mechanism. These can be of the second kind also, because the auto-ionization to the higher ionization continuum to which the Rydberg states converge is possible by the second mechanism.

The superexcited states, especially those of the first kind, are not well known in spite of their importance in various dynamic processes. Information on $\mu_A(R)$ and $\Gamma(R)$ (especially on $\Gamma(R)$) is very scarce. Figure 20 shows the potential curves of NO taken from the review by Mitchels (1981). This immediately indicates that there must be many superexcited states of the first kind which go into the first ionization continuum at small

internuclear distances. There must be a very large number of these states playing a significant role in 'high-energy chemistry'. Recent progress in multiphoton ionization spectroscopy and synchrotron radiation spectroscopy will surely reveal this scientifically rich interesting world.

4.2. *Multichannel quantum defect theory*

The MQDT was first established by Seaton (1983) and his co-workers for treating atomic Rydberg states and continuum in a unified way. This was extended by Fano (1970) to the coupling in molecules between electronic and nuclear rotational motions based on the frame transformation. The generalization of the theory to the molecular rovibronic coupling problems was made by Jungen and Atabek (1977). Raoult and Jungen (1981) and Giusti-Suzor and Lefebvre-Brion (1980) have further extended the theory so that one can deal with the auto-ionization problem. The essences of the MQDT are explained here. For simplicity, the theory is presented here only for the case of no l mixing and no electronic core excitation.

In the inner region ($r \lesssim r_0$) of electron coordinate space, the total wavefunction is expanded in terms of the Born–Oppenheimer basis functions and is explicitly expressed as follows at $r \approx r_0$:

$$\Psi_{\mathrm{BO}} = \sum_{v\Lambda} A_{v\Lambda} \Phi^{\mathrm{BO}}_{v\Lambda}, \tag{4.5}$$

$$\Phi^{\mathrm{BO}}_{v\Lambda} \overset{r \approx r_0}{\approx} \phi^{\mathrm{BO}}_{v\Lambda}(\hat{r}, \mathbf{r}', \mathbf{R})\{f_l(v,r)\cos[\pi\mu_\Lambda(R)] + g_l(v,r)\sin[\pi\mu_\Lambda(R)]\}, \tag{4.6}$$

where $\phi^{\mathrm{BO}}_{v\Lambda}$ represents the total wavefunctions for the angular part ($\hat{r}$) of the Rydberg electron, for the core electrons $\mathbf{r}'$ and nuclear rovibrational motions, $f_l(v,r)$ is the energy-normalized one-centre Coulomb function which is regular at the origin and $g_l(v,r)$ is the corresponding one-centre Coulomb function which is irregular at origin; $f_l(v,r)$ and $g_l(v,r)$ have the following asymptotic forms ($\nu = \mathrm{i}/k$):

$$\left.\begin{aligned} f_l &\overset{r\to\infty}{\to} \left(\frac{2}{\pi k}\right)^{1/2} \sin\zeta \\ g_l &\overset{r\to\infty}{\to} \left(\frac{2}{\pi k}\right)^{1/2} \cos\zeta \end{aligned}\right\} \tag{4.7}$$

with

$$\zeta = kr - \frac{l}{2}\pi + \frac{1}{k}\ln(2kr) + \arg\left[\Gamma\left(l+1-\frac{\mathrm{i}}{k}\right)\right]. \tag{4.8}$$

The term within the braces in equation (4.6) is the radial part of the Rydberg electron. The R-dependent quantum defect $\mu_\Lambda(R)$ effectively represents all the interactions (including exchange interaction) between the Rydberg electron and the core electrons.

In the outer region ($r \gtrsim r_0$), on the other hand, the total wavefunction is expanded in the way of close coupling as

$$\Psi_{\mathrm{cc}} = \sum_{v^+N^+} \Phi^{\mathrm{cc}}_{v^+N^+}, \tag{4.9}$$

$$\Phi^{\mathrm{cc}}_{v^+N^+} = \phi^{\mathrm{cc}}_{v^+N^+}(\hat{r}, \mathbf{r}', \mathbf{R})[f_l(v_{v^+N^+}, r)\alpha_{v^+N^+} + g_l(v_{v^+N^+}, r)\beta_{v^+N^+}], \tag{4.10}$$

where v^+ and N^+ stand for the vibrational and rotational quantum numbers of the core. The radial part of the Rydberg electron (the term in square brackets in equation

(4.10)) is now R independent. Since the (v^+, N^+) represents a channel (either open or closed) at $r \to \infty$, the energy parameter ν depends on them. In the intermediate region ($r \approx r_0$) (boundary between the two regions), both approximations (4.5) and (4.9) are assumed to hold well and the energy parameter ν becomes almost independent of (v^+, N^+), because the kinetic energy of the Rydberg electron becomes much larger than the rovibrational energy spacing. Thus, by taking a projection between the two basis functions, we obtain

$$\alpha_{v^+N^+} = \sum_{v\Lambda} A_{v\Lambda} \mathscr{C}_{v^+N^+, v\Lambda}, \tag{4.11a}$$

$$\beta_{v^+N^+} = \sum_{v\Lambda} A_{v\Lambda} \mathscr{S}_{v^+N^+, v\Lambda}, \tag{4.11b}$$

where

$$\mathscr{C}_{v^+N^+, v\Lambda} = \langle N^+|\Lambda\rangle \langle v^+|\cos[\pi\mu_\Lambda(R)]|v\rangle, \tag{4.12a}$$

$$\mathscr{S}_{v^+N^+, v\Lambda} = \langle N^+|\Lambda\rangle \langle v^+|\sin[\pi\mu_\Lambda(R)]|v\rangle. \tag{4.12b}$$

The quantity $\langle N^+|\Lambda\rangle$ represents the frame transformation of the angular parts (nuclear rotation plus Rydberg electron's angular part) between Hund's two coupling cases b and d (Fano 1970, Jungen and Atabek 1977, Chang and Fano 1972). $|v^+\rangle$ and $|v\rangle$ are the vibrational states of the core and the Rydberg state. Insertion of equation (4.11) into equation (4.10) and application of the proper boundary conditions to equation (4.9) lead to the expression for the scattering matrix. The Coulomb functions f_l and g_l have the following asymptotic expressions at negative energies $\epsilon = -\frac{1}{2}\nu^2$:

$$f_l(\nu, r) \overset{r\to\infty}{\to} \sin(\pi\nu)\, u(\nu, r) - \cos(\pi\nu)\, v(\nu, r), \tag{4.13a}$$

$$g_l(\nu, r) \to \cos(\pi\nu)\, u(\nu, r) + \sin(\pi\nu)\, v(\nu, r), \tag{4.13b}$$

where $u(\nu, r) \propto \exp(r/\nu)$ and $v(\nu, r) \propto \exp(-r/\nu)$. The coefficients of the function $u(\nu, r)$ in the total wavefunction should be zero. Following the procedure by Seaton (1983) and introducing the reactance matrix $\mathbf{R}$, we obtain

$$\mathbf{R} = \mathfrak{R}_{oo} - \mathfrak{R}_{oc}[\mathfrak{R}_{cc} + \tan(\pi\nu)]^{-1}\mathfrak{R}_{co} \tag{4.14}$$

with

$$\mathfrak{R} = \mathscr{S}\mathscr{C}^{-1}, \tag{4.15}$$

where the matrix $\mathbf{R}$ is related to the scattering matrix as

$$\mathbf{S} = (1 + i\mathbf{R})(1 - i\mathbf{R})^{-1}, \tag{4.16}$$

$\mathscr{S}$ and $\mathscr{C}$ are the matrices whose elements are given by equation (4.12), and the subscripts o and c in equation (4.14) mean open and closed respectively. The second term in equation (4.14) represents the contribution from the closed channel (resonant scattering part). If there is no open channel, we obtain the following eigenvalue equation:

$$\det|\mathfrak{R}_{cc} + \tan(\pi\nu)| = 0. \tag{4.17}$$

This gives a spectrum of infinite number of perturbed Rydberg states. Since the vibrational states v^+ of ionic core and v of Rydberg state are almost the same, the R dependence of the quantum defect $\mu_\Lambda(R)$ is the most decisive factor for the various dynamic processes involving vibrational transitions.

As can be understood from the above introduction, the MQDT provides a unified description of Rydberg states and ionization continuum. The matrix $\mathfrak{R}$ is the most basic quantity for describing uniformly either the perturbed bound-state problem or the scattering problem. In order to treat a process such as dissociative recombination, the theory should be extended so as to incorporate the effects of dissociative superexcited state of the first kind. This can be done by the two-step treatment proposed by Giusti (1980). The scattering problem associated with the electronic coupling $V(R)$ between the dissociative superexcited state and the electronic continuum is described by the integral equation for the reactance matrix $\mathbf{K}$:

$$K_{jj'}(E,E')=\langle jE|V(R)|j'E'\rangle+\sum_{j''}\mathrm{Pv.}\int dE''\frac{\langle jE|V(R)|j''E''\rangle}{E-E''}K_{j''j'}(E'',E'), \quad (4.18)$$

where j, j' and j'' represent the vibrational (v) or nuclear dissociation (d) state. Next, we introduce the matrix $\{U_{j\alpha}\}$ which diagonalizes the on-the-energy-shell $\mathbf{K}$ matrix, that is

$$\sum_{j'}K_{jj'}U_{j'\alpha}=-\frac{1}{\pi}\tan\eta_\alpha U_{j\alpha}, \quad (4.19)$$

where $-(\tan\eta_\alpha)/\pi$ is the eigenvalue of the $\mathbf{K}$ matrix. If we employ the first-order perturbation theory, we have

$$K_{jj'}=\begin{cases}\langle v|V(R)|F_d\rangle\equiv\dfrac{1}{\pi}\xi_v, & \text{for } j=v \text{ and } j'=d,\\ 0, & \text{otherwise,}\end{cases} \quad (4.20)$$

$$\eta_\alpha=\begin{cases}0 & ((I-2)\text{ fold degenerate}),\\ \pm\tan^{-1}\xi,\end{cases} \quad (4.21)$$

where

$$\xi^2=\sum_v\xi_v^2, \quad (4.22)$$

I is the total number of channels (one dissociation channel and $I-1$ vibrational channels) and F_d is the nuclear dissociation wavefunction. The basis function in the inner region is now taken to be

$$\psi_\alpha=\sum_q U_{q\alpha}(\varphi_q\cos\eta_\alpha-\bar{\varphi}_q\sin\eta_\alpha), \quad (4.23)$$

where for the ionization channel $q=v\Lambda$

$$\varphi_q=\Phi^{\mathrm{BO}}_{v\Lambda}, \quad (4.24a)$$

$$\bar{\varphi}_q=\phi^{\mathrm{BO}}_{v\Lambda}\{-g_l(v,r)\cos[\pi\mu_\Lambda(R)]+f_l(v,r)\sin[\pi\mu_\Lambda(R)]\}, \quad (4.24b)$$

and for the dissociation channel $q=d$

$$\varphi_q=\phi_d(\mathbf{r}:R)F_d(R), \quad (4.25a)$$

$$\bar{\varphi}_q=\phi_d(\mathbf{r}:R)G_d(R). \quad (4.25b)$$

The function ϕ_d represents the electronic wavefunction of the dissociative superexcited state, and $G_d(R)$ is the nuclear dissociation wavefunction which has a cosine asymptotic form. Here the function φ_q plays the role of f_l in equation (4.6), and $\bar{\varphi}_q$ that of g_l. In the

outer region, in addition to the ionization channel $i=v^+$ defined by equation (4.10), the following dissociation channel is introduced:

$$\Phi_d=\phi_d(\mathbf{r}:R)(F_d\alpha_d+G_d\beta_d). \tag{4.26}$$

Exactly the same procedure as before can be used. Equation (4.14)–(4.16) hold with the matrices $\mathscr{C}$ and $\mathscr{S}$ generalized as follows:

$$\mathscr{C}_{v^+,\alpha}=\sum_v \langle v^+|\cos[\pi\mu_A(R)+\eta_\alpha]|v\rangle U_{v\alpha}, \tag{4.27a}$$

$$\mathscr{S}_{v^+,\alpha}=\sum_v \langle v^+|\sin[\pi\mu_A(R)+\eta_\alpha]|v\rangle U_{v\alpha} \tag{4.27b}$$

for the ionization channel ($i=v^+$), and

$$\mathscr{C}_{d,\alpha}=U_{d\alpha}\cos\eta_\alpha, \tag{4.28a}$$

$$\mathscr{S}_{d,\alpha}=U_{d\alpha}\sin\eta_\alpha \tag{4.28b}$$

for the dissociation channel ($i=d$). It should be noted that the rotational degrees of freedom are neglected here for simplicity and thus the factor $\langle N^+|A\rangle$ is missing. The unitarity of the S matrix can easily be shown to be guaranteed. This is proved in Appendix C.

Once the matrix $\mathfrak{R}$ and then the scattering matrix S are obtained, the following various dynamic processes can be investigated uniformly.

(1) Dissociative recombination: the partial cross-section for the dissociation into channel d from the initial vibrational state v_i^+ is given by

$$\sigma_{d,v_i^+}=\frac{\pi}{k^2}\rho_i|S_{d,v_i^+}|^2, \tag{4.29}$$

where ρ_i represents the statistical factor and k is the initial (electron) wavenumber.

(2) Vibrational transition $v_i^+\to v_f^+$: the partial cross-section is given by

$$\sigma_{v_f^+,v_i^+}=\frac{\pi}{k^2}\rho_i|S_{v_f^+,v_i^+}|^2. \tag{4.30}$$

(3) Associative ionization $d\to v_f^+$: the cross-section is

$$\sigma_{v_f^+,d}=\frac{\pi}{k^2}\rho_d\sum_L(2L+1)|S^{(L)}_{v_f^+,d}|^2, \tag{4.31}$$

where k is the initial wavenumber of nuclear relative motion, ρ_d is the statistical factor of the initial dissociative state and L is the angular momentum of the nuclear relative motion. Here only one partial wave of the ejected electron and only one initial dissociative state are assumed.

(4) Photo-ionization and photodissociation: the rotationally unresolved cross-section is (Seaton 1983, Greene and Jungen 1985)

$$\sigma_\beta=\frac{4\pi^2}{3}\alpha\hbar\omega|D_\beta|^2 \qquad (\beta\equiv\text{ionization, dissociation}), \tag{4.32}$$

where α is the fine-structure constant, $\hbar\omega$ is the photon energy and D_β represents the reduced dipole-matrix element which is given by

$$D_\beta = D_\beta^{(\text{open})} - \chi_{oc}[\chi_{cc} - \exp(-2\pi i\nu)]^{-1} D_\beta^{(\text{closed})}. \tag{4.33}$$

The first term represents the direct process, and the second term describes the indirect process via the closed channel (Rydberg states). This second term can be used to analyse the auto-ionization and pre-dissociation mechanisms.

The matrix χ used in equation (4.33) is defined in terms of the Jost matrices $\mathbf{J}^\pm$ as

$$\chi = \mathbf{J}^+(\mathbf{J}^-)^{-1}, \tag{4.34}$$

with

$$\mathbf{J}^\pm = \mathscr{C} \pm i\mathscr{S}. \tag{4.35}$$

The scattering matrix $\mathbf{S}$ and the matrix $\mathfrak{R}$ are related to χ by

$$\mathbf{S} = \chi_{oo} - \chi_{oc}[\chi_{cc} - \exp(-2\pi i\nu)]^{-1}\chi_{co}, \tag{4.36}$$

$$\mathfrak{R} = i(1-\chi)(1+\chi)^{-1}. \tag{4.37}$$

4.3. *Photo-ionization and auto-ionization*

We discuss here the mechanisms and physics of the photon impact processes in the energy region near the first ionization threshold. There exist some intriguing problems such as

(1) the role of auto-ionization (pre-dissociation) in photo-ionization (photodissociation),
(2) the different mechanisms of auto-ionization (vibrational and electronic auto-ionization) and
(3) the competition between auto-ionization and pre-dissociation.

These problems can be investigated in a unified way by the MQDT, as is explained in the previous section. Unfortunately, however, information is very scarce for the basic physical parameters: the R-dependent quantum defect $\mu_\Lambda(R)$, the electronic coupling $V(R)$ and the reduced transition dipole moments. More challenge by the quantum chemists is desired. On the other hand, high-resolution spectroscopy, especially the resonantly enhanced multiphoton ionization (REMPI) spectroscopy is now well developed (for example Kimura (1987)). It enables us to derive useful information on the superexcited states and stimulates theoretical studies.

The most extensively studied molecules are H_2 and NO. The studies up to 1985 have been summarized by Greene and Jungen (1985). In the case of H_2, photo-ionization, auto-ionization and photoelectron angular distributions were studied with the use of the MQDT by Jungen and co-workers (Dill and Jungen 1980, Jungen and Dill 1980, Raoult *et al.* 1980, Jungen and Raoult 1981, Raoult and Jungen 1981). In these studies, only the one-photon ionization process is considered and thus no superexcited state of the first kind is involved, since the lowest doubly excited state (near the ionization threshold) is that of the $^1\Sigma_g$ symmetry (figure 21). Auto-ionization occurs only by the vibrational auto-ionization mechanism. Since information on the various doubly excited states of H_2 is now available (Collins and Schneider 1983, Hazi 1983, Guberman 1983, Takagi and Nakamura 1983, Hara and Sato 1984, Tennyson and Noble 1985, Sato and Hara 1986) and the REMPI experiment is possible (Pratt

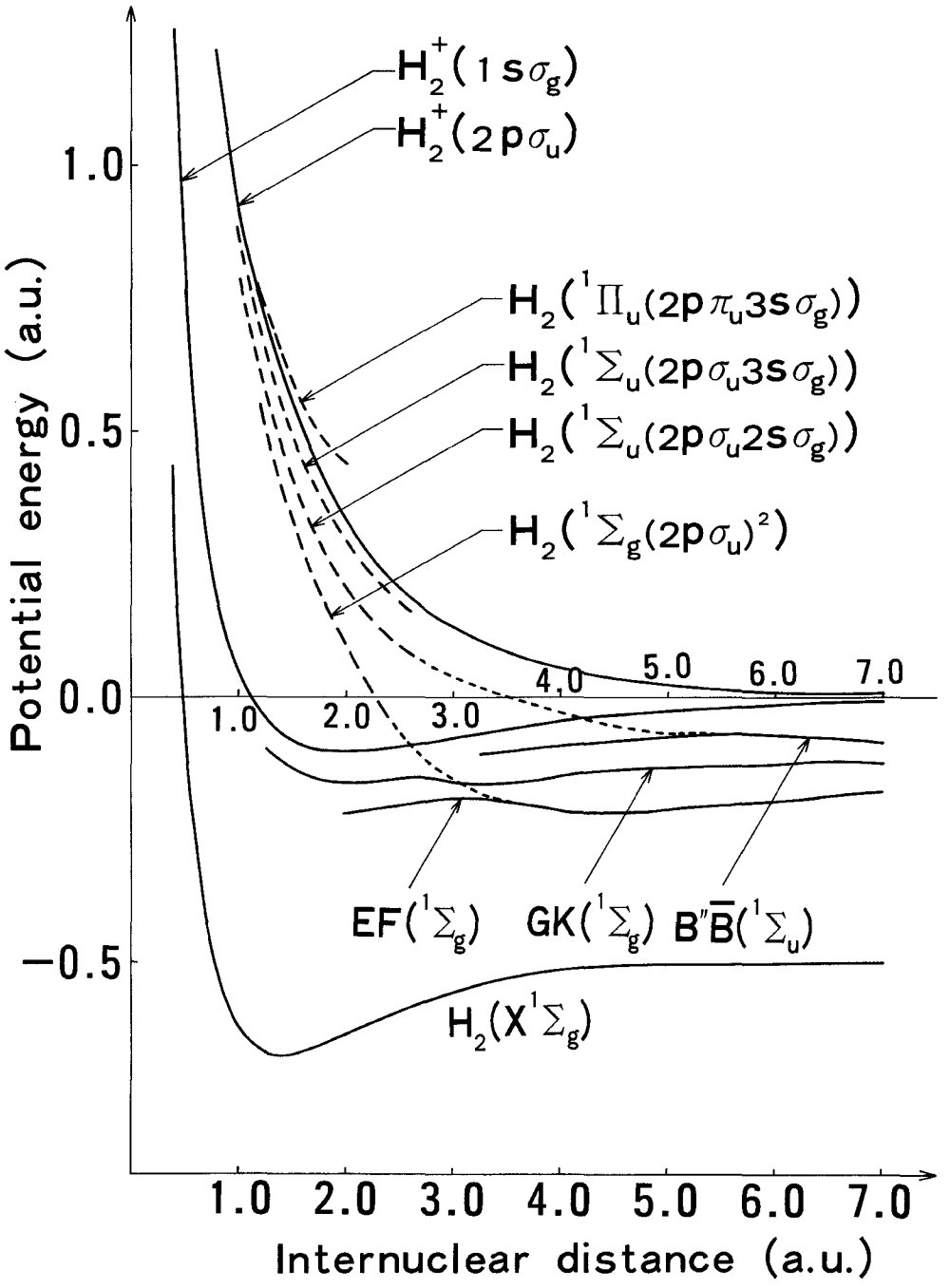

Figure 21. Potential curves of H_2 near the lowest ionic state.

et al. 1984, 1986, Verschuur and Van Linden van den Heuvell 1989), more extensive theoretical studies of H_2 should now be carried out. See also the studies by Dastidar and Lambropoulos (1982, 1984), Dastidar (1983), Dastidar *et al.* (1986), Ganguly *et al.* (1986), Rudolph *et al.* (1987), Ganguly and Dastidar (1988) and Dixit *et al.* (1989). The NO molecule has also been a good target of theoretical studies using the MQDT approach (Giusti-Suzor and Jungen 1984, Li 1986, Fredin *et al.* 1987, Raoult 1987, Sobolewski 1987, Rudolph *et al.* 1988, Pratt *et al.* 1989, Nakashima *et al.* 1989). There exist many dissociative superexcited states, and both vibrational and electronic auto-ionizations are possible. The REMPI technique can specify the symmetry of the states, pinpoint the energy region to be investigated and provide us with very useful information on the superexcited states. It is remarkable that the electronic auto-ionization via dissociative superexcited state of the first kind plays a significant role in auto-ionization (Giusti-Suzor and Jungen 1984, Nakashima *et al.* 1989). One example of analysis is given below. The MQDT approach has also been applied to some other diatomic molecules (Morin *et al.* 1982, Raoult *et al.* 1983, Giusti-Suzor and Lefebvre-Brion 1984, Lefebvre-Brion *et al.* 1985, Bordas *et al.* 1989, Lefebvre-Brion and Keller 1989).

In the following, by taking some practical examples we explain the applications of the MQDT, clarify the mechanisms of auto-ionization and analyse the REMPI experiment on NO (Achiba and Kimura 1989).

First, we derive the analytical expression for the vibrational auto-ionization width (Takagi and Nakamura 1981). In the case of relatively low Rydberg states ($n \lesssim 10$) which can be specified well by the quantum number Λ, the vibrational auto-ionization can be treated in a two-state (v_i^+ (initial closed channel) and v_f^+ (final open channel)) approximation. Applying the boundary conditions of closed channel to equation (4.9) with the use of equations (4.11)–(4.13), we have

$$\sum_v [\sin(\pi\nu_i)\mathscr{C}_v^{v_i^+} + \cos(\pi\nu_i)\mathscr{S}_v^{v_i^+}]A_v = 0, \tag{4.38}$$

where $\mathscr{C}_v^{v_i^+}$ and $\mathscr{S}_v^{v_i^+}$ are those defined by equations (4.12) without $\langle N^+|\Lambda\rangle$. The standing-wave boundary condition for the open channel v_f^+ leads to

$$\sum_v [\sin(\eta_f)\mathscr{C}_v^{v_f^+} - \cos(\eta_f)\mathscr{S}_v^{v_f^+}]A_v = 0, \tag{4.39}$$

where η_f is the scattering phase shift. Equations (4.38) and (4.39) are reduced to

$$\begin{vmatrix} K_f^f \sin(\eta_f - \theta_f^f), & K_i^f \sin(\eta - \theta_i^f) \\ K_f^i \sin(\pi\nu_i + \theta_f^i), & K_i^i \sin(\pi\nu_i + \theta_i^i) \end{vmatrix} = 0, \tag{4.40}$$

where

$$K_\alpha^\beta \cos\theta_\alpha^\beta = \mathscr{C}_\alpha^\beta \equiv \mathscr{C}_{v_\alpha^+}^{v_\beta^+}, \tag{4.41 a}$$

$$K_\alpha^\beta \sin\theta_\alpha^\beta = \mathscr{S}_\alpha^\beta \equiv \mathscr{S}_{v_\alpha^+}^{v_\beta^+}, \quad (\alpha,\beta) \equiv (i,f) \tag{4.41 b}$$

and $|v\rangle$ is assumed to be equal to $|v^+\rangle$. By fitting the energy dependence of the phase shift η_f derived from equation (4.40) to a form

$$\eta_f = \eta_p - \tan^{-1}\left(\frac{\Gamma/2}{E - E_r}\right), \tag{4.42}$$

the resonance energy E_r and the vibrational auto-ionization width Γ_v can be obtained as

$$E_r = -\frac{1}{2(n-\beta)^2}, \tag{4.43}$$

$$\Gamma_v = \frac{-2}{\pi}\frac{\tan\bar{\eta}}{1+\epsilon^2}\frac{1}{(n-\beta)^3}, \tag{4.44}$$

where

$$\tan\bar{\eta} = \frac{4K}{(1-K)^2}\frac{\tan\delta_i \tan\delta_f}{1+\tan^2(\eta_p-\theta_f)}, \tag{4.45a}$$

$$\epsilon = \tan\bar{\eta}\tan(\eta_p-\theta_f)+\tan(\eta_p-\theta_i), \tag{4.45b}$$

$$\beta = \frac{\theta_i - \tan^{-1}\epsilon}{\pi}, \tag{4.45c}$$

$$\theta_\alpha = \tfrac{1}{2}(\theta_i^\alpha + \theta_f^\alpha), \quad \alpha \equiv i, f, \tag{4.45d}$$

$$\delta_\alpha = \tfrac{1}{2}(\theta_f^\alpha - \theta_i^\alpha), \quad \alpha \equiv i, f, \tag{4.45e}$$

$$\tan(\eta_p-\theta_\alpha) = \frac{1+K}{1-K}\tan\delta_\alpha \quad \alpha \equiv i, f, \tag{4.45f}$$

$$K = \frac{K_i^f K_f^f}{K_i^i K_f^i}, \tag{4.45g}$$

and n is the principal quantum number. Equation (4.44) is an exact expression within the two-state approximation and shows the well known n^{-3} dependence of Γ. When K can be assumed to be small, which is expected to hold well quite generally, equation (4.44) can be simplified to

$$\Gamma_v \approx -\frac{2}{\pi}K\frac{\sin(2\delta_i)\sin(2\delta_f)}{(n-\theta_i^i/\pi)^3}. \tag{4.46}$$

If we retain only the first term in the expansion of the quantum defect number around the equilibrium distance R_e, then we have

$$\Gamma_v \approx \frac{2\pi}{(n-\mu_0)^3}|\langle v_f^+|R-R_e|v_i^+\rangle \mu_1|^2, \tag{4.47}$$

where

$$\mu(R) = \sum_{m=0}^{\infty}\mu_m(R-R_e)^m. \tag{4.48}$$

If we can further use the harmonic oscillator approximation, then we obtain

$$\Gamma_v(\Delta v=1) \approx \frac{\pi}{(n-\mu_0)^3}\mu_1^2\frac{v_i^+}{m\omega}, \tag{4.49a}$$

$$\frac{\Gamma_v(\Delta v=2)}{\Gamma(\Delta v=1)} \approx \left(\frac{\mu_2}{\mu_1}\right)^2\frac{v_i^+-1}{2m\omega}, \tag{4.49b}$$

where $\Delta v = |v_i^+ - v_f^+|$, m is the reduced mass and ω is the angular frequency of the harmonic oscillator. Equations (4.47) and (4.49) are equivalent to the crude Born–Oppenheimer approximation (Herzberg and Jungen 1972, Dehmer and Chupka 1976). Figures 22 and 23 show the v_i^+ dependence of Γ_v and $\Gamma_v(\Delta v)/\Gamma_v(\Delta v = 1)$ against Δv for H_2 ($np\sigma$) respectively. The results obtained by Berry and Nielsen (1970) and by Shaw and Berry (1972) are those of the first-order perturbation of non-adiabatic coupling. The present results (equation (4.44)) are in good agreement with experiment (Dehmer and Chupka 1976). Figure 23 clearly indicates the well known propensity rule, $\Gamma_v(\Delta v = 1) \gg \Gamma_v(\Delta v = 2) \gg \ldots$. The crude Born–Oppenheimer approximations (4.47) and (4.49) were shown not to hold well always, because the linear dependence on R of

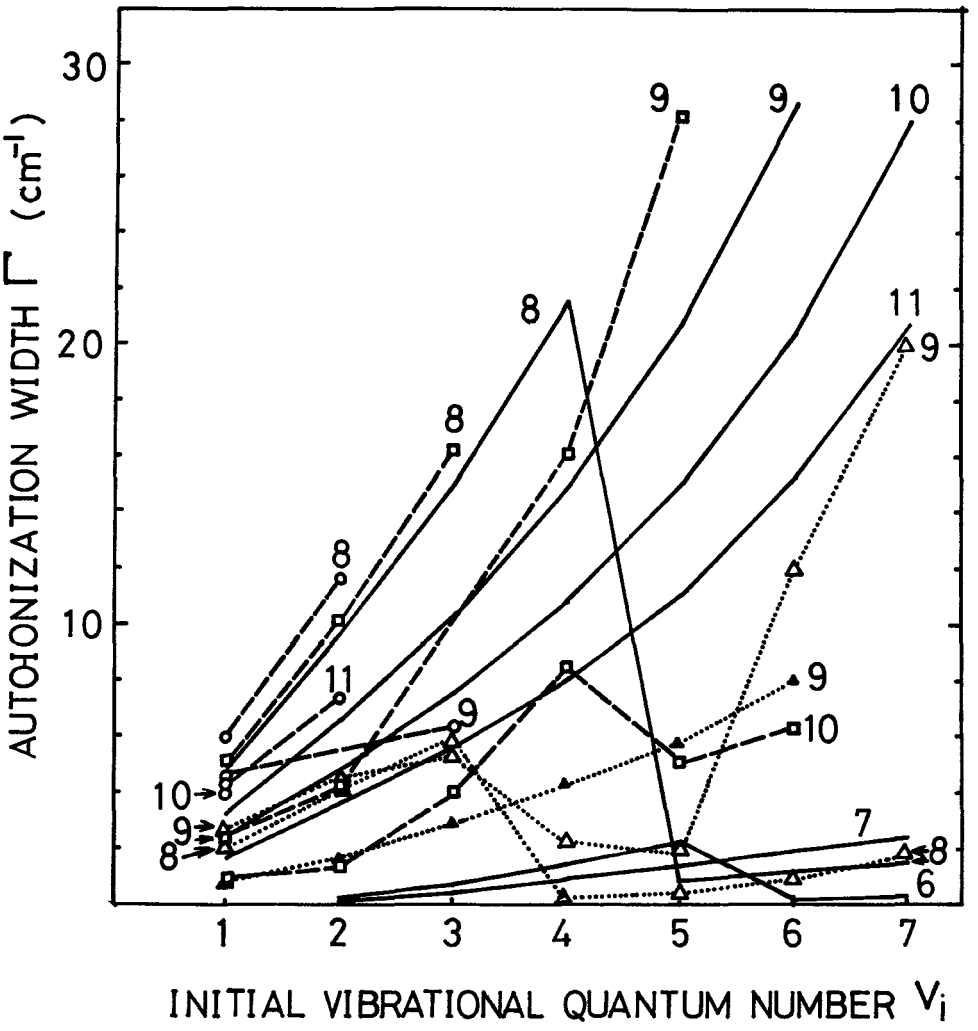

Figure 22. Vibrational auto-ionization width ($\Sigma_{\Delta v}\Gamma(\Delta v)$) as a function of the initial vibrational quantum number in the case of H_2 ($np\sigma$) (the numbers on the lines indicate the principal quantum numbers): (——), Takagi and Nakamura (1981); (· · · · ·), Berry and Nielsen (1970); (· · · △ · · ·), Shaw and Berry (1972); (– – ○ – –), *ortho*-H_2, experiment (Dehmer and Chupka 1976); (– – □ – –), *para*-H_2, experiment (Dehmer and Chupka 1976).

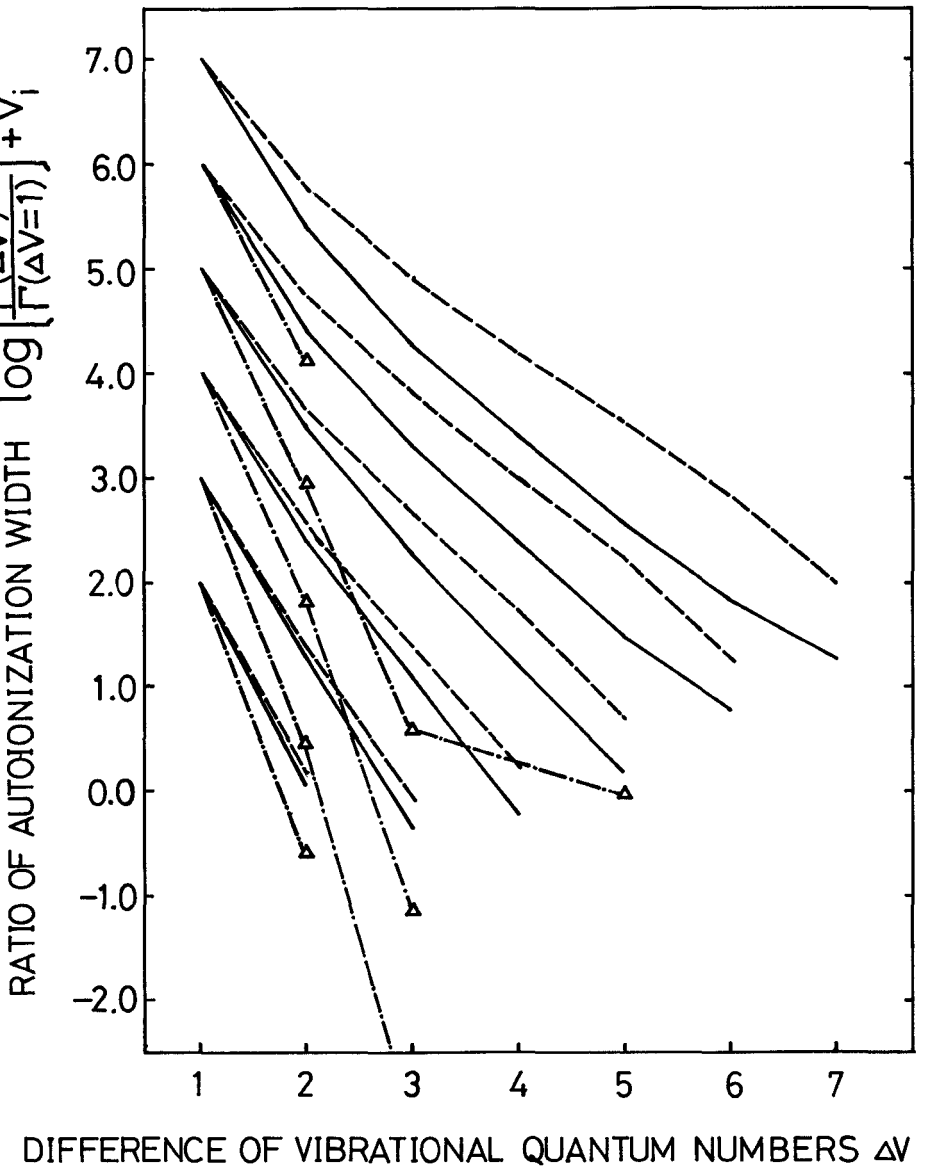

Figure 23. Propensity of vibrational auto-ionization in the case of H_2 ($np\sigma$): (——), Takagi and Nakamura (1981); (···△···), Berry and Nielsen (1970); (– – –), crude Born–Oppenheimer approximation.

the quantum defect does not necessarily hold well and the anharmonicity becomes important sometimes, especially for $\Delta v \geqslant 2$. Equation (4.46) is quite accurate but is unfortunately still complicated. So, we recommend here the following expression for practical use:

$$\Gamma_v \approx \frac{2\pi}{(n-\mu_0)^3} |\langle v_f^+ | \mu(R) | v_i^+ \rangle|^2. \tag{4.50}$$

Pure rotational de-excitation within the same vibrational level can also lead to auto-ionization. In this case the R dependence of the quantum defect can be disregarded, and $\mathscr{C}$ and $\mathscr{S}$ are reduced to

$$\mathscr{C}_\Lambda^{N^+} = \langle N^+ | \Lambda \rangle \cos(\pi \mu_\Lambda), \tag{4.51 a}$$

$$\mathscr{S}_\Lambda^{N^+} = \langle N^+ | \Lambda \rangle \sin(\pi \mu_\Lambda). \tag{4.51 b}$$

The procedure and the formulae described above hold with the various quantities defined below. For simplicity, we consider here the case of the two channels $N^+ = 0$ and 2 (thus $\Lambda = 0$ (σ) and 1 (π). Then we have

$$\langle N^+ | \Lambda \rangle = \begin{bmatrix} \cos\alpha, & \sin\alpha \\ -\sin\alpha, & \cos\alpha \end{bmatrix} = \begin{bmatrix} \sqrt{\frac{1}{3}} & \sqrt{\frac{2}{3}} \\ -\sqrt{\frac{2}{3}} & \sqrt{\frac{1}{3}} \end{bmatrix}, \tag{4.52 a}$$

$$\theta_\Lambda^{N^+} = \pi \mu_\Lambda, \tag{4.52 b}$$

$$K = -\tan^2\alpha, \tag{4.52 c}$$

$$\delta_i = \delta_f = \frac{\pi(\mu_\sigma - \mu_\pi)}{2} \equiv \delta \tag{4.52 d}$$

$$\theta_i = \theta_f = \frac{\pi(\mu_\sigma + \mu_\pi)}{2}, \tag{4.52 e}$$

$$\tan(\eta_p - \theta_i) = \tan(\eta_p - \theta_f) = \tan\delta \cos(2\alpha), \tag{4.52 f}$$

$$\tan\bar{\eta} = \frac{-\sin^2(2\alpha)\sin^2\delta}{1 - \sin^2(2\alpha)\sin^2\delta}. \tag{4.52 g}$$

The expression for the phase shift η_f derived from equation (4.40) is the same as equation (34) of Fano (1970). If we can assume that $|\delta| \ll 1$, $|\epsilon| \ll 1$ and $|\beta| \ll n$, then we find that

$$\Gamma_r \approx \frac{4\pi}{9} \frac{1}{n^3} (\mu_\sigma - \mu_\pi)^2. \tag{4.53}$$

This is equivalent to the formula employed by Herzberg and Jungen (1972).

Next, let us consider the case in which a dissociative superexcited state of first kind coexists and electronic auto-ionization is also involved. For clarity, we take, as an example, the recent MQDT analysis (Nakashima *et al.* 1989) of the REMPI experiment on NO (Achiba and Kimura 1989). Using the (2+1)-photon process, Achiba and Kimura (1989) measured the photo-ionization and photoelectron kinetic energy spectra. Figure 24(*a*) shows the photo-ionization spectrum against the wavelength of the third photon (second laser). Figure 25 shows the kinetic energy spectrum of the photoelectrons originating from the $nd\delta$ ($v = 4$) Rydberg states ($n = 5$–9). Although the $v^+ = 3$ peak is the highest, $v^+ = 0$ gives the second highest. This clearly contradicts the

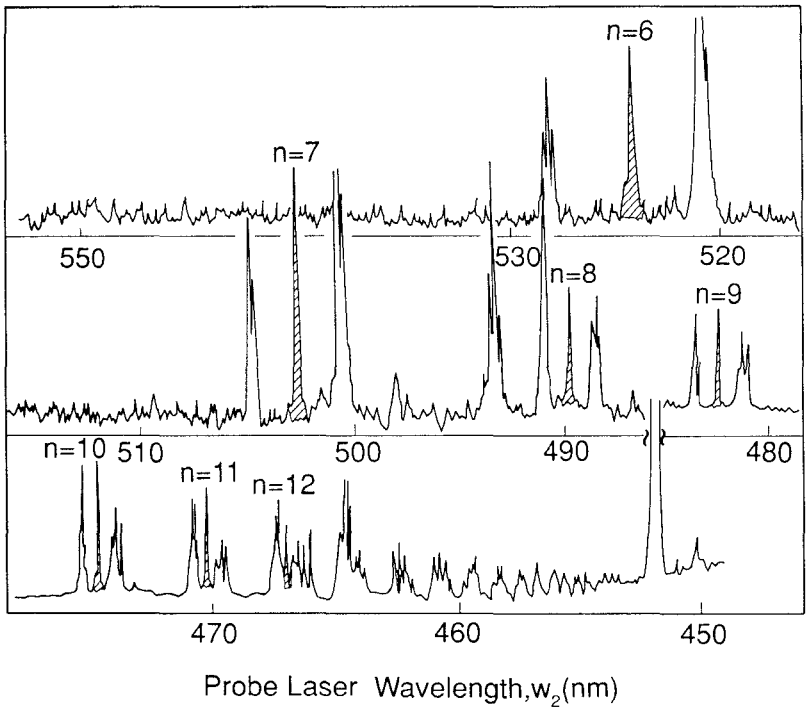

(*a*)

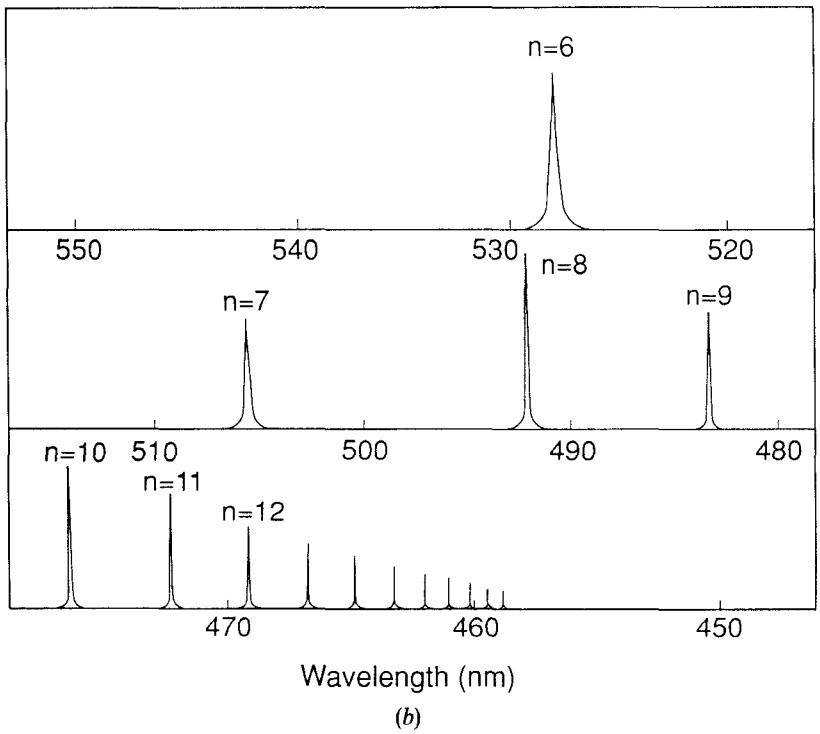

(*b*)

Figure 24. Photo-ionization spectra. (*a*) The experimental MPI spectrum (Achiba and Kimura 1989). The shaded peaks correspond to $nd\delta$ ($v=4$). (*b*) Theoretical calculation of $nd\delta$ peaks (Nakashima *et al.* 1989).

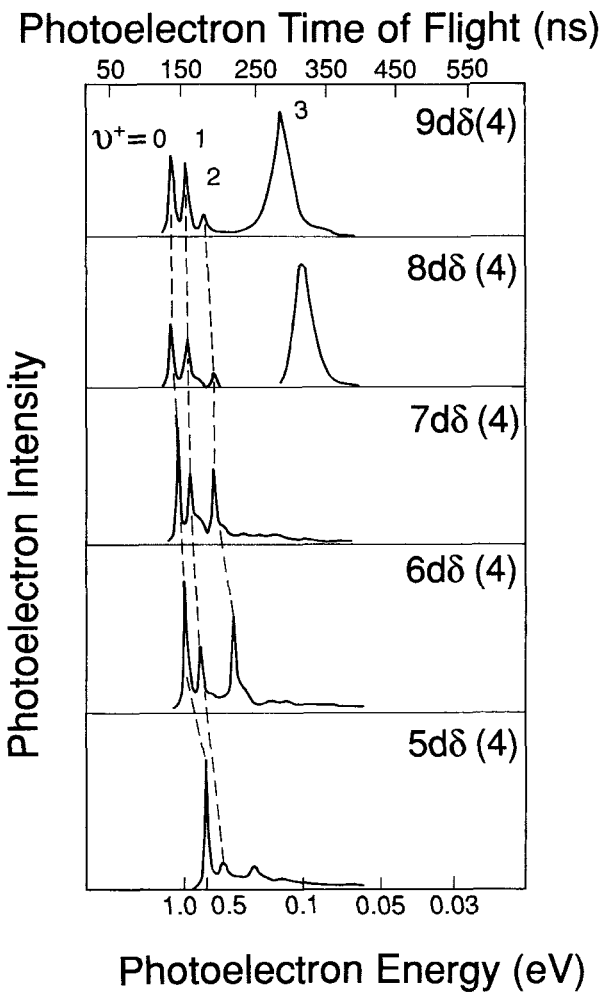

Figure 25. Photo-ionization kinetic energy spectra of NO for ndδ ($v=4$) ($n=5$–9) (Achiba and Kimura 1989).

propensity rule of vibrational auto-ionization and suggests a large contribution of the electronic auto-ionization via the dissociative superexcited state B′ $^2\Delta$, which is expected to be located near the equilibrium internuclear distance. In order to make this clear first, we have calculated the quantum defects at various internuclear distances. Table 1 gives a rough estimate of $\Gamma_v(\Delta v=2)/\Gamma_v(\Delta v=1)$ with use of equation (4.49 b) and the calculated quantum defects. This result clearly tells that the vibrational auto-ionization is not dominant, at least for $\Delta v \geqslant 2$. Analysis of the experiment was carried out based on the two-step MQDT formalism described in section 4.2. Since this is a resonant process, we concentrate on the second term of equation (4.33):

$$D_{v^+}^{(\mathrm{res})} \approx -\chi_{v^+ v_R}[\chi_{v_R v_R} - \exp(-2\pi i\nu)]^{-1} D_{v_R}, \tag{4.54}$$

where only one closed channel v_R (Rydberg state ndδ ($v=4$)) is assumed. If we note that the Jost matrices $\mathbf{J}^{\pm}$ defined by equation (4.35) can be expressed as

$$\mathbf{J}^{\pm} = \mathbf{X}^{\pm}\mathbf{U}\mathbf{A}^{\pm}, \tag{4.55}$$

Table 1. Ratio of the vibrational auto-ionization widths $\Gamma(\Delta v=2)/\Gamma(\Delta v=1)$ for the NO Rydberg states (Nakashima *et al.* 1989).

$l\lambda$	sσ	pσ	pπ	dσ	dπ	dδ
$\frac{\Gamma(\Delta v=2)}{\Gamma(\Delta v=1)}$	$4{\cdot}36\times10^{-3}$	$5{\cdot}60\times10^{-3}$	$6{\cdot}43\times10^{-3}$	$7{\cdot}14\times10^{-6}$	$1{\cdot}99\times10^{-4}$	$1{\cdot}32\times10^{-4}$

where

$$(X^{\pm})_{ij}=\begin{cases}1, & i=j=1,\\ 0, & (i=1, j\neq 1),\quad (i\neq 1, j=1),\\ \langle i|\exp[\pm i\pi\mu(R)]|j\rangle, & \text{otherwise},\end{cases} \tag{4.56}$$

$$(A^{\pm})_{ij}=\exp(\pm i\eta_i)\,\delta_{ij}, \tag{4.57}$$

then we can easily show that

$$\boldsymbol{\chi}=\mathbf{X}^{+}(\mathbf{U}\mathbf{A}^{+}\mathbf{U}^{\mathrm{T}})^{2}(\mathbf{X}^{-})^{-1}. \tag{4.58}$$

Here the channel $i=1$ (I) corresponds to dissociation (Rydberg state v_{R}) and $i=2-(I-1)$ correspond to ionization continua (v^{+}). Using the explicit expressions for **U** (Giusti 1980) and **K** (equation (4.20)), we obtain

$$(\mathbf{U}\mathbf{A}^{+}\mathbf{U}^{\mathrm{T}})^{2}=1-\frac{2\mathrm{i}}{\xi^{2}+1}\pi K-\frac{2}{\xi^{2}+1}(\pi K)^{2}. \tag{4.59}$$

Neglecting the R dependence of the quantum defect ($\mu(R)\approx\bar{\mu}$), we can obtain

$$\chi_{v^{+}v_{\mathrm{R}}}=-\frac{2}{\xi^{2}+1}\exp(\pm i\pi\bar{\mu})\,\xi_{v^{+}}\xi_{v_{\mathrm{R}}}, \tag{4.60a}$$

$$\chi_{v_{\mathrm{R}}v_{\mathrm{R}}}=\exp(2i\pi\bar{\mu})\left(1-\frac{2}{\xi^{2}+1}\xi_{v_{\mathrm{R}}}^{2}\right). \tag{4.60b}$$

As is seen from equations (4.54) and (4.60*a*), the final vibrational state distribution in photo-ionization is proportional to $\xi_{v^{+}}^{2}$, that is

$$\text{vibrational branching ratio}\propto\xi_{v^{+}}^{2}. \tag{4.61}$$

On the other hand, the resonant photo-ionization profile is determined by the second term of equation (4.54). Expanding the energy parameter ν around the resonance position $\nu_0=1/(2\epsilon_0)^{1/2}=n_*$ (effective principal quantum number) as $\nu-\nu_0\approx\frac{1}{2}\nu_0^{3}(\epsilon-\epsilon_0)$, we have

$$|\chi_{v_{\mathrm{R}}v_{\mathrm{R}}}-\exp(-2\pi i\nu)|^{-2}\approx\frac{(\Gamma/2)^{2}}{(\epsilon-\epsilon_0)^{2}+(\Gamma/2)^{2}}\Big/\left(\frac{2}{\xi^{2}+1}\xi_{v_{\mathrm{R}}}^{2}\right)^{2}, \tag{4.62}$$

where the bandwidth Γ is given by

$$\Gamma=\frac{1}{\pi n_*^{3}}\frac{4}{\xi^{2}+1}\xi_{v_{\mathrm{R}}}^{2}. \tag{4.63}$$

Using equation (4.61) and assuming that $\xi_{v^{+}}\approx V_0\langle v^{+}|F_{\mathrm{d}}\rangle$, where V_0 represents the average strength of electronic coupling $V(R)$, we have determined the repulsive part of

the potential curve of the dissociative superexcited state B' $^2\Delta$ from the experimentally observed vibrational branching ratio. Then, by using equation (4.63), the electronic coupling strength V_0 is estimated to be about 0·002 atomic units from the observed bandwidth of $6\,\mathrm{d}\delta(v=4)$. In order to make sure that the above-mentioned simple Franck–Condon factor analysis is valid, a full MQDT calculation with the information obtained above is also carried out. The results are shown in table 2. This table clearly proves that the vibrational auto-ionization can be safely neglected for the $\Delta v \geqslant 2$ transitions. The photo-ionization spectrum corresponding to the $n\mathrm{d}\delta$ resonances is also calculated theoretically and is shown in figure 24(*b*) in comparison with experiment.

The analysis explained above clearly indicates that the combination of the REMPI experiment and its analysis by MQDT is very useful and effective for revealing the nature of the superexcited states. The information deduced from this kind of analysis can be usefully employed to investigate other various dynamic processes involving these superexcited states. Another significant and intriguing fact is the role of the electronic auto-ionization via a dissociative superexcited state of the first kind. The electronic auto-ionization gives a very different propensity rule from that of the vibrational auto-ionization, and the vibrational distribution is essentially given by the Franck–Condon-like factor ξ_v. It is rather surprising that the two-step ionization process, Rydberg state→dissociative state→auto-ionization, dominates the one-step vibrational auto-ionization. This phenomenon was actually first found and analysed by Giusti and Jungen (1984) for the case of NO $^2\Pi$. This is expected to be a general phenomenon, because the electronic coupling seems to be generally quite strong compared with the rovibrational coupling represented by the R dependence of the quantum defect.

The importance of the dissociative superexcited state should also be noted in the analysis of photoelectron spectrum in the case when only the first kind of superexcited states are involved (Nakamura 1975). Figure 26 shows a schematic potential diagram which includes one attractive ($E_s(R)$) and one dissociative ($E_d(R)$) superexcited state of the first kind. The observed photoelectron spectrum or vibrational state distribution of a molecular ion is a superposition of two transitions: auto-ionization from the attractive superexcited state, and autoionization from the dissociative state. Since such a transition that conserves the internal (electronic) energy is considered to be dominant, these two are expected to give very different vibrational state distributions as designated by the curves E' and E'', respectively. These two curves are defined as

$$E - E_s(R) = E' - E_{\mathrm{ion}}(R), \tag{4.64a}$$

$$E - E_d(R) = E'' - E_{\mathrm{ion}}(R). \tag{4.64b}$$

Table 2. Photoelectron branching ratio. Comparison of the Franck–Condon factor analysis (FCF) and the MQDT analysis (Nakashima *et al.* 1989).

	$v_f=0$		$v_f=1$		$v_f=2$	
State	FCF	MQDT	FCF	MQDT	FCF	MQDT
5dδ	1·00	1·00	0·10	0·10	0·18	0·21
6dδ	1·00	1·00	0·40	0·39	0·30	0·32
7dδ	1·00	1·00	0·50	0·50	0·48	0·54
8dδ	1·00	1·00	0·85	0·86	0·20	0·20
9dδ	1·00	1·00	0·96	0·97	0·15	0·16

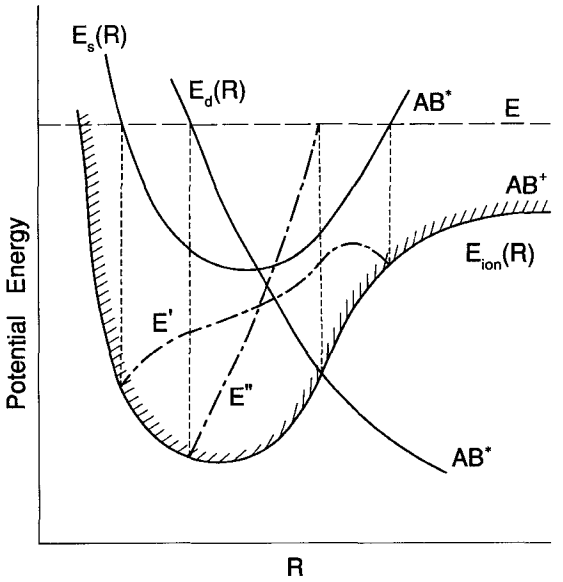

Figure 26. Internal (vibrational) energy distribution of molecular ion by electronic auto-ionization. E' represents that for the case of auto-ionization of the attractive superexcited state $E_s(R)$. E'' represents that in the case of $E_d(R)$.

The auto-ionization from the dissociative state gives a higher vibrational state distribution. Since dissociative superexcited states are not well known despite the fact that these are expected to exist in various molecules, analysis of the photoelectron spectrum should be carried out with care.

4.4. *Dissociative recombination, vibrational transition and associative ionization*

Dissociative recombination is a process to produce neutral species (atoms or moleclues) from positive molecular ions by recombination collisions with slow electrons. A dissociative superexcited state of the first kind plays a crucial role in this process. This is considered to be an important process in various application fields such as dense plasma and astronomy and has been attracting much academic interest as well (Mitchell and Guberman 1989). There are two kinds of process:

(1) a direct process, in which an incident electron is captured directly into the dissociative superexcited state and
(2) an indirect process, in which an electron is first captured into a rovibrationally excited Rydberg state.

Thus both kinds of superexcited state again participate in the process, and the two-step formalism of MQDT described in section 4.2 can be usefully employed. The effects of a countable infinite number of Rydberg states can be taken into account nicely by this theory. The most decisive factor is whether the dissociative state crosses the ionic state near the equilibrium internuclear distance or not.

Here, we discuss, as an example, the dissociative recombination of H_2^+ and its isotopic molecules via the lowest doubly excited dissociative state $^1\Sigma_g\,(2p\sigma_u)^2$ (Takagi and Nakamura 1986, Nakashima *et al.* 1987). Information on the basic quantities $\mu(R)$ and $V(R)$ and also the potential energy curves of the dissociative state is taken from previous scattering calculations (Takagi and Nakamura 1981). The potential energy

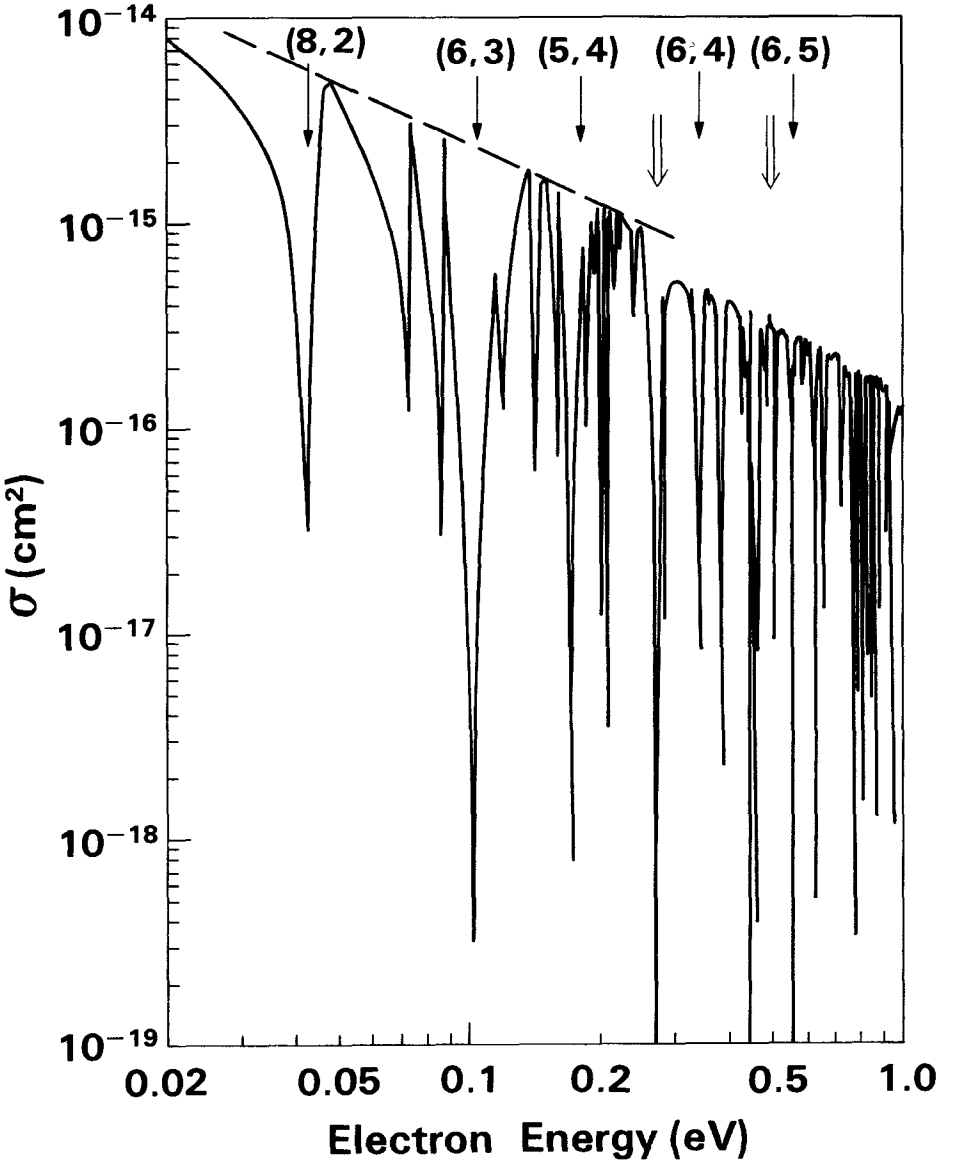

Figure 27. Dissociative recombination cross-section as a function of electron energy for H_2^+ ($v=1$). Single arrows indicate the closed-channel Rydberg states (n, v) and double arrows show the opening of the inelastic channels $v=2$ and 3 (Nakashima *et al.* 1987).

curves of H_2 near the ionization threshold are shown in figure 21. The doubly excited state $^1\Sigma_g(2p\sigma_u)^2$ is known to couple almost exclusively to the dδ partial wave, and thus the cross-sections for dissociative recombination and vibrational transition are given by equations (4.29) and (4.30) with $\rho_i=\frac{1}{4}$. This statistical factor comes from the fact that only the singlet scattering contributes to the dissociative recombination. Thus the cross-sections for the vibrational transitions calculated from equation (4.30) are those for the singlet dδ partial wave scattering. Figures 27, 29 and 30 show some of the calculated results. Figure 27 shows the cross-section for the dissociative recombination

of H_2^+ ($v_i = 1$). The rich structure seen in this figure is due to the infinite number of closed-channel Rydberg states. Each dip represents a resonance, corresponding to a vibrationally excited Rydberg state (n, v). Some of them are indicated by arrows. The double arrows in the figure indicate the opening of vibrationally inelastic channels ($v^+ = 2, 3$). The broken curve is the envelope of the curves, indicating roughly the E^{-1} dependence on the electron energy E, which essentially comes from the $1/k^2$ in equation (4.29). Figure 28 shows the recent merging beam experiment (Hus *et al.* 1988). Although

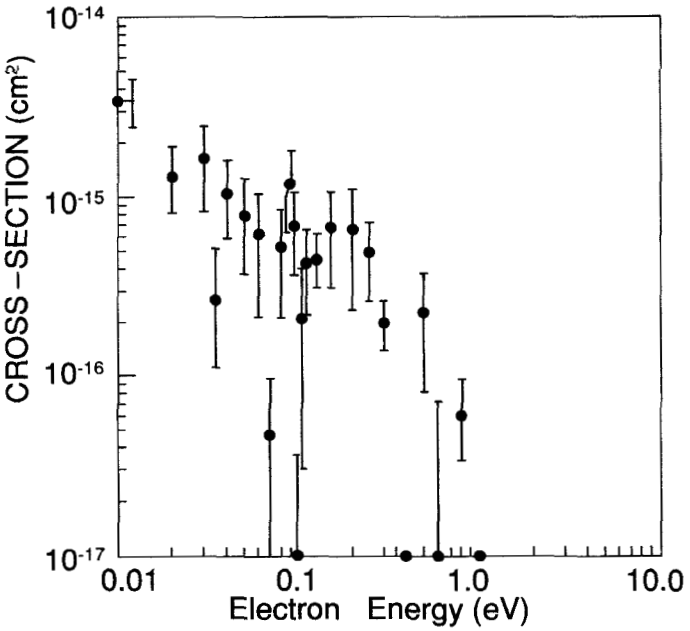

Figure 28. Experimentally observed cross-section of dissociative recombination (Hus *et al.* 1988).

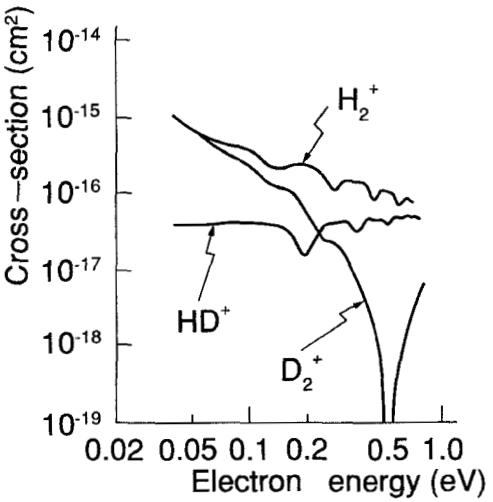

Figure 29. Isotope effect in dissociative recombination of H_2^+ ($v = 3$). The cross-sections are convoluted as described in the text.

a detailed comparison with our theoretical work is still premature, the agreement seems to be quite good (the main vibrational state in the H_2^+ beam is considered to be $v=1$). Not only the sharp dip at $E\approx 0{\cdot}1$ eV but also the absolute value of the cross-section are in good accordance with each other. Figure 29 shows an interesting isotope effect for the case $v_i=3$. In order to make a direct comparison possible, the cross-sections are convoluted with use of the triangular apparatus function of half-width 0·04 eV. This isotope effect can be explained by the two facts that the energy dependence apart from the $1/k^2$ dependence is mainly determined by the factor ξ_v defined by equation (4.20) and the fact that this factor has different energy dependences for H_2^+ ($v=3$), HD^+ ($v=3$) and D_2^+ ($v=3$). $\xi_{v=3}(D_2^+)$ happens to have a zero at $E\approx 0{\cdot}5$ eV, which causes a large dip in the cross-section there. On the other hand, $|\xi_{v=3}(HD^+)|$ increases strongly with increasing energy in the energy region that we are interested in and roughly cancels the factor $1/k^2$. Figure 30 shows the convoluted cross-sections for the dissociative recombination cross-section and also the vibrational transitions ($v_f^+=0$–3) for HD^+ ($v=1$). This figure tells clearly that the energy dependence of the vibrational transitions resembles very much that of the dissociative recombination. This implies that even the vibrational transitions are dictated by the factors ξ_v. That is to say, the dominant pathway for the vibrational transition $v_i\rightarrow v_f$ is the two-step process via the dissociative superexcited state d, that is $v_i\rightarrow d\rightarrow v_f$.

The above-mentioned features can be substantiated by the following simple analysis of the MQDT approach. Assuming that no closed channel is involved, employing the first-order perturbation approximation to the **K** matrix as we did in section 4.2, and using the results described in the Appendix of the paper by Giusti (1980), we can obtain the following expressions for the **S** matrix elements:

$$S_{dv_i}\approx\frac{-2\mathrm{i}}{1+\xi^2}\sum_v \xi_v M_{vv_i}, \tag{4.65}$$

$$S_{v_fv_i}\approx\sum_v M_{v_fv}M_{vv_i}-\frac{2}{1+\xi^2}\sum_{v,v'} M_{v_fv'}\xi_{v'}\xi_v M_{vv_i}, \tag{4.66}$$

where

$$M_{vv'}=\langle v|\exp[\mathrm{i}\pi\mu(R)]|v'\rangle. \tag{4.67}$$

Since the R dependence of $\mu(R)$ is not strong and thus the $|M_{vv'}|$ ($v\neq v'$) values are small compared with the diagonal elements $|M_{vv}|$, we retain only the diagonal elements of **M**. Then we have

$$S_{dv_i}\approx-\frac{2\mathrm{i}}{1+\xi^2}\xi_{v_i}M_{v_iv_i}, \tag{4.68}$$

$$S_{v_iv_i}\approx M_{v_iv_i}^2\left(1-\frac{2}{1+\xi^2}\xi_{v_i}^2\right), \tag{4.69}$$

$$S_{v_fv_i}\approx-\frac{2}{1+\xi^2}M_{v_fv_f}\xi_{v_f}\xi_{v_i}M_{v_iv_i}. \tag{4.70}$$

Since $|M_{vv}|\approx 1$, the similar energy dependence of the various cross-sections can be explained by the fact that the common factor ξ_{v_i} appears in the above expressions.

The role played by the dissociative superexcited state in the vibrational transitions gives another example to show the importance of this kind of state. It should not be

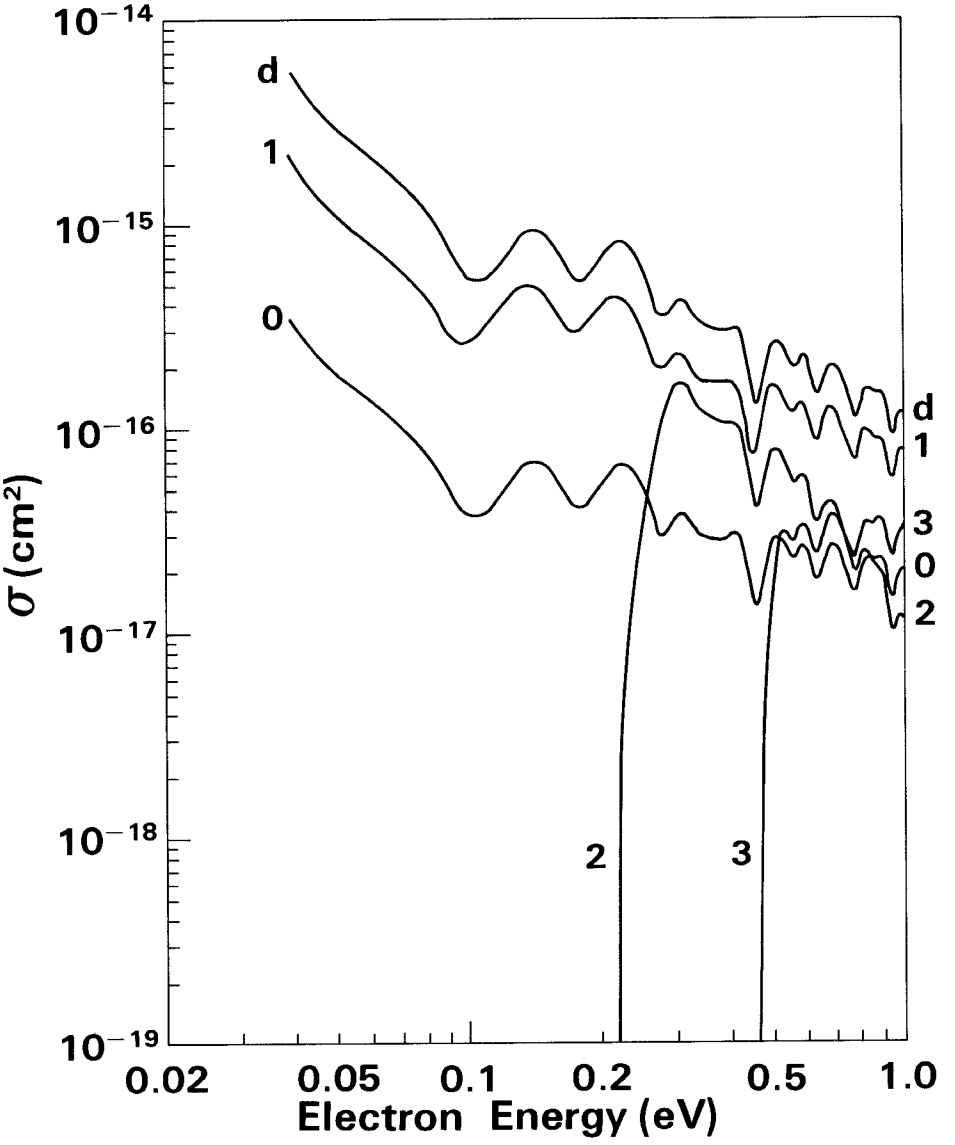

Figure 30. Convoluted cross-sections for dissociative recombination (*d*) of HD^+ ($v=1$) and for vibrational transitions $v=1\rightarrow 0$–3.

Table 3. Dissociative recombination rate $\alpha=\alpha_0\,[100/T(\mathrm{K})]^{\gamma}\,\mathrm{cm^3\,s^{-1}}$ (Nakashima *et al.* 1987).

	H_2^+		HD^+		D_2^+	
v_i	α_0	γ	α_0	γ	α_0	γ
0	$2{\cdot}31\times10^{-8}$	0·29	$2{\cdot}26\times10^{-8}$	0·44	$4{\cdot}11\times10^{-9}$	0·12
1	$1{\cdot}81\times10^{-7}$	0·50	$1{\cdot}54\times10^{-7}$	0·47	$1{\cdot}19\times10^{-7}$	0·49
2	$1{\cdot}34\times10^{-8}$	0·66	$1{\cdot}58\times10^{-7}$	0·60	$1{\cdot}54\times10^{-7}$	0·52
3	$1{\cdot}98\times10^{-8}$	0·32	$6{\cdot}46\times10^{-10}$	−0·16	$6{\cdot}34\times10^{-8}$	0·83
4	$3{\cdot}26\times10^{-8}$	0·77	$5{\cdot}55\times10^{-8}$	0·58	$4{\cdot}02\times10^{-8}$	0·43

forgotten, however, that the complicated resonance structures in the cross-section as a function of energy are the manifestations of the interference between the indirect and direct processes and thus are produced by the existence of the closed-channel Rydberg states. Interestingly, these resonances appear almost exclusively as dips. This can be explained again by the fact that the off-diagonal elements $M_{vv'}$ are smaller than ξ_v values, since Fano's resonance profile index q corresponds to $M_{vv_i}/\xi_v\xi_{v_i}$. A very rough estimate of the rate constants of dissociative recombination was made by using the straight-line envelopes like that shown in figure 27. Assuming the energy dependence of the cross section to be $\sigma = AE^{-\beta}$, we have the following expression for the rate constant α:

$$\alpha = A\left(\frac{8}{\pi m_e}\right)^{1/2}\Gamma(2-\beta)(k_B T)^{1/2-\beta}, \tag{4.71}$$

where m_e is the electron mass, k_B is the Boltzmann constant and T is the temperature. The results are summarized in table 3.

As has frequently been pointed out so far, information on the quantum defect $\mu(R)$, the electronic coupling $V(R)$ and the potential curves of superexcited states is crucial to understanding the dynamic processes such as dissociative recombination. Such information is, however, very scarce. Quantum-chemical calculations of these quantities and also the MQDT analyses of the REMPI experiments are really desired. A nice example of the former case is CH. Recently, Takagi *et al.* (1990) carried out an elaborate quantum-chemical calculation for this system and estimated the dissociative recombination rate constant to be about $1{\cdot}12 \times 10^{-7}\,\mathrm{cm^3\,s^{-1}}$ at $T = 120\,\mathrm{K}$ which is in fairly good agreement with the merging-beam experiment (Mitchell and McGowan 1978). A good example for the second case is NO as described in the previous section. With use of the information obtained there (Nakashima *et al.* 1989) and also by Raoult (1987), the various dynamic processes of NO can be investigated.

The inverse process of dissociative recombination, that is associative ionization, has also been studied recently (Urbain and Giusti-Suzor 1987, Takagi and Nakamura 1988). Although some additional care is required with respect to the initial state, the calculations can be done essentially in the same way as dissociative recombination. The rotationally unresolved results are shown in figure 31 for the process $H(2s) + H \rightarrow H_2^+(v)$

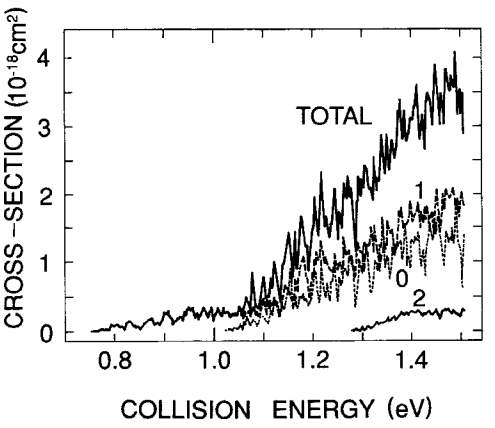

Figure 31. Cross-section for the associative ionization $H(2s) + H \rightarrow H_2^+(v) + e$. The numbers in the figure indicate the final vibrational quantum numbers.

+e. The dominant contribution comes from $v=0$ and 1. There are many resonances caused by the indirect processes via intermediate vibrationally excited Rydberg states. These have survived the summation over L and v (see equation (4.31)).

5. Concluding remarks

The basic interactions governing electronic transitions in various molecular dynamic processes are classified into the following four types:

(1) non-adiabatic radial coupling,
(2) non-adiabatic rotational (Coriolis) coupling,
(3) configuration interaction between discrete superexcited state of first kind and electronic continuum and
(4) rovibronic coupling among Rydberg states.

The first two can be treated in a unified way by introducing the DS representation in spite of their difference in nature. The semiclassical theory for these non-adiabatic transitions was proved to be powerful. The wide applicability of the semiclassical theory was demonstrated. The significance of non-adiabatic tunnelling is emphasized and the working equations are proposed. Although no discussion was given here, the ordinary atom–diatom chemical reaction can be viewed as a vibrationally non-adiabatic transition and can be treated in some cases even analytically by using the semiclassical theory. By employing the hyperspherical coordinate system, a reactive transition (particle rearrangement) can be explicitly shown to occur in a spatially localized region near the so-called 'potential ridge', the watershed dividing the initial and final channel valleys. These features of the chemical reaction are summarized in a recent review article by Ohsaki and Nakamura (1990). This gives another example of the interdisciplinarity of the concept of the non-adiabatic transition.

Superexcited states are classified into two kinds, and their difference in decay mechanism is clarified. A variety of their dynamic processes can be analysed in a unified way to some extent by using the MQDT. A combination of the REMPI experiment and the MQDT analysis was demonstrated to be very powerful and useful to explore the world of highly excited states of molecules. Electronic auto-ionization was shown generally to dominate vibrational auto-ionization. In particular, a dissociative superexcited state of the first kind was found to play an important role in various processes and much more care should be devoted to its existence and dynamical role.

In conclusion, the developments to be made in future are summarized based on the present author's viewpoint. The semiclassical theory for the non-adiabatic transition should be extended to multidimensional cases. This is one of the most challenging and significant problems, since most of the physical phenomena intrinsically occur in a multidimensional space. Although a perturbative golden rule approach to tunnelling proved to be quite successful in some cases (Pacey *et al.* 1986, Siebrand *et al.* 1984a, b), the basic non-perturbative semiclassical theory for multidimensional non-adiabatic tunnelling as well as simple tunnelling should be further developed. The theory should also be generalized into the statistical mechanical framework so that the effects of fluctuation and dissipation can be taken into account (Nasu and Kayanuma 1980, Kayanuma 1982, 1984a, b, 1985, Wolynes 1987, Leggett *et al.* 1987). See also the following works concerning tunnelling (Caldeira and Leggett 1983, Razavy and Pimpale 1988). The role of avoided crossing in the classical chaotic behaviour of the quantum energy spectrum would also be an interesting subject to be investigated

further. An electronically non-adiabatic chemical reaction should of course be an important target of the semiclassical theory. Much effort should also be devoted to non-adiabatic tunnelling which is supposed to play a crucial role in phase change in various fields. Even the most basic two-state one-dimensional theory is not very satisfactory yet.

Concerning the superexcited states, more studies, both spectroscopic and dynamical, are needed without doubt. The dynamics of superexcited states, especially of polyatomic molecules, would open up new interesting fields of physics and chemistry. Complicated chaotic behaviour in both the electronic degrees of freedom and the nuclear (vibrational) degrees of freedom are involved and coupled. Since information on the basic parameters of the superexcited states is so scarce at present, not only the more extensive challenge of quantum chemistry is desired, but also the elaborate interplay between the REMPI-type high-resolution experiment and the MQDT-type theoretical analysis is also required. Another challenging subject is to find and understand uniformly some peculiar modes of collective motion in a variety of quantum-mechanical finite many-body systems with strong interparticle correlation. The interesting collective motions in doubly excited states of atoms have been quite successfully analysed by the algebraic approach and the hyperspherical coordinate approach (for example Herrick (1983), Watanabe and Lin (1986) and Iwai and Nakamura (1989)). On the other hand, mode couplihg and normal-to-local mode transformation in the vibrationally highly excited states have also been extensively studied (for example Child and Halonen (1984) and Levine and Kinsey (1986)). Such systematic studies from the viewpoint of collective motion should be carried out for the superexcited (doubly excited) states of molecules. Generally speaking, strong interparticle coupling causes some kind of phase transition and collective motion of a whole system. It would be a challenging subject to find, if any, a universality or isomorphism among and to comprehend in a unified context the peculiar properties and dynamics of the various kinds of finite many-body system such as systems of nucleons, atomic and molecular electrons, and atoms and molecules.

Acknowledgments

The author would like to thank Mr M. Namiki, Ms R. Suzuki, Dr H. Takagi and Dr K. Nakashima for the collaborations in some of the works reported in this review article. This work was supported in part by a Grant in Aid from the Ministry of Education, Science and Culture of Japan. The numerical computations were carried out at the Computer Center of Institute for Molecular Science.

Appendix A

Derivation of the semiclassical S matrix for the Landau–Zener- and Rosen–Zener-type non-adiabatic transitions

Here we derive the explicit expressions of the semiclassical S matrix given in section 3.3. The method described below is based on the comparison equation method (Miller and Good 1953, Berry and Mount 1972, Dubrovskii 1964).

We start with the conventional time-dependent Schrödinger equation in the diabatic state representation,

$$\mathrm{i}\frac{\mathrm{d}}{\mathrm{d}x}(a_1)=\frac{V}{v}\exp\left(\frac{\mathrm{i}}{v}\int_{-\infty}^{x}\omega(x')\,\mathrm{d}x'\right)a_2, \qquad \text{(A 1 } a\text{)}$$

$$i\frac{d}{dx}(a_2)=\frac{V}{v}\exp\left(-\frac{i}{v}\int_{-\infty}^{x}\omega(x')\,dx'\right)a_1, \tag{A 1 b}$$

where a_n is the expansion coefficient for the diabatic state $n(=1,2)$, $\hbar V$ is the diabatic coupling, $x=vt$ with velocity v, and $\hbar\omega$ represents the difference of the two diabatic state potential energies. The transformation

$$a_2(x)=V^{1/2}\exp\left(-\frac{i}{2v}\int_{-\infty}^{x}\omega(x')\,dx'\right)A(x) \tag{A 2}$$

leads to the following single equation:

$$\left(\frac{d}{dx^2}+\frac{1}{v^2}\Omega^2(x,v)\right)A(x)=0, \tag{A 3}$$

where

$$\Omega^2(x,v)=\frac{1}{4}\left(\frac{\Delta E}{\hbar}\right)^2-\frac{iv}{2}V\frac{d}{dx}\left(\frac{\omega}{V}\right)-v^2\{V,x\}, \tag{A 4}$$

$$(\Delta E)^2=\hbar^2\omega^2(x)+4\hbar^2V^2(x) \tag{A 5}$$

is the adiabatic state energy difference and

$$\{V,x\}=-\frac{1}{2}\frac{d}{dx}\left(\frac{1}{V}\frac{dV}{dx}\right)+\frac{1}{4}\left(\frac{1}{V}\frac{dV}{dx}\right)^2 \tag{A 6}$$

is the Schwartz derivative. The asymptotic solutions of equation (A 3) are written as

$$A(x)\approx\begin{cases}\left(\dfrac{v}{2\Omega}\right)^{1/2}\left[C_1\exp\left(-\dfrac{i}{v}\displaystyle\int_x^{x_1}\Omega\,dx'\right)\right.\\ \left.+C_2\exp\left(\dfrac{i}{v}\displaystyle\int_x^{x_1}\Omega\,dx'\right)\right], \quad \text{for } x\to-\infty & \text{(A 7 a)}\\ \left(\dfrac{v}{2\Omega}\right)^{1/2}\left[C_7\exp\left(\dfrac{i}{v}\displaystyle\int_{x_2}^{x}\Omega\,dx'\right)\right.\\ \left.+C_8\exp\left(-\dfrac{i}{v}\displaystyle\int_{x2}^{x}\Omega\,dx'\right)\right], \quad \text{for } x\to\infty, & \text{(A 7 b)}\end{cases}$$

where x_j $(j=1,2)$ represent the real parts of the complex zeros (b_j) of Ω $(x_1<0,\ x_2>0)$. The transition matrix **T** is defined by

$$\begin{bmatrix}C_7\\C_8\end{bmatrix}=\mathbf{T}\begin{bmatrix}C_1\\C_2\end{bmatrix} \tag{A 8}$$

and is equivalent to the scattering matrix apart from the phase factor.

In order to derive the analytical expression of **T** we employ the following approximations.

(1) ΔE dominancy: at low velocities, ΔE becomes dominant and $\Omega(x,v)$ can be expressed as

$$\Omega(x,v)\approx\frac{1}{2}\frac{\Delta E}{\hbar}-\frac{i}{2}v\frac{1}{(1+W^2)^{1/2}}\frac{dW}{dx}+Q(x,v), \tag{A 9}$$

where $W=(\omega/2)/V$ and $Q(x,v)$ represents a correction. The complex zeros b_j of Ω are approximated by those of ΔE.

(2) The avoided crossing points x_j $(j=1,2)$ are located far from the turning point $x=0$.

Thus the whole problem is divided into the two problems: one for $\mathrm{Re}\,x<0$, the connection between (C_1, C_2) and (C_3, C_4), and the other for $\mathrm{Re}\,x>0$, the connection between (C_5, C_6) and (C_7, C_8) (see figure A 1). Each problem represents a two-transition point problem with order unity in the theory of asymptotic solution of the second-order differential equation (Evgrafov and Fedoryuk 1966, Shibuya 1975); thus this can be solved in terms of the properties of the Weber equation which is the standard equation of this kind (Heading 1962). By the transformation

$$\frac{1}{v}\int_{b_{1,2}}^{x}\Omega(x,v)\,\mathrm{d}x=\frac{1}{2}\int_{\mp 2i\epsilon^{1/2}}^{\xi}(\xi^2+4\epsilon)^{1/2}\,\mathrm{d}\xi, \tag{A 10}$$

the solution $A(x)$ can be expressed in terms of the Weber (parabolic cylinder) function $U(\xi(x))$ as

$$A(x)\approx\left(\frac{v^2(\xi^2+4\epsilon)}{4\Omega^2}\right)^{1/4}U(\xi(x)), \tag{A 11}$$

where

$$\epsilon=\frac{1}{\mathrm{i}\pi v}\int_{b_1}^{b_2}\Omega(x,v)\,\mathrm{d}x\approx\frac{1}{\pi v}\int_{0}^{\mathrm{Im}\,b_2}\mathrm{Re}\left(\frac{\Delta E}{\hbar}\right)\mathrm{d}y+\tfrac{1}{2}\mathrm{i}\equiv\gamma+\tfrac{1}{2}\mathrm{i} \tag{A 12}$$

with $y=\mathrm{Im}\,x$. This method is called the comparison equation method (Miller and Good 1953, Berry and Mount 1972). The connection between the two asymptotic expansions of the Weber function is well known from its Stokes phenomenon (Heading 1962). This is explicitly given as follows:

$$\begin{bmatrix}d_1\\ d_2\end{bmatrix}=D_1\begin{bmatrix}d_3\\ d_4\end{bmatrix}, \tag{A 13}$$

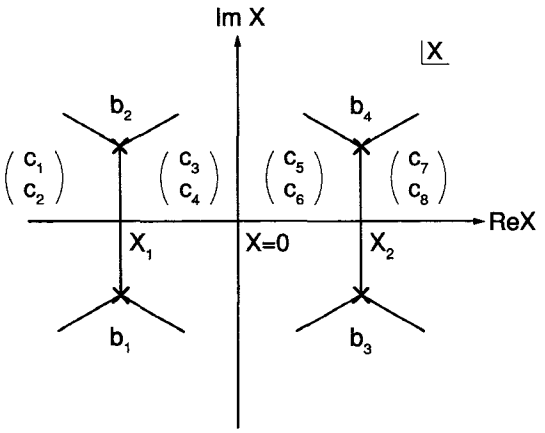

Figure 32. Complex x plane where the b_j $(j=1$–$4)$ are the transition points (zero points of ΔE): (——), the Stokes lines.

where

$$U(\xi\to\mp\infty)=(\xi^2+4\epsilon)^{-1/4}\left[d_{1(3)}\exp\left(\frac{\mathrm{i}}{2}\int_0^{\xi}(\xi^2+4\epsilon)^{1/2}\,\mathrm{d}\xi\right)\right.$$
$$\left.+d_{2(4)}\exp\left(-\frac{\mathrm{i}}{2}\int_0^{\xi}(\xi^2+4\epsilon)^{1/2}\,\mathrm{d}\xi\right)\right], \tag{A 14}$$

$$D_1=\begin{pmatrix} f(\epsilon)[1+\exp(-2\pi\epsilon)]^{1/2}\exp[\mathrm{i}\phi(\epsilon)] & \mathrm{i}\exp(-\pi\epsilon) \\ -\mathrm{i}\exp(-\pi\epsilon) & f^{-1}(\epsilon)[1+\exp(-2\pi\epsilon)]^{1/2}\exp[-\mathrm{i}\phi(\epsilon)] \end{pmatrix}, \tag{A 15}$$

$$f(\epsilon)=|\Gamma(\tfrac{1}{2}+\mathrm{i}\epsilon)|\left(\frac{1}{\pi}\cosh(\pi\epsilon)\right)^{1/2}, \tag{A 16}$$

$$\phi(\epsilon)=\epsilon-\epsilon\ln\epsilon+\arg[\Gamma(\tfrac{1}{2}+\mathrm{i}\epsilon)]. \tag{A 17}$$

First we derive the connection between (C_1, C_2) and (C_3, C_4). Since from equation (A 10) we have

$$\frac{1}{2}\int_0^{\xi}(\xi^2+4\epsilon)^{1/2}\,\mathrm{d}\xi=\frac{1}{v}\int_{x_1}^{x}\Omega\,\mathrm{d}x-\Phi_1 \tag{A 18}$$

with

$$\Phi_1=\frac{1}{2v}\left(\int_{x_1}^{b_1}\Omega\,\mathrm{d}x+\int_{x_1}^{b_2}\Omega\,\mathrm{d}x\right)$$
$$\approx\frac{1}{2v}\int_0^{\mathrm{Im}\,b_1}\frac{1}{\hbar}\Delta E\,\mathrm{d}y,\quad y=\mathrm{Im}\,x, \tag{A 19}$$

we can obtain the following connection formula:

$$\begin{bmatrix}C_3\\C_4\end{bmatrix}=\mathbf{I}\begin{bmatrix}C_1\\C_2\end{bmatrix}. \tag{A 20}$$

where

$$\mathbf{I}=\begin{bmatrix}\exp(\mathrm{i}\Phi_1) & 0\\ 0 & \exp(-\mathrm{i}\Phi_1)\end{bmatrix}\mathbf{D}_1^{-1}\begin{bmatrix}\exp(-\mathrm{i}\Phi_1) & 0\\ 0 & \exp(\mathrm{i}\Phi_1)\end{bmatrix}. \tag{A 21}$$

The same procedure can be employed to derive the connection formula between (C_5, C_6) and (C_7, C_8):

$$\begin{bmatrix}C_7\\C_8\end{bmatrix}=\mathbf{O}\begin{bmatrix}C_5\\C_6\end{bmatrix}, \tag{A 22}$$

where

$$\mathbf{O}=\begin{bmatrix}\exp(\mathrm{i}\Phi_2) & 0\\ 0 & \exp(-\mathrm{i}\Phi_2)\end{bmatrix}\mathbf{D}_2^{-1}\begin{bmatrix}\exp(-\mathrm{i}\Phi_2) & 0\\ 0 & \exp(\mathrm{i}\Phi_2)\end{bmatrix}$$
$$=\mathbf{I}^{\mathrm{T}}\ \text{(transposed)}, \tag{A 23}$$

$$\Phi_2=\frac{1}{2v}\left(\int_{x_2}^{b_3}\Omega\,\mathrm{d}x+\int_{x_2}^{b_4}\Omega\,\mathrm{d}x\right)$$
$$\approx-\frac{1}{2v}\int_0^{\mathrm{Im}\,b_3}\frac{1}{\hbar}\Delta E\,\mathrm{d}y \tag{A 24}$$

and $\mathbf{D}_2$ is the same as $\mathbf{D}_1$ except for ϵ replaced by ϵ' with

$$\epsilon' = \frac{1}{\mathrm{i}\pi v}\int_{b_3}^{b_4} \Omega(x,v)\,\mathrm{d}x \approx \frac{1}{\pi v}\int_0^{\mathrm{Im}\,b_4} \mathrm{Re}\left(\frac{\Delta E}{\hbar}\right)\mathrm{d}y - \frac{\mathrm{i}}{2} = \gamma - \frac{\mathrm{i}}{2}. \tag{A 25}$$

The connection between (C_3, C_4) and (C_5, C_6) is obtained simply as

$$\begin{bmatrix} C_5 \\ C_6 \end{bmatrix} = \begin{bmatrix} \exp(\mathrm{i}\Phi) & 0 \\ 0 & \exp(-\mathrm{i}\Phi) \end{bmatrix}\begin{bmatrix} C_3 \\ C_4 \end{bmatrix}, \tag{A 26}$$

with

$$\Phi = \frac{1}{v}\int_{x_1}^{x_2} \Omega(x,v)\,\mathrm{d}x \approx \frac{1}{v}\int_0^{x_2} \frac{\Delta E}{\hbar}\,\mathrm{d}x + \tau \tag{A 27}$$

and

$$\tau = \tfrac{1}{2}\tan^{-1}\left(\frac{1}{2\gamma}\right) + \gamma \ln\left(\frac{\gamma}{(\gamma^2+\frac{1}{4})^{1/2}}\right), \tag{A 28}$$

where the correction $Q(x,v)$ in equation (A 9) gives the term τ in equation (A 27) within the original Landau–Zener model. The contributions of Q to $\epsilon, \epsilon', \Phi_1$ and Φ_2 are usually neglected. This point remains to be further investigated. The transition matrix $\mathbf{T}$ is given by

$$\mathbf{T} = \mathbf{O}\begin{bmatrix} \exp(\mathrm{i}\Phi) & 0 \\ 0 & \exp(-\mathrm{i}\Phi) \end{bmatrix}\mathbf{I}, \tag{A 29}$$

where

$$\mathbf{I} = \begin{bmatrix} [1-\exp(-2\pi\gamma)]^{1/2}\exp[-\mathrm{i}\phi_0(\gamma)] & \exp(-\pi\gamma)\exp(\mathrm{i}\sigma_0) \\ -\exp(-\pi\gamma)\exp(-\mathrm{i}\sigma_0) & [1-\exp(-2\pi\gamma)^{1/2}\exp[\mathrm{i}\phi_0(\gamma)] \end{bmatrix}, \tag{A 30}$$

$$\phi_0(\gamma) = \tfrac{1}{2}[\phi(\epsilon) + \phi(\epsilon')]$$

$$= \gamma - \frac{\gamma}{2}\ln\left(\gamma^2+\frac{1}{4}\right) + \arg[\Gamma(1+\mathrm{i}\gamma)] - \frac{\pi}{4} + \frac{1}{2}\tan^{-1}\left(\frac{1}{2\gamma}\right), \tag{A 31}$$

$$\sigma_0 = -2\Phi_1 = 2\Phi_2. \tag{A 32}$$

$|T_{12}|^2$ obtained from equation (A 29) gives the same overall transition probability as equation (3.31) in the main text. However, we want to generalize the theory so as to be extendable to a multilevel problem in the spirit of path-integral formulation (Miller and George 1972, Miller 1974). In the above procedure we have been considering the time evolution of the system, assuming tacitly a certain kind of common trajectory $R(t)$. Now, we take into account the fact that there are two possible classical trajectories along the adiabatic potential curves $E_n(R)$ $(n=1,2)$ $(E_2(R) > E_1(R))$ and that there holds a general correspondence

$$\frac{1}{v}\int \Delta E\,\mathrm{d}x \leftrightarrow \int [k_1(R) - k_2(R)]\,\mathrm{d}R, \tag{A 33}$$

where

$$k_n(R) = \left(\frac{2\mu}{\hbar^2}[E - E_n(R)]\right)^{1/2}. \tag{A 34}$$

Then, we can generalize the quantities γ, σ_0 and Φ in the spirit of the path-integral formulation. Taking into account the phase contribution from the scattering at $R > R_X$ and also the requirement that the scattering matrix should coincide with the proper potential scattering matrix in the adiabatic ($\delta \to \infty$) and the diabatic ($\delta \to 0$) limits, we finally obtain the expression for the **S** matrix in the form (2.1). It should be noted that γ is replaced by δ/π and $\phi_S = \tau - \phi_0$. In the above-mentioned procedure based on the comparison equation method it is assumed that the adiabatic potential energy difference ΔE has complex zeros of order $\frac{1}{2}$ (thus the corresponding non-adiabatic coupling always has poles of order unity there), as is seen from the transformation (A 10). See also Crothers (1971) for other derivations.

The method mentioned above cannot be used to derive the Rosen–Zener formula (3.36). Employing the transformation used by Dykhne and Chaplik (1963) and a new asymptotic expansion of the Weber function (Crothers 1972), Crothers derived equation (3.36) with sech δ in place of $2[p_{RZ}(1-p_{RZ})]^{1/2}$ (Crothers 1976). It should be noted that there is no Stokes phase correction. In the Landau–Zener model the ordinary asymptotic expansion of the Weber function for a large argument is used. The large argument physically corresponds to the divergence of the diabatic potential curves away from the crossing point. In the Rosen–Zener model a new asymptotic expansion is required for the case when both the argument and the index are large, which corresponds to strong diabatic coupling. The scattering matrix expression (2.1) with equations (3.34) and (3.35) is a simple generalization in the same spirit of path-integral formulation as that used in the Landau–Zener case.

Appendix B

Derivation of equations (3.77)

Being based on the diagram in figure 15, we derive here the expressions for the matrix $\tilde{\mathbf{A}}^{H}$ given by equations (3.77). The quantities V'_n and V''_n ($n = 1, 2$) in this diagram represent as before the coefficients of the outgoing and incoming waves respectively along the adiabatic potential $E_n(R)$ on the right side of the crossing region and U'_n and U''_n ($n = 1, 2$) those on the left side (see equations (3.69) and (3.70)). In terms of these coefficients we introduce the following vectors:

$$\mathbf{U}'^{(n)} = \begin{bmatrix} U_1'^{(n)} \\ U_2'^{(n)} \end{bmatrix}$$
$$\mathbf{V}'^{(n)} = \begin{bmatrix} V_1'^{(n)} \\ V_2'^{(n)} \end{bmatrix}. \tag{B 1}$$

Now U' and V' are connected by the non-adiabatic transition

$$V' = \mathbf{O}_X U' \tag{B 2a}$$

and U'' and V'' by

$$U'' = \mathbf{I}_X V'' \tag{B 2b}$$

where $\mathbf{O}_X$ and $\mathbf{I}_X$ are given by equations (3.22) and (3.23). Since U_2' and U_2'' and also V_2'' and V_2' are directly related by wave propagation and reflection along $E_2(R)$, we have

$$\begin{aligned} \frac{U_2'}{U_2''} &= L^2(b_2, R_X) \\ \frac{V_2''}{V_2'} &= L^2(R_X, c_2), \end{aligned} \tag{B 3}$$

where

$$L(A,B) = \exp\left(\mathrm{i}\gamma_2(A,B) + \frac{\pi}{4}\mathrm{i}\right). \tag{B 4}$$

From equations (B 2) and (B 3) we can obtain the following expressions for the matrix $\tilde{\mathbf{A}}^H$ (see the definition of the matrix $\mathbf{A}$ in equation (3.68)):

$$\tilde{A}^H_{11} = \frac{L(b_2,c_2)\exp(\pi\mathrm{i}/4)O_{12}I_{21}}{L^*(b_2,c_2)\exp(-\pi\mathrm{i}/4) - L(b_2,c_2)\exp(\pi\mathrm{i}/4)O_{22}I_{22}}, \tag{B 5a}$$

$$\tilde{A}^H_{22} = \frac{L^*(b_2,R_X)L(R_X,c_2)I_{12}O_{21}}{L^*(b_2,c_2)\exp(-\pi\mathrm{i}/4) - L(b_2,c_2)\exp(\pi\mathrm{i}/4)O_{22}I_{22}}, \tag{B 5b}$$

$$\tilde{A}^H_{12} = \tilde{A}^H_{21} = \frac{L^*(b_2,c_2)\exp(-\pi\mathrm{i}/4)O_{11} - L(b_2,c_2)\exp(\pi\mathrm{i}/4)I_{22}}{L^*(b_2,c_2)\exp(-\pi\mathrm{i}/4) - L(b_2,c_2)\exp(\pi\mathrm{i}/4)O_{22}I_{22}}, \tag{B 5c}$$

where O_{nm} and I_{nm} are the (n,m) elements of the matrices $\mathbf{O}_X$ and $\mathbf{I}_X$ respectively. Insertion of equation (B 4) and the explicit expressions for O_{nm} and I_{nm} given by equations (3.22) and (3.23) leads directly to equations (3.77). Unitarity and symmetry of the matrix $\tilde{\mathbf{A}}^H$ can be directly proved.

Appendix C

Unitarity of the S matrix defined by equation (4.16)

We prove here the symmetry of the real matrix $\mathfrak{R}$ of equation (4.15), because this guarantees the unitarity of $\mathbf{S}$.

First, we show the unitarity of $\mathbf{J}^{\pm}$ which is expressed as (see equations (4.27), (4.28) and (4.35))

$$J^{\pm}_{i\alpha} = \begin{cases} \sum_v \langle \mathrm{i}|\exp[\pm\mathrm{i}(\pi\mu\pi_A(R)+\eta_\alpha)]|v\rangle U_{v\alpha}, & \text{for } i = v^+, \\ U_{d\alpha}\exp(\pm\mathrm{i}\eta_\alpha), & \text{for } i = d. \end{cases} \tag{C 1}$$

From this expression, we have

$$\begin{aligned} \sum_i (J^{\pm})^{\dagger}_{\alpha' i} J^{\pm}_{i\alpha} &= \sum_{v^+}\sum_v\sum_{v'} (U^{-1})_{\alpha' v'} U_{v\alpha} \\ &\quad \times \langle v'|\exp[\mp\mathrm{i}(\pi\mu_A(R)+\eta_{\alpha'})]|v^+\rangle\langle v^+|\exp[\pm\mathrm{i}(\pi\mu_A(R)+\eta_\alpha)]|v\rangle \\ &\quad + \sum_d (U^{-1})_{\alpha' d} U_{d\alpha}\exp[\pm\mathrm{i}(\eta_\alpha - \eta_{\alpha'})] \\ &= \sum_{\gamma = v^+, d} (U^{-1})_{\alpha'\gamma} U_{\gamma\alpha}\exp[\pm\mathrm{i}(\eta_\alpha - \eta_{\alpha'})] \\ &= \delta_{\alpha\alpha'}. \end{aligned} \tag{C 2}$$

Here the completeness of the vibrational manifold $\{v^+\}$ and the unitarity of $\mathbf{U}$ are assumed. Next, the unitarity of $\boldsymbol{\chi}$ can be proved:

$$\begin{aligned}\boldsymbol{\chi}^\dagger\boldsymbol{\chi} &= (\mathbf{J}^{-\dagger})^{-1}\mathbf{J}^{+\dagger}\mathbf{J}^{+}(\mathbf{J}^{-})^{-1} \\ &= (\mathbf{J}^{-\dagger})^{-1}(\mathbf{J}^{-})^{-1} \\ &= (\mathbf{J}^{-}\mathbf{J}^{-\dagger})^{-1} = 1. \end{aligned} \tag{C 3}$$

Finally, the symmetry of $\mathfrak{R}$ is shown as follows:

$$\begin{aligned}\mathfrak{R}^{\mathrm{T}}(\text{transposed}) &= \mathrm{i}(1+\boldsymbol{\chi}^{\mathrm{T}})^{-1}(1-\boldsymbol{\chi}^{\mathrm{T}}) \\ &= \mathrm{i}[1+(\boldsymbol{\chi}^{-1})^*]^{-1}[1-(\boldsymbol{\chi}^{-1})^*] \\ &= -\mathrm{i}(1+\boldsymbol{\chi}^*)^{-1}\boldsymbol{\chi}^*(\boldsymbol{\chi}^{-1})^*(1-\boldsymbol{\chi}^*) \\ &= [\mathrm{i}(1+\boldsymbol{\chi})^{-1}(1-\boldsymbol{\chi})]^* \\ &= \mathfrak{R}^* \\ &= \mathfrak{R}. \end{aligned} \tag{C 4}$$

References

ABE, Y., and PARK, J. Y., 1983, *Phys. Rev.* C, **28,** 2316.

ACHIBA, Y., and KIMURA, K., 1989, *Chem. Phys.*, **129,** 11.

BAER, M., 1985, *Theory of Chemical Reaction Dynamics*, Vol. II, edited by M. Baer (Boca Raton, Florida: CRC), p. 219.

BARANY, A., 1979, Uppsala University Institute of Theoretical Physics, Report No. 25.

BERKOWITZ, J., 1979, *Photoabsorption, Photoionization, and Photoelectron Spectroscopy* (New York: Academic).

BERRY, M. V., and MOUNT, K. E., 1972, *Rep. Prog. Phys.*, **35,** 315.

BERRY, R. S., and NIELSEN, S. E., 1970, *Phys. Rev.* A, **1,** 395.

BESWICK, J. A., SHAPIRO, M., and SHARON, R., 1977, *J. chem. Phys.*, **67,** 4045.

BORDAS, C., LABASTIE, P., CHEVALEYRE, J., and BROYER, M., 1989, *Chem. Phys.*, **129,** 21.

CALDEIRA, A. O., and LEGGETT, A. J., 1983, *Ann. Phys., N.Y.*, **149,** 374.

CHANG, E. S., and FANO, U., 1972, *Phys. Rev.* A, **6,** 173.

CHILD, M. S., 1974a, *J. molec. Spectrosc.*, **53,** 280; 1974b, *Molecular Collision Theory* (New York: Academic); 1979, *Atom–Molecule Collision Theory*, edited by R. B. Bernstein (New York: Plenum), p. 427.

CHILD, M. S., and HALONEN, L., 1984, *Adv. chem. Phys.*, **57,** 1.

COLLINS, L. A., and SCHNEIDER, B. I., 1983, *Phys. Rev.* A, **27,** 101.

COVENEY, P. V., CHILD, M. S., and BARANY, A., 1985, *J. Phys.* B, **18,** 4557.

CROTHERS, D. S. F., 1971, *Adv. Phys.*, **20,** 405; 1972, *J. Phys.* A, **5,** 1680; 1976, *J. Phys.* B, **9,** 635; 1981, *Adv. atom. molec. Phys.*, **17,** 55.

DASTIDAR, K. R., 1983, *Chem. Phys. Lett.*, **101,** 254.

DASTIDAR, K. R., GANGULY, S., and DASTIDAR, T. K. R., 1986, *Phys. Rev.* A, **33,** 2106.

DASTIDAR, K. R., and LAMBROPOULOS, P., 1982, *Chem. Phys. Lett.*, **93,** 273; 1984, *Phys. Rev.* A, **29,** 183.

DEHMER, P. M., and CHUPKA, W. A., 1976, *J. chem. Phys.*, **65,** 2243.

DEMKOV, Y. N., 1964, *Soviet Phys. JETP*, **18,** 138.

DEMKOV, Y. N., and OSHEROV, V. I., 1968, *Soviet Phys. JETP*, **26,** 916.

DEMKOV, Y. N., OSTROVSKII, V. N., and SOLOV'EV, E. A., 1978, *Phys. Rev.* A, **18,** 2089.

DEVAULT, D., 1984, *Quantum Mechanical Tunneling in Biological Systems* (Cambridge University Press).

DILL, D., and JUNGEN, CH., 1980, *J. phys. Chem.*, **84,** 2116.

DIXIT, S. N., LYNCH, D. L., MCKOY, B. V., and HAZI, A. U., 1989, *Phys. Rev.* A, **40,** 1700.

DUBROVSKII, G. V., 1964, *Soviet Phys. JETP*, **19,** 591.

DYKHNE, A. M., and CHAPLIK, A. V., 1963, *Soviet Phys. JETP*, **16,** 631.

EU, B. C., 1984, *Semiclassical Theories of Molecular Scattering* (Berlin: Springer).
EVGRAFOV, M. A., and FEDORYUK, M. V., 1966, *Russian mathematical Surveys*, **21**, 1.
FANO, U., 1970, *Phys. Rev.* A, **2**, 353; 1975, *J. opt. Soc. Am.*, **65**, 979; 1981, *Comments atom molec. Phys.*, **10**, 223; 1983, *Comments atom. molec. Phys.*, **13**, 157.
FREDIN, S., GAUYACQ, D., HORAIN, M., JUNGEN, CH., and LEFEBVRE, G., 1987, *Molec. Phys.*, **60**, 825.
GANGULY, S., and DASTIDAR, T. R., 1988, *Phys. Rev.* A, **37**, 1363.
GANGULY, S., DASTIDAR, K. R., and DASTIDAR, T. K. R., 1986, *Phys. Rev.* A, **33**, 337.
GASPARD, P., RICE, S. A., and NAKAMURA, K., 1989, *Phys. Rev. Lett.*, **63**, 930.
GIUSTI, A., 1980, *J. Phys.* B, **13**, 3867.
GIUSTI-SUZOR, A., and JUNGEN, CH., 1984, *J. chem. Phys.*, **80**, 986.
GIUSTI-SUZOR, A., and LEFEBVRE-BRION, H., 1980, *Chem. Phys. Lett.*, **76**, 132; 1984, *Phys. Rev.* A, **30**, 3057.
GOLUBKOV, G. V., and IVANOV, G. K., 1981, *Soviet Phys. JETP*, **53**, 674; 1984, *J. Phys.* B, **17**, 747.
GOLUBKOV, G. V., IVANOV, G. K., and CHERLINA, I. E., 1983, *Opt. Spectrosc.*, **54**, 251.
GREENE, C. H., and JUNGEN, CH., 1985, *Adv. atom. molec. Phys.*, **21**, 51.
GUBERMAN, S. L., 1983, *J. chem. Phys.*, **78**, 1404.
HARA, S., and SATO, H., 1984, *J. Phys.* B, **17**, 4301.
HATANO, Y., 1988, *Radiochim. Acta*, **43**, 119.
HAZI, A. U., 1983, *Electron–Atom and Electron–Molecule Collisions*, edited by J. Hinze (New York: Plenum), p. 103.
HEADING, J., 1962, *An Introduction to Phase-integral Methods* (London: Methuen).
HERRICK, D. R., 1983, *Adv. chem. Phys.*, **52**, 1.
HERZBERG, G., 1950, *Molecular Spectra and Molecular Structure, I, Spectra of Diatomic Molecules* (Cincinnati, Ohio: Van Nostrand Reinhold).
HERZBERG, G., and JUNGEN, CH., 1972, *J. molec. Spectrosc.*, **41**, 425.
HUS, H., YOUSIF, F., NOREN, C., SEN, A., and MITCHELL, J. B. A., 1988, *Phys. Rev. Lett.*, **60**, 1006.
IMANISHI, B., and VON OERTZEN, W., 1987, *Phys. Rep.*, **155**, 29.
INOKUTI, M., 1967, *Butsuri*, **22**, 196 (in Japanese); 1981, *Bunko Kenkyu*, **30**, 393 (in Japanese).
IWAI, M., and NAKAMURA, H., 1989, *Phys. Rev.* A, **40**, 2247.
JORTNER, J., and PULLMAN, B. (editors), 1986, *Tunneling*, The Jerusalem Symposia on Quantum Chemistry and Biochemistry, Vol. 19 (Dordrecht: D. Reidel).
JUNGEN, CH., and ATABEK, O., 1977, *J. chem. Phys.*, **66**, 5584.
JUNGEN, CH., and DILL, D., 1989, *J. chem. Phys.*, **73**, 3338.
JUNGEN, CH., and RAOULT, M., 1981, *Faraday Disc. chem. Soc.*, **71**, 253.
KAYANUMA, Y., 1982, *J. phys. Soc. Japan*, **51**, 3526; 1984a, *Ibid.*, **53**, 108; 1984b, *Ibid.*, **53**, 118; 1985, *Ibid.*, **54**, 2037.
KIMURA, K., 1987, *Int. Rev. phys. Chem.*, **6**, 195.
KLEPPNER, D., LITTMAN, M. G., and ZIMMERMAN, M. L., 1983, *Rydberg States of Atoms and Molecules*, edited by R. F. Stebbings and F. B. Dunning (Cambridge University Press), p. 73.
KORSCH, H. J., 1983, *Molec. Phys.*, **49**, 325.
LAING, J. R., YUAN, J. M., ZIMMERMAN, H., DEVRIES, P. L., and GEORGE, T. F., 1977, *J. chem. Phys.*, **66**, 2801.
LAM, K. S., and GEORGE, T. F., 1979, *Semiclassical Methods in Molecular Scattering and Spectroscopy*, edited by M. S. Child (Dordrecht: D. Reidel), p. 179.
LANDAU, L., 1932, *Phys. Z. Sowjun.*, **2**, 46.
LAWLEY, K. P. (editor), 1985, *Adv. chem. Phys.*, **60**.
LEFEBVRE-BRION, H., GIUSTI-SUZOR, A., and RASEEV, G., 1985, *J. chem. Phys.*, **83**, 1557.
LEFEBVRE-BRION, H., and KELLER, F., 1989, *J. chem. Phys.*, **90**, 7176.
LEGGETT, A. J., CHAKRAVARTY, S., DORSEY, A. T., FISHER, M. P. A., GARG, A., and ZWERGER, W., 1987, *Rev. mod. Phys.*, **59**, 1.
LEVINE, R. D., and KINSEY, J. L., 1986, *J. phys. Chem.*, **90**, 3653.
LI, J. M., 1986, *Electronic and Atomic Collisions*, Invited Papers of the 15th International Conference on Physics of Electronic and Atomic Collisions (Amsterdam: North-Holland), p. 621.
LIGHT, J. C., and WALKER, R. B., 1976, *J. chem. Phys.*, **65**, 4272.
MCGOWAN, J. W. (editor), 1981, *Adv. chem. Phys.*, **45**.

MIES, F. H., 1980, *Molec. Phys.*, **41**, 973; 1984, *J. chem. Phys.*, **80**, 2514.
MIES, F. H., and JULIENNE, P. S., 1984, *J. chem. Phys.*, **80**, 2526.
MILLER, S. C., and GOOD, R. H., 1953, *Phys. Rev.*, **91**, 174.
MILLER, W. H., 1970, *J. chem. Phys.*, **52**, 3563; 1974, *Adv. chem. Phys.*, **25**, 69.
MILLER, W. H., and GEORGE, T. F., 1972, *J. chem. Phys.*, **56**, 5637.
MITCHELL, J. B. A., and GUBERMAN, S. L. (editor), 1989, *Dissociative Recombination: Theory, Experiment and Applications* (Singapore: World Scientific).
MITCHELL, J. B. A., and MCGOWAN, J. W., 1978, *Astrophys. J.*, **222**, L77.
MITCHELL, A. C. G., and ZEMANSKY, M. W., 1934, *Resonance Radiation and Excited Atoms* (Cambridge University Press).
MITCHELS, H. H., 1981, *Adv. chem. Phys.*, **45**, 225.
MORIN, P., NENNER, I., ADAM, M. Y., HUBIN-FRANSKIN, M. J., DELWICHE, J., LEFEBVRE-BRION, H., and GIUSTI-SUZOR, A., 1982, *Chem. Phys. Lett.*, **92**, 609.
MOTT, N. F., and MASSEY, H. S. W., 1965, *The Theory of Atomic Collisions* (Oxford: Clarendon), chap. XIII.
NAKAMURA, H., 1969, *J. phys. Soc. Japan*, **26**, 1473; 1971, *J. phys. Soc. Japan*, **31**, 574; 1975, *Chem. Phys.*, **10**, 271; 1982, *Phys. Rev.* A, **26**, 3125 (erratum, 1983, *Phys. Rev.* A, **28**, 486); 1983, *Chem. Phys.*, **78**, 235; 1984a, *J. phys. Chem.*, **88**, 4812; 1984b, *Electronic and Atomic Collisions*, Invited Papers of the 13th International Conference on Photoelectric, Electronic and Atomic Collisions (Amsterdam: North-Holland), p. 661; 1986, *Butsuri*, **41**, 413 (in Japanese); 1987, *J. chem. Phys.*, **87**, 4031; 1988, *Electronic and Atomic Collisions*, Invited Papers of the 15th International Conference on Photoelectric, Electronic and Atomic Collisions (Amsterdam: North-Holland), p. 413.
NAKAMURA, H., and MATSUZAWA, M., 1970, *Butsuri*, **25**, 727 (in Japanese).
NAKAMURA, H., and NAMIKI, M., 1980, *J. phys. Soc. Japan*, **49**, 843; 1981, *Phys. Rev.* A, **24**, 2963.
NAKAMURA, H., and TAKAGI, H., 1990, *Butsuri*, **45**, 87 (in Japanese).
NAKASHIMA, K., NAKAMURA, H., ACHIBA, Y., and KIMURA, K., 1989, *J. chem. Phys.*, **91**, 1603.
NAKASHIMA, K., TAKAGI, H., and NAKAMURA, H., 1987, *J. chem. Phys.*, **86**, 726.
NASU, K., and KAYANUMA, Y., 1980, *Butsuri*, **35**, 226 (in Japanese).
NIEHAUS, A., 1981, *Adv. chem. Phys.*, **45**, 399.
NIKITIN, E. E., and UMANSKII, S. YA., 1984, *Theory of Slow Atomic Collisions* (Berlin: Springer).
OHSAKI, A., and NAKAMURA, H., 1990, *Phys. Rep.*, **187**, 1.
OVCHINNIKOVA, M. YA., 1965, *Dokl. phys. Chem.*, **161**, 259.
PACEY, P. D., SIEBRAND, W., and WILDMAN, T. A., 1986, *Tunneling*, edited by J. Jortner and B. Pullman (Dordrecht: D. Reidel), p. 117.
PLATZMAN, R. L., 1962a, *Vortex*, **23**, 372; 1962b, *Radiat. Res.*, **17**, 419.
PRATT, S. T., DEHMER, P. M., and DEHMER, J. L., 1984, *Chem. Phys. Lett.*, **105**, 28; 1986, *J. chem. Phys.*, **85**, 3379.
PRATT, S. T., JUNGEN, CH., and MIESCHER, E., 1989, *J. chem. Phys.*, **90**, 5971.
RAMASWAMY, R., and MARCUS, R. A., 1981, *J. chem. Phys.*, **74**, 1385.
RAOULT, M., 1987, *J. chem. Phys.*, **87**, 4736.
RAOULT, M., and JUNGEN, CH., 1981, *J. chem. Phys.*, **74**, 3388.
RAOULT, M., JUNGEN, CH., and DILL, D., 1980, *J. chim. Phys.*, **77**, 599.
RAOULT, M., LE ROUZO, H., RASEEV, G., and LEFEBVRE-BRION, H., 1983, *J. Phys.* B, **16**, 4601.
RAZAVY, M., and PIMPALE, A., 1988, *Phys. Rep.*, **168**, 306.
ROSEN, N., and ZENER, C., 1932, *Phys. Rev.*, **40**, 502.
RUDOLPH, H., DIXIT, S. N., MCKOY, V., and HUO, W. M., 1988, *J. chem. Phys.*, **88**, 1516.
RUDOLPH, H., LYNCH, D. L., DIXIT, S. N., MCKOY, V., and HUO, W. M., 1987, *J. chem. Phys.*, **86**, 1748.
RUSSEK, A., 1971, *Phys. Rev.* A, **4**, 1918.
SATO, H., and HARA, S., 1986, *J. Phys.* B, **19**, 2611.
SATO, K., ACHIBA, Y., NAKAMURA, H., and KIMURA, K., 1986, *J. chem. Phys.*, **85**, 1418.
SCHWARZSCHILD, B., 1986, *Phys. Today*, **39**, 17.
SEATON, M. J., 1983, *Rep. Prog. Phys.*, **46**, 167.
SHAW, G. S., and BERRY, R. S., 1972, *J. chem. Phys.*, **56**, 5808.
SHIBUYA, Y., 1975, *Global Theory of a Second Order Linear Ordinary Differential Equation with a Polynomial Coefficient* (Amsterdam: North-Holland).

SIEBRAND, W., WILDMAN, T. A., and ZGIERSKI, M. Z., 1984a, *J. Am. chem. Soc.*, **106**, 4083; 1984b, *Ibid.*, **106**, 4089.
SOBOLEWSKI, A. L., 1987, *J. chem. Phys.*, **87**, 331.
SOBOLEWSKI, A. L., and DOMCKE, W., 1987, *J. chem. Phys.*, **86**, 176; 1988, *J. chem. Phys.*, **88**, 5571.
STÜCKELBERG, E. C. G., 1932, *Helv. phys. Acta*, **5**, 369.
SUZUKI, R., NAKAMURA, H., and ISHIGURO, E., 1984, *Phys. Rev.* A, **29**, 3060.
TAKAGI, H., KOSUGI, N., and LEDOURNEUF, M., 1990, *J. Phys.* B (to be published).
TAKAGI, H., and NAKAMURA, H., 1981, *J. chem. Phys.*, **74**, 5808; 1983, *J. chem. Phys.* A, **27**, 691; 1986, *J. chem. Phys.*, **84**, 2431; 1988, *Ibid.*, **88**, 4552.
TAKATSUKA, K., and GORDON, M. S., 1981, *J. chem. Phys.*, **74**, 5718.
TENNYSON, J., and NOBLE, C. J., 1985, *J. Phys.* B, **18**, 155.
THORSON, W. R., 1961, *J. chem. Phys.*, **34**, 1744.
URBAIN, X., and GIUSTI-SUZOR, A., 1987, *Abstracts of the 15th International Conference on Physics of Electronic and Atomic Collisions* (Amsterdam: North-Holland), p. 174.
VERSCHUUR, J. W. J., and VAN LINDEN VAN DEN HEUVELL, H. B., 1989, *Chem. Phys.*, **129**, 1.
WATANABE, S., and LIN, C. D., 1986, *Phys. Rev.* A, **34**, 823.
WILLE, U., and HIPPLER, R., 1986, *Phys. Rep.*, **132**, 129.
WOLYNES, P., 1987, *J. chem. Phys.*, **86**, 1957.
WOOLLEY, A. M., 1971, *Molec. Phys.*, **22**, 607.
YOSHIMORI, A., and TSUKADA, M. (editors), 1985, *Dynamical Processes and Ordering on Solid Surfaces* (Berlin: Springer).
ZENER, C., 1932, *Proc. R. Soc.* A, **137**, 696.